THE ANALYSIS OF ACOUSTIC NOISE IN A SUBMERGED ARC FURNACE

by

J. Chadowitz

Submitted in fulfilment of
the requirements of a Masters
Degree in Electrical Engineering.

University of Cape Town,
September, 1977.

ACKNOWLEDGEMENTS

My thanks to:

The National Institute for Metallurgy for their sponsorship.

The staff of the Instruments Division at N.I.M. for their advice and aid with my work at the furnace.

Dr. A. Semmilink for his advice on acoustic instrumentation.

Dr. D. Swingler for his advice on Digital Signal Processing and his FFT package.

Dr. D.E. Naudé for his general supervision.

CONTENTS

INTRODUCTION

This project deals with Acoustic Noise Analysis in a submerged Arc Furnace. Operators and Metallurgists believe that the acoustic noise coming from the furnace conveys information as to the operating conditions of the furnace.

This submerged arc furnace reduces ferrochrome ore to the metal. A carefully made-up mixture of ore and slag producing materials is continually fed into the furnace. Three large carbon electrodes provide the heat to melt the ore by means of resistance heating and/or arcing. The exact mechanism is unknown. The furnace is rated at 48 MVA maximum and the electrodes carry currents of the order of 100 kiloamperes. The metal is tapped approximately every four hours. The term submerged arc is used because the furnace is completely enclosed and the arc occurs below a layer of ore mix.

This differs from an open arc furnace which does not have a roof and where the operators can actually see into the top of the furnace.

The operation of the submerged arc furnace is also different from that of a scrap melting electric arc furnace. A scrap furnace has set melting cycles and has acoustic noise changes determined by falling metal, melting and initial arcing. Higgs, Papadakis and Sheets (Ref.1) performed signature analysis on acoustic noise from a scrap furnace to differentiate between different operating conditions in the furnace.

The aim of the present project was to collect and analyze data records of acoustic noise and operating conditions from the number four furnace at Ferrometals, Witbank. The data was recorded on analogue and computer magnetic tape and analyzed at UCT. The analysis was aimed at explaining the operators' theory of the acoustic noise relating to operating conditions of the furnace.

This procedure is different from that of Reference 1 in that they did their analysis with an on-plant analyzing computer, and that their furnace had a set defined cycle whereas the submerged arc furnace is a continuous feed system. Reference 1 is the only known information relating to the analysis of noise in the electric arc furnaces, and their furnace operation is largely different to that of the furnace used in this project.

CHAPTER 1.

COLLECTION AND RECORDING OF ACOUSTIC NOISE DATA, AND DATA DESCRIBING FURNACE OPERATING CONDITIONS

1.1 DESCRIPTION OF THE FURNACE ENVIRONMENT

The acoustic noise to be analysed is produced by the furnace and heard by the operators. The furnace as shown in diagram 1.1 consists of a metal tank standing on a platform made of concrete and iron girders.

At the tank roof level, the surrounding structure has a floor completely surrounding the furnace and providing access to the firebrick roof. This level also holds the two exhaust gas plants and the numerous material feeding chutes. The operating room is built on this floor alongside the furnace.

Above this level is a floor providing access to the electrode movement machinery and electrical power connections. At the bottom of the furnace there is a platform used in tapping the metal into ladles which are moved by a gantry alongside the furnace.

From inspection of the furnace, and the use of a sound level meter, the following was determined.

(a) The top level holding the electrode equipment had a low noise level (65dB) when most of the surrounding machinery

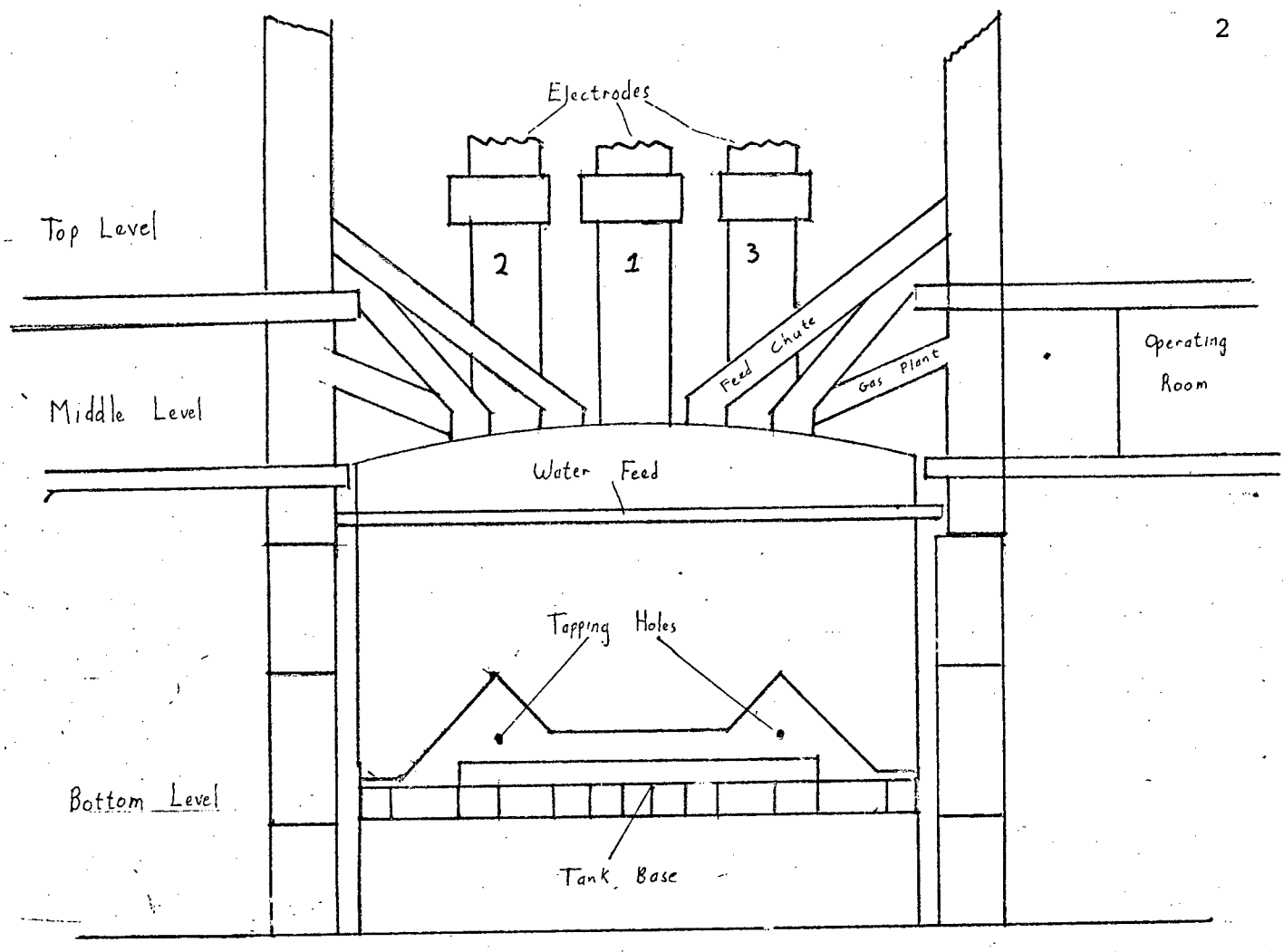

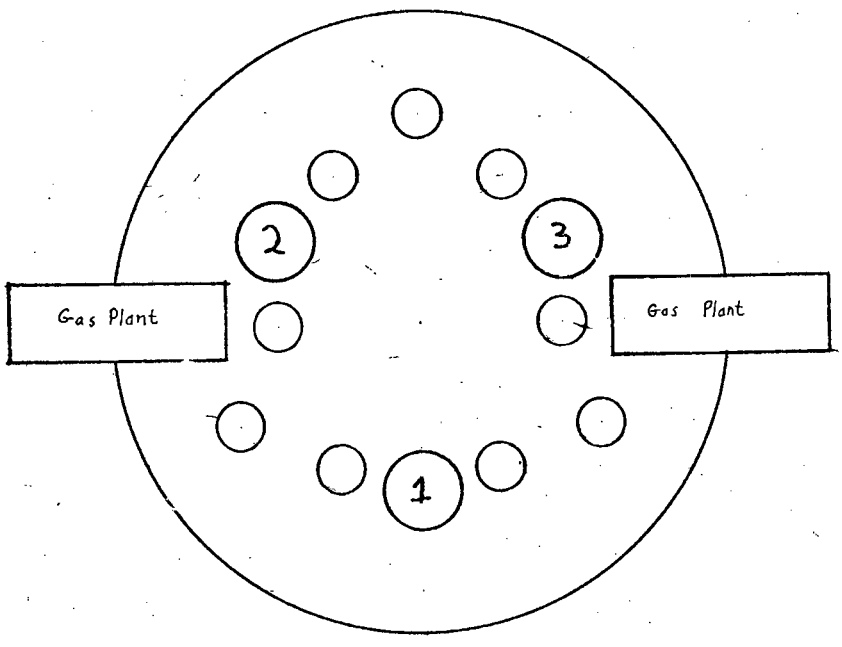

Furnace Roof.

Diagram 1.1

and workmen were quiet. The noise in this area is not heard by the operators and consists mainly of machinery noise. Any instrumentation mounted on this floor would have to cope with electrical and magnetic field problems caused by the close proximity of cables carrying of order 100 000 amps. For the above reasons it was decided that acoustic noise data would not be collected from this area.

(b) The middle level was considered a good location for the collection of acoustic data as this was the area most frequented by the operators. The sound level was of the order of 85dB but there was a large amount of external machinery noise as well as the furnace noise. The machinery noise was created by the two gas plants and numerous material feeding chutes.

(c) The bottom level around the base of the furnace had a low noise level (65dB), made up of furnace noise, machinery noise and passing vehicle noise. Near the tapping holes machinery and gantry noises dominated. The area around the tapping holes was considered unsuitable for instrumentation due to the extreme heat and harsh environmental conditions. The floor of the furnace was accessible via tunnels formed by the iron girders upon which it rested. The floor and tank, apart from near the tapping holes, were considered to be suitable for acoustic noise data collection.

1.2 CHOICE OF TRANSDUCERS

The transducers used to detect the sound and transform it into an electrical signal must fulfil the following requirements:

(a) They should be, as much as is possible, capable of detecting the same noise as the human ear.

(b) They must endure the harsh environmental conditions of large electrical and magnetic fields, heat, and in some cases, water.

(c) The transducers must be mounted such that they are not vulnerable to theft or interference.

(d) The transducers must feed into a recording device, from which the data can be reproduced for analysis.

The common transducers used to collect acoustic noise data are microphones and piezoelectric accelerometers.

Microphones are sensitive to sound pressure and are designed to detect airborne noise. Accelerometers are vibration transducers and are normally attached firmly to the vibrating noise source. Many types of microphones are sensitive to electric or magnetic fields, but Condenser Microphones, which do not have this problem, are too fragile for plant use and also require a multi-core cable to provide power for operation. Because of these problems and the extraneous airborne noise, it was decided that microphones would not be used.

Piezoelectric accelerometers must be firmly attached to the noise source where they convert vibration into electric signals. They are insensitive to airborne sound and have a low transverse sensitivity. Piezoelectric transducers are unaffected to a large extent by electric and magnetic fields. Accelerometers can be obtained for use in almost all operating conditions and with a wide range of frequency bandwidths and sensitivities. It was decided that accelerometers would be used as they fulfil the necessary requirements.

The characteristics of the specific accelerometer required were established from the following considerations:

The human ear in young persons has a frequency bandwidth of up to 15 kHz (Ref. 4). Older people have a lower high frequency limit which can drop to below 10 kHz with age and hearing damage. Working from these estimates it was decided that it was very unlikely that the operators were hearing noise above 10 kHz. This determined the high frequency limit of the instrumentation. The furnace vibration was visually estimated at less than 1 g by scattering sand and watching for jumping. The temperature of the furnace shell is kept below 100^{o}C by a curtain of water flowing down it. The roof and floor have temperatures below 200^{o}C.

The accelerometer selected for use was an ENDEVCO HIGH SENSITIVITY ACCELEROMETER MODEL 213 E. Its characteristics are described in Appendix 1. It has a 10 kHz bandwidth, and will withstand the environmental conditions described above. Four

of these accelerometers were ordered along with high temperature cables (ENDEVCO No. 3090A).

The ear has a dynamic range of 120dB and is able to detect a sinusoidal signal 60dB down in noise. The accelerometer does not have this discriminating characteristic but being a vibration transducer which is insensitive to airborne noise, it should only detect vibration from the body to which it is fixed.

1.3 ACOUSTIC NOISE RECORDING EQUIPMENT

The electrical signal generated in the accelerometer had to be transmitted along cables, amplified then recorded on a magnetic tape recorder. The tape recorder was positioned in the computer room which was a separate airconditioned part of the operating room.

The tape recorder used was a PHILLIPS EL1020/07 PORTABLE INSTRUMENTATION RECORDER having seven instrumentation channels and one audio channel. The channels can be used in a Direct (D.R.) mode or Frequency Modulation (F.M.) mode and combined with the four tape speeds, allowed signals from d.c. to 100 kHz to be recorded. The signal to noise ratio was specified at -36dB using the D.R. mode and was measured at -32dB at tape speed 3¾"/sec. using the F.M. mode. Further specifications on the tape recorder are given in Appendix 3.4.

The following sections describe the instrumentation necessary

for noise free transmission and amplification of the accelerometer signal.

1.4 RECORDING INSTRUMENTATION

In order to design or select instrumentation to transform and transmit the signal produced by the accelerometer, the operation and characteristics of the accelerometer must be known.

Appendix 2 describes the operation and characteristics of accelerometers when used in charge and voltage modes.

(a) CHOICE OF AMPLIFIERS

In order to optimize the instrumentation, the type of amplifier was chosen on its suitability to the requisites summarized below:

1. The instrumentation must have a similar bandwidth to that of the human ear (30 Hz to 10 kHz).

2. The instrumentation must withstand a plant environment or must be mounted in a protected area.

The description of accelerometer characteristics in Appendix 2 indicates that two types of amplifiers are suitable for use with accelerometers.

Charge Amplifier

The Charge Amplifier need not be mounted close to the accelerometer as cable capacitance does not affect sensitivity or

frequency response. Commercially available are the Brüel and Kjaer range of which the 2324 is designed for field operation. These charge amplifiers were rejected for the following reasons: the low frequency response is much better than is needed and, as the cost of this type of amplifier is very high, one is paying for unrequired capabilities. The insensitivity of the available charge amplifier systems to Plant electrical noise was unspecified and the successful operation of this equipment in the furnace environment was not guaranteed.

Voltage Amplifier

The Voltage Amplifier for reasons of sensitivity, and susceptibility to electrical noise, must be mounted as close to the accelerometer as possible. The output of the voltage amplifier is a low impedance line whose length does not affect the sensitivity or susceptibility to electrical noise. The preamplifier must withstand the plant environment at the accelerometer mounting position and should be internally battery-powered to avoid noise sensitive power supply cables. The Brüel and Kjaer preamplifiers Types 2616 and 2625 are battery-powered but are only designed for brief use in the field, and would not withstand continuous use in the harsh environment for a few weeks. The mounting positions of the accelerometers are not always easily accessible, and once installed, instrumentation would remain for the duration of the data collection.

It was decided that commercially available preamplifiers were not ideally suited to the required application. A suitable simple, high input impedance voltage preamplifier was designed and constructed.

(b) VOLTAGE PREAMPLIFIER DESIGN

The main requisites of the preamplifier are high input impedance and low power consumption. Field Effect Transistors are capable of very high input impedances but have a large power consumption. The LM 4250 is a versatile programmable monolithic operational amplifier. A single external master bias setting resistor programs the input bias current, input offset current, quiescent power consumption, slew rate, input noise and the gain-bandwidth product. This amplifier was used in an a.c. amplifier bootstrap circuit to produce a high input impedance voltage preamplifier with low power consumption. The circuit is shown in Diagram 1.2.

The set current of the operational amplifier was 1 μA giving a quiescent current of less than 10 μA. The preamplifier was powered by two 1.4 volt 210 mAH mercury cells which have constant a voltage and long shelf life. The actual operating current drawn was dependent on the pre-amplifier load. The largest signal delivered by the pre-amplifier into a 1KΩ load was 10 mV which results in a current flow of 10 μA. This current flow as well as the quiescent current gave the preamplifier an acceptable continuous operation life of one year. The pre-amplifier was designed for unity gain giving an adequate bandwidth of 40 kHz. The measured low frequency 3dB point was 8 Hz and the amplifier was designed to critically damp low frequency ringing. The input impedance was greater than 100MΩ the input capacitance was 1nF and the output impedance was of the order of 1Ω .

VOLTAGE PREAMPLIFIER CIRCUIT.

See Appendix 3.

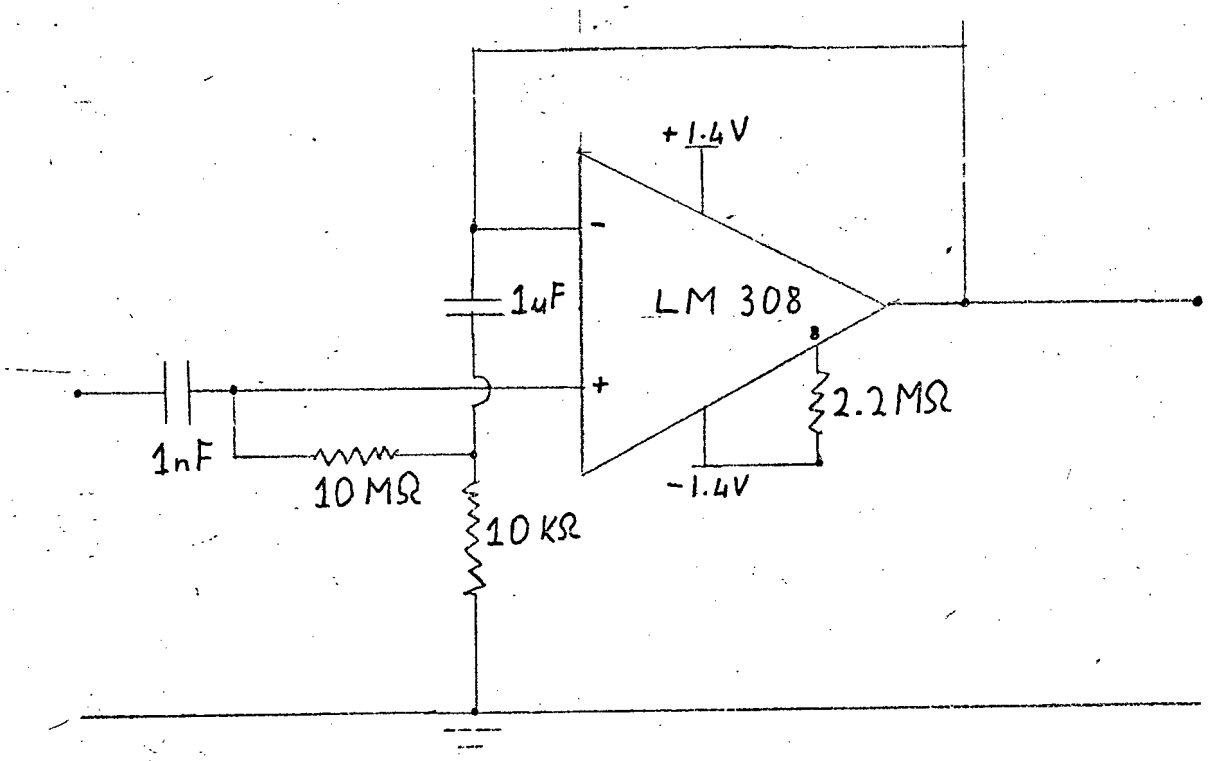

DIAGRAM 1.2

The amplifier was assembled on a fibre-glass printed circuit board which was mounted in a 25 x 50 x 100 mm industrial plastic box. The circuit board made direct contact with both batteries, holding them in place as well as making an electrical contact. The interior of the box was sprayed with graphite particles suspended in a plastic solvent, which formed a conductive layer used as an effective earth screen. The box contents were encapsulated in a water-resistant silastic rubber which also protects the circuitry from physical shock. This rubber was easily removable for battery replacement or amplifier repair. The pre-amplifier was tested for noise rejection and harsh environmental conditions.

(c) SYSTEM OPERATION

The complete instrumentation system consisted of four accelerometers, with their respective remote voltage pre-amplifiers, feeding via 50Ω co-axial cables into a common four-channel voltage amplifier. These amplifiers were simple inverting X100 amplifiers which brought the signals within the input ranges of the tape recorder amplifiers (see Diagram 1.3).

The input impedances of the 4-channel voltage amplifier was 1kΩ. This was the lowest value the pre-amplifiers could drive while having a reasonable battery life. The pre-amplifier output impedance is of the order of 1Ω. The entire transmission section is at a low impedance and therefore is insensitive to noise.

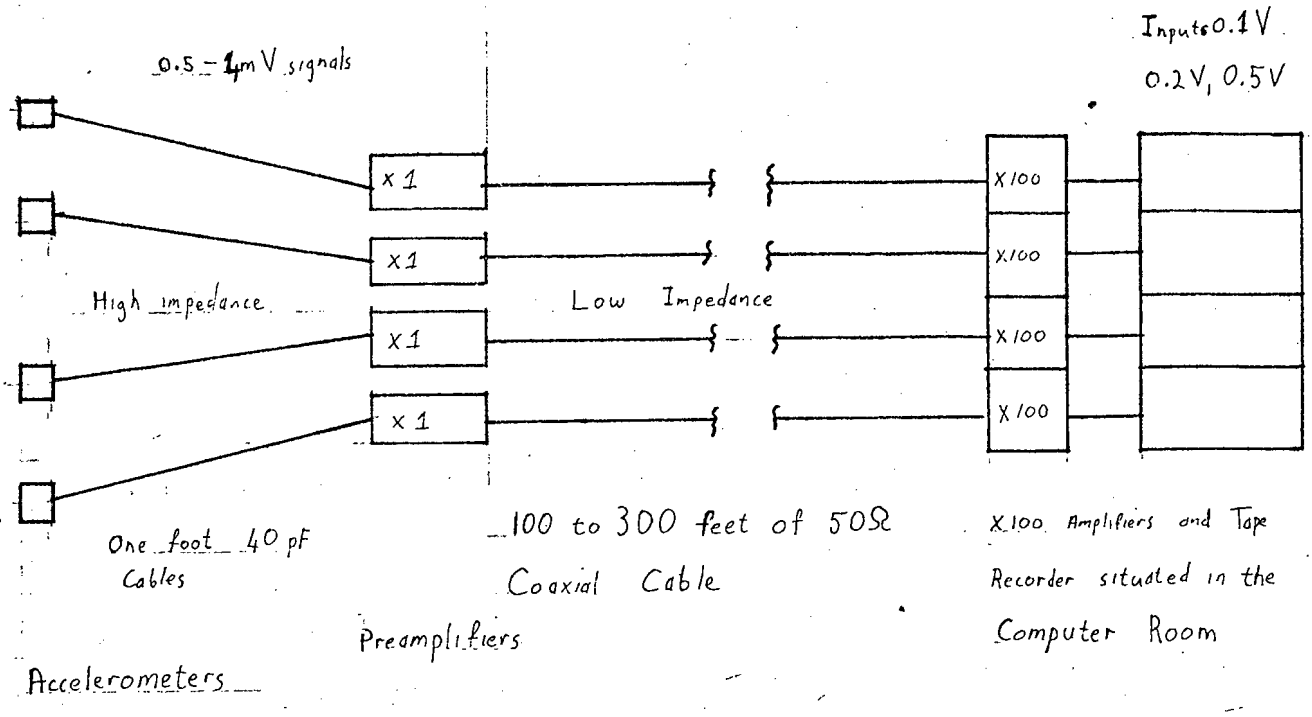

DIAGRAM 1.3

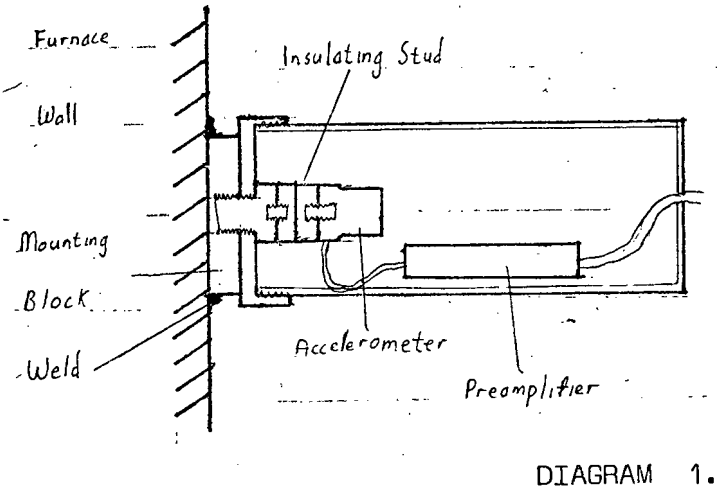

DIAGRAM 1.5

The earthing point of the instrumentation was very important as earth current loops create large electrical noise signals. These loops are avoided by earthing the instrumentation at only one point.

The accelerometer case is connected to the "low" side of its transducer as isolating the case permits capacitive coupling of AC noise. This means that if the accelerometer is mounted directly onto a metal object the "instrumentation" is earthed, and must not be earthed at any other point. The four accelerometers were all mounted on metal surfaces and connected to a four channel amplifier with a common earth. Earth current loops were avoided by electrically insulating the accelerometers while keeping them in good mechanical contact with the furnace wall. The only earth connection was made at the four channel amplifier.

An insulating stud was used to isolate the accelerometer from the mounting point. The stud was constructed from two pieces of machined brass hex-bar each fitted with 10-32 NF thread studs. The pieces were glued together with epoxy putty. The insulation between the studs was greater than 100MΩ and could withstand 500 volts A.C. The stud could withstand twice the mounting torque the accelerometer required and was capable of withstanding the environmental conditions. Tests done on the study to establish its effect on the high frequency response of the accelerometer, showed that the stud had no detectable influence on the frequency response of the amplifier.

1.5 POSITIONING THE ACCELEROMETERS

(a) CHOICE OF POSITIONS

Accelerometers, being vibration transducers, have to be fixed firmly to the vibrating noise source. In the case of a furnace, the added weight of the accelerometer will not affect the noise produced. Accelerometers can be attached to noise sources by the following means:

1. Bolting the accelerometer onto a stud fixed in a flat surface of the noise source.
2. Cementing the accelerometer on with dental cement.
3. In the case of attaching to certain metals a magnet fitted with a stud can be used.

The mode of mounting is important as a mechanical coupling which is "soft" will tend to reduce the high frequency range of the accelerometer due to the formation of a mechanical low pass filter. Methods 2 and 3 described above might fall into that category, depending on the cement and magnetic strength.

The initial experimentation involved finding the best positions for mounting the accelerometers. To do this it was not feasible to drill a hole and tap to mount an accelerometer at every likely position. Instead, a heavy steel block was welded to the back of a powerful magnet onto which an accelerometer was bolted using the insulating study described previously. The effect of the magnetic coupling was very small and found to be

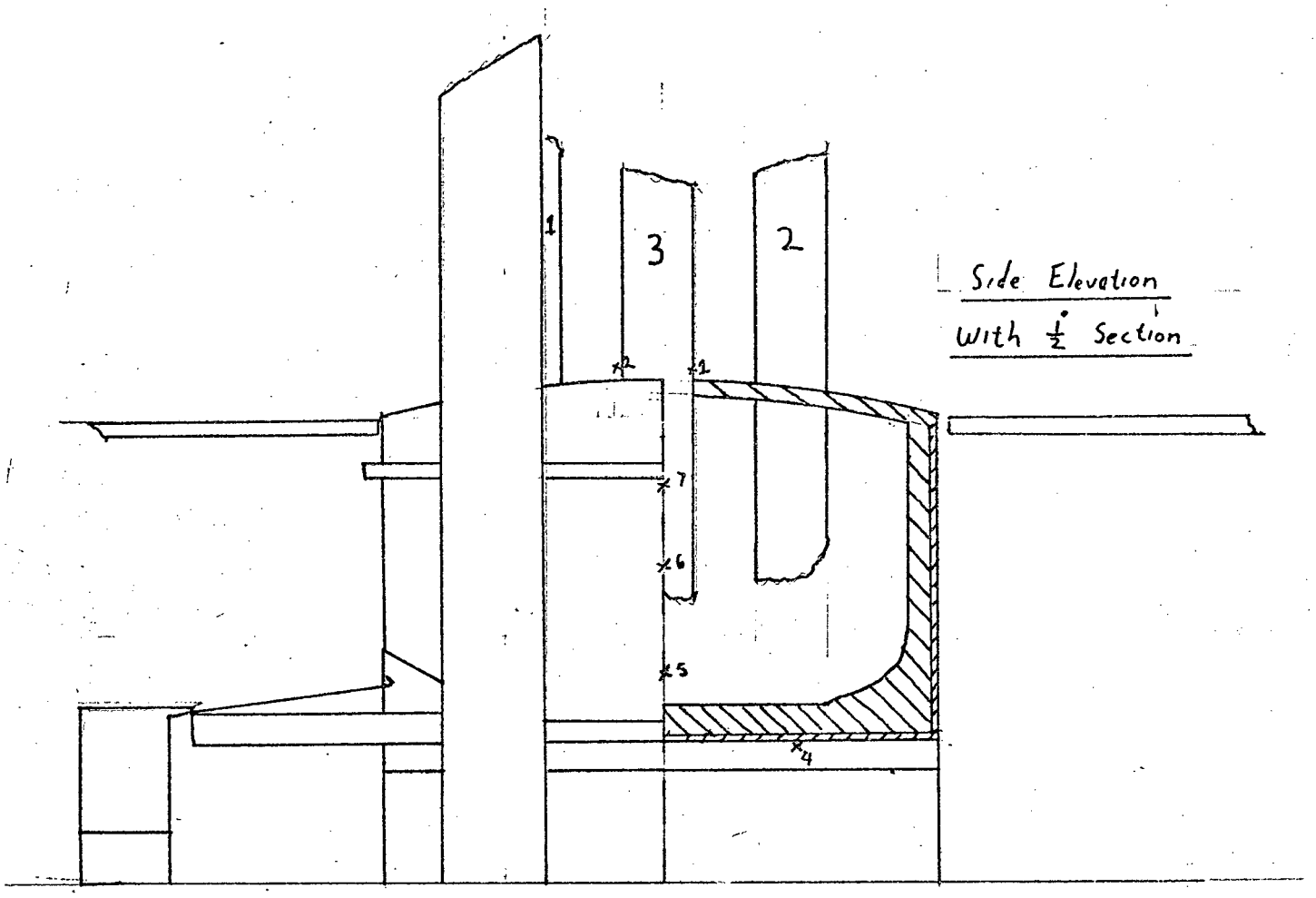

Side Elevation
With $\frac{1}{2}$ Section

Accelerometer positions ·····x

Roof Plan

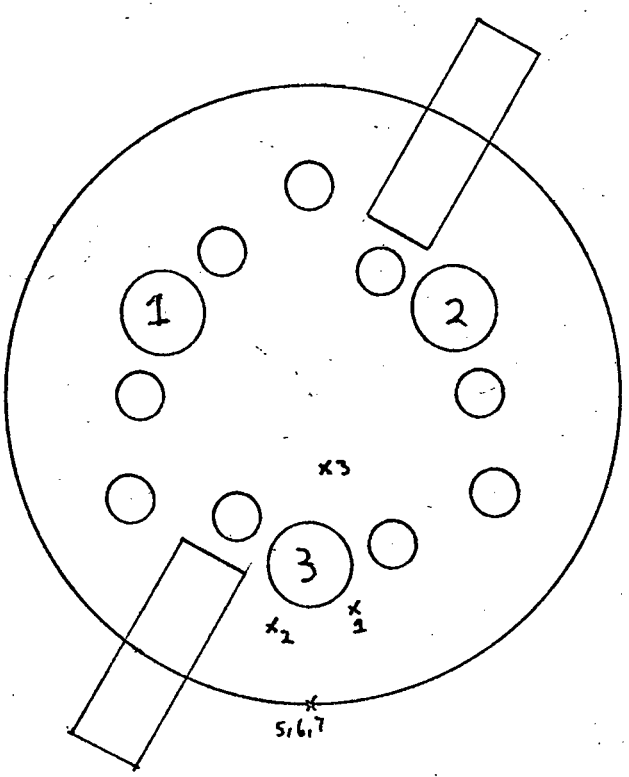

Diagram 1.4

negligible in this application. A pair of headphones with a portable audio preamplifier was used to listed to the noise at the positions investigated. A co-axial cable was run to the operating room so that the signal could be observed on an oscilloscope and recorded on magnetic tape.

The following seven positions were investigated in the areas chosen by inspection as described previously:

(a) Under the furnace;

(b) On the furnace walls;

(c) On the furnace roof;

The positions are shown in Diagram 1.4.

Positions 1, 2 and 3, all on the furnace roof, produced large noise amplitudes of approximately 8 mV at the accelerometer. On hearing the noise via the accelerometer, amplifier and headphones, it was decided that a large amount of the noise was mechanical noise from feed chutes and the gas plants. An attempt was made to attach the clamp onto the metal case of the electrode but, due to the strong a.c. magnetic field associated with the electrode, the d.c. field of the magnet was swamped and the magnet would not hold.

Position 4 was under the furnace floor between two steel girders on which the furnace rests. The noise level was 0.5 mV at the accelerometer. This low level is to be expected due to the damping effect of the thick graphite floor.

Positions 5, 6 and 7 were down the side of the furnace wall opposite electrode 3. The accelerometers, which have a low transverse sensitivity and high directivity, were positioned opposite a specific electrode as it was hoped that the majority of the noise would be associated with that electrode. The noise level increased from the bottom to the top of the wall. At position 7, the amplitude was 3 mV which fell to 2 mV at position 6, and 1 mV at position 5. This was probably due to the wall thickness increasing down the furnace (see section in Diagram 1.4). The noise heard via the headphones gave little indication of mechanical noise. The furnace wall has cooling water flowing down it which would wet the accelerometer, and short circuit the insulating stud. This was avoided by coating the stud and accelerometer with silastic rubber. The sound of the running water was detected by the accelerometer but the furnace noise was still dominant.

From the above investigation, it was decided that the accelerometers would be mounted at positions 6 and 7 opposite electrode three, and at corresponding positions opposite electrode two. These positions were well within the temperature range of the instrumentation, but the cooling water was a problem in that it adds extraneous noise and would short circuit the insulating stud. The use of silastic rubber for insulation involved turning off the cooling water for the time required to mount an accelerometer and allow the silastic rubber to dry. This was difficult to accomplish and was not popular with the furnace administrators.

The other positions did not have water problems but had either too much extraneous noise to too low a noise level.

A protective mount for the accelerometers was therefore developed which eliminated these problems.

(b) MOUNTING THE ACCELEROMETERS IN THEIR POSITIONS

The mounting unit as shown in Diagram 1.5 consists of a piece of 3" steam piping with a threaded heavy steel cap. The cap has a ½" steel bolt through its centre and welded in place. The top of the bolt is faced and tapped to take the insulating stud. The back of the pipe is closed but has a gland for the output cable. The preamplifier is mounted in the pipe and is connected to the accelerometer by a short lead. The pipe, with cap screwed on and sealed, provides a complete pre-assembled robust and waterproof unit. The ½" bolt screws into tapped steel blocks welded to the furnace wall. The accelerometer via the bolt is in good mechanical contact with the furnace, and the pipe prevents water falling on the accelerometer and short-circuiting the insulating stud. The water noise is not significantly detected by the accelerometer as no water falls directly upon it, and the vibration of the pipe due to the water has no effect at the mounting bold. The section of the instrumentation most susceptible to electrical noise is the cable between accelerometer and pre-amplifier. This section is within a continuous magnetic and electric shield formed by the pipe and earthed to the furnace. The complete units were easily mounted on the furnace wall without disruption of the cooling water.

Co-axial cables (50Ω) were laid in conduit from the mounting positions to the computer room. Although the instrumentation was only intended to be on plant for less than one month, the conduit was necessary to prevent theft of, or interference with, the cables.

The mounting positions were fortunately out of reach of the platforms around the furnace wall. For theft, interference, installation or removal of instrumentation, a large monkey wrench and long ladder was required. The "transducer unit" cables were joined to the transmission cables via "in-line" BNC connectors which were encapsulated in silastic rubber and taped up after connecting. Excess cable was non-inductively coiled and placed in the metal boxes terminating the conduit.

(c) RECORDING PROCEDURE

As described in Appendix 4, the tape recorder has four speeds and seven separate instrument channels each usable in the Frequency Modulator (F.M.) or Direct (D.R.) mode. The tapes available were extended play (E.P.) usable for F.M. recording only and Long Play (L.P.) which were half the length of the E.P. tapes, but could be used for Direct or F.M. recording. The frequency bandwidth is proportional to tape speed. In order to have the maximum amount of tape available for data collection, initial recordings were made to establish the bandwidth of the signal. The tape speed used was 30"/sec. and F.M. gave a bandwidth of 0-10 kHz which was also the bandwidth of the transducer.

The signal was frequency analyzed and showed harmonics of 100 Hz with very little signal above 1 kHz. (see Diagram 1.6).

This established the signal bandwidth of 1 kHz and allowed a tape speed of 3¾" per second to be used giving a bandwidth of 1250 Hz on F.M. recording. At this speed the playing time was 3 hours for the E.P. tapes and 1½ hours for the L.P. tapes.

There was no experimental way of determining the length of the data records needed. The only known cycle time in the furnace operation is the metal tapping procedure which occurs approximately every four hours. In order to collect data which would cover time variations over a long period of time, an on-off timer was used to switch on the tape recorder for ¾ of a minute every 10 minutes. In this way a sampled record length of approximately 48 hours was available. The timer used was a high stability industrial timer which was connected to the 12 volt diode logic of the tape recorder via the tape remote control switch. Two types of data record were recorded, giving short continuous records of up to 3 hours and long sampled records of up to 48 hours.

From Diagram 1.7 it was observed that harmonics of 100 Hz dominate the acoustic noise. The dynamic range of the tape recorder on F.M. is 32dB which reduces the level of the recorded noise other than harmonics, to the same level as recorder noise. To investigate the noise other than the harmonics, the following active filters were designed and built.

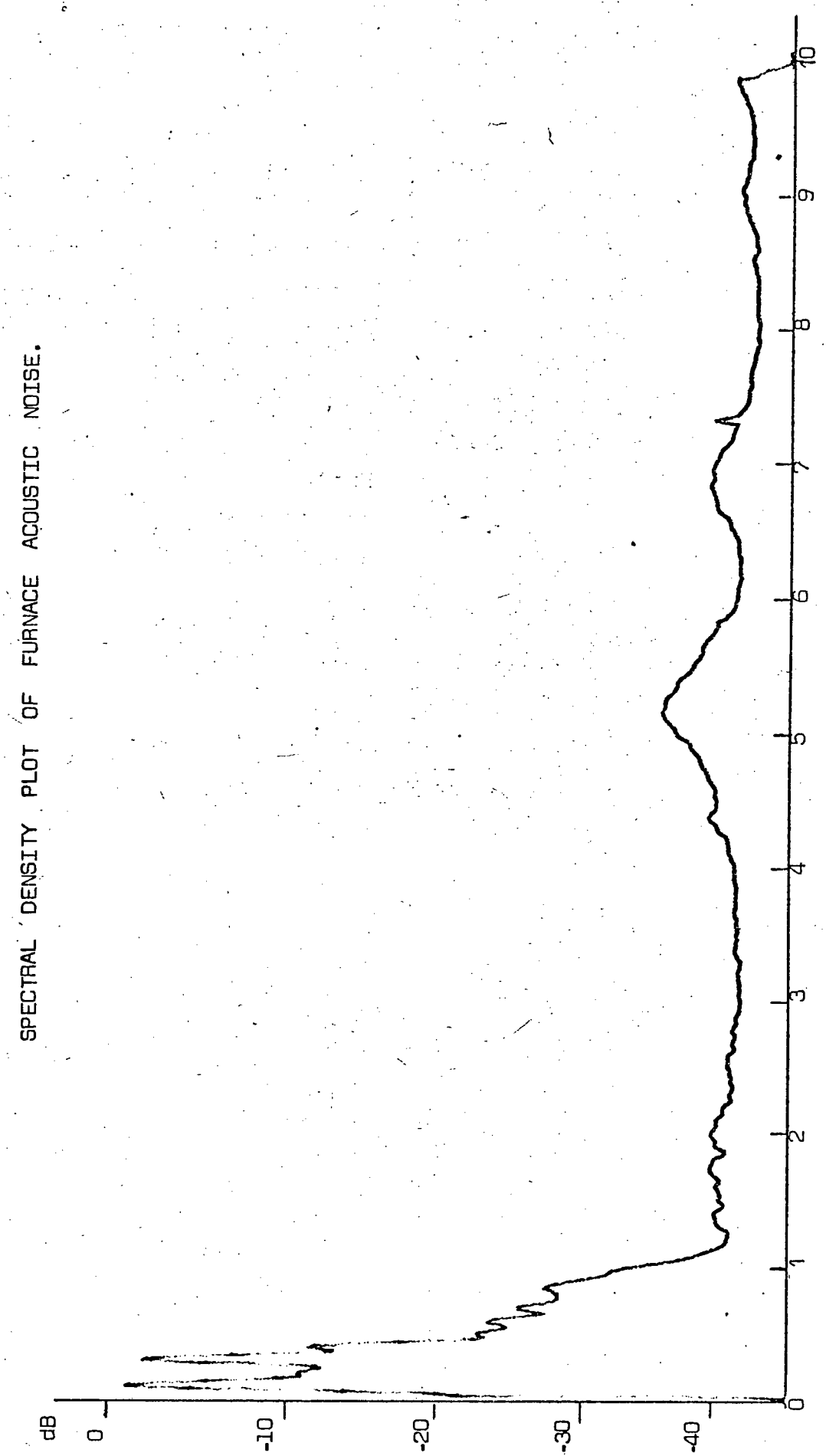
SPECTRAL DENSITY PLOT OF FURNACE ACOUSTIC NOISE.
dB
0
-10
-20
-30
-40
0
1
2
3
4
5
6
7
8
9
10
Frequency kHz

DIAGRAM 1.6

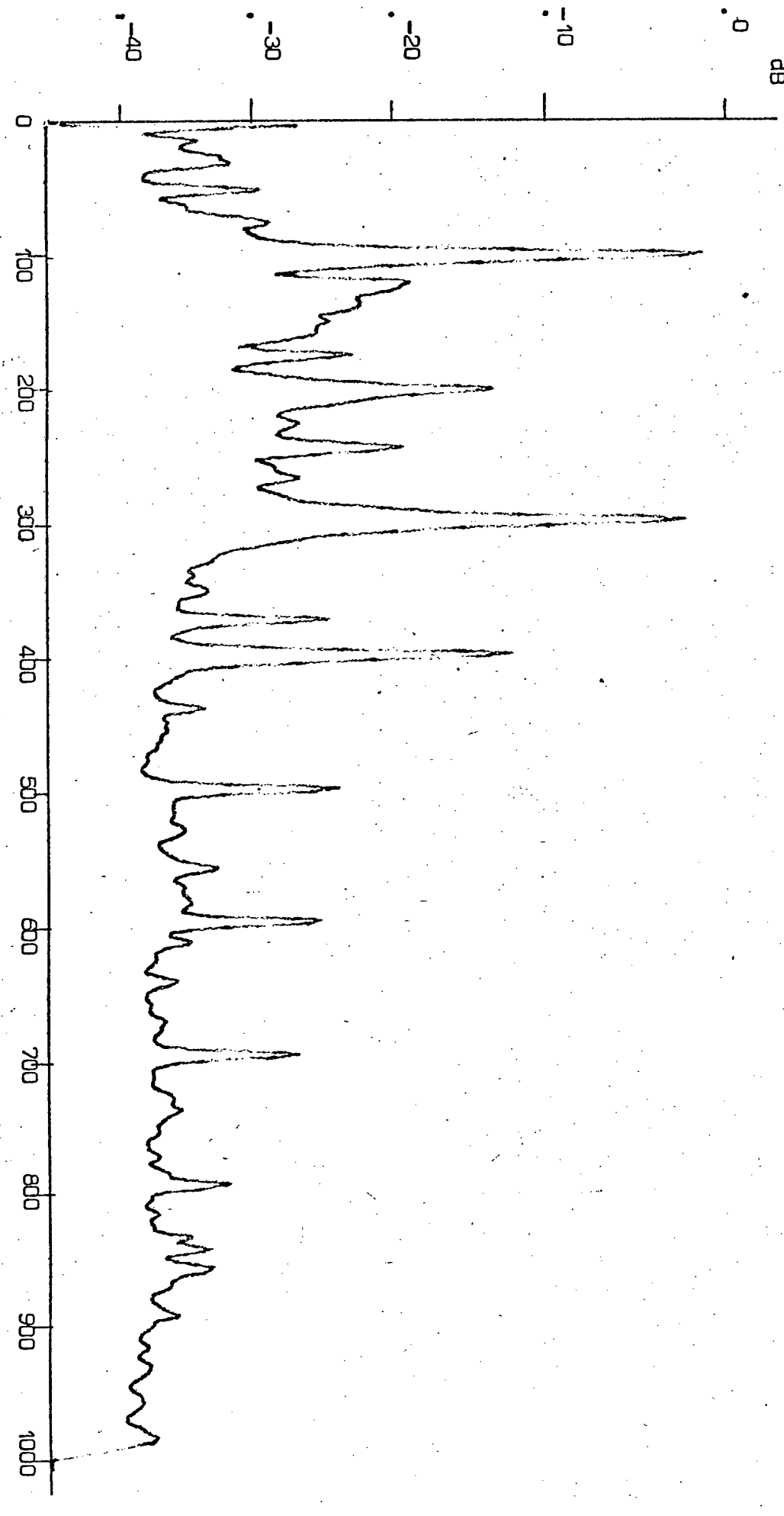

SPECTRAL DENSITY PLOT OF FURNACE ACOUSTIC NOISE.

DIAGRAM 1.7

A set of high Q notch filters at the harmonic frequencies which eliminated the harmonics and allowed the noise between harmonics as well as the noise above 1 kHz to be recorded.

These filters were active and were chosen for their high Q, component insensitivity and ease of tuning. The frequency response of the 50 Hz Notch Filter is shown in Diagram 1.8. Further Filter details are given in Appendix 5.

Using these filters a continuous recording was made to establish whether relevant information was in the noise other than harmonic noise.

1.6 THE COLLECTION OF OPERATING CONDITIONS DATA

Number four furnace of Ferometals, Witbank, has a Nova Computer System with RTP interface equipment, installed in a room next to the operating room.

The N.I.M. CANCER project used this system to log one minute averages of 25 selected data channels to a wrap-around disc file. The data channels logged are described in Appendix 6.

Their objects of logging the data in this way were:

1. To keep a detailed history of plant operation for up to one week, so that in the event of plant failure, the data could be examined for the cause of the failure.

2. To obtain a record of plant operation in the computer, so

FREQUENCY RESPONSE OF THE 50 Hz NOTCH FILTER

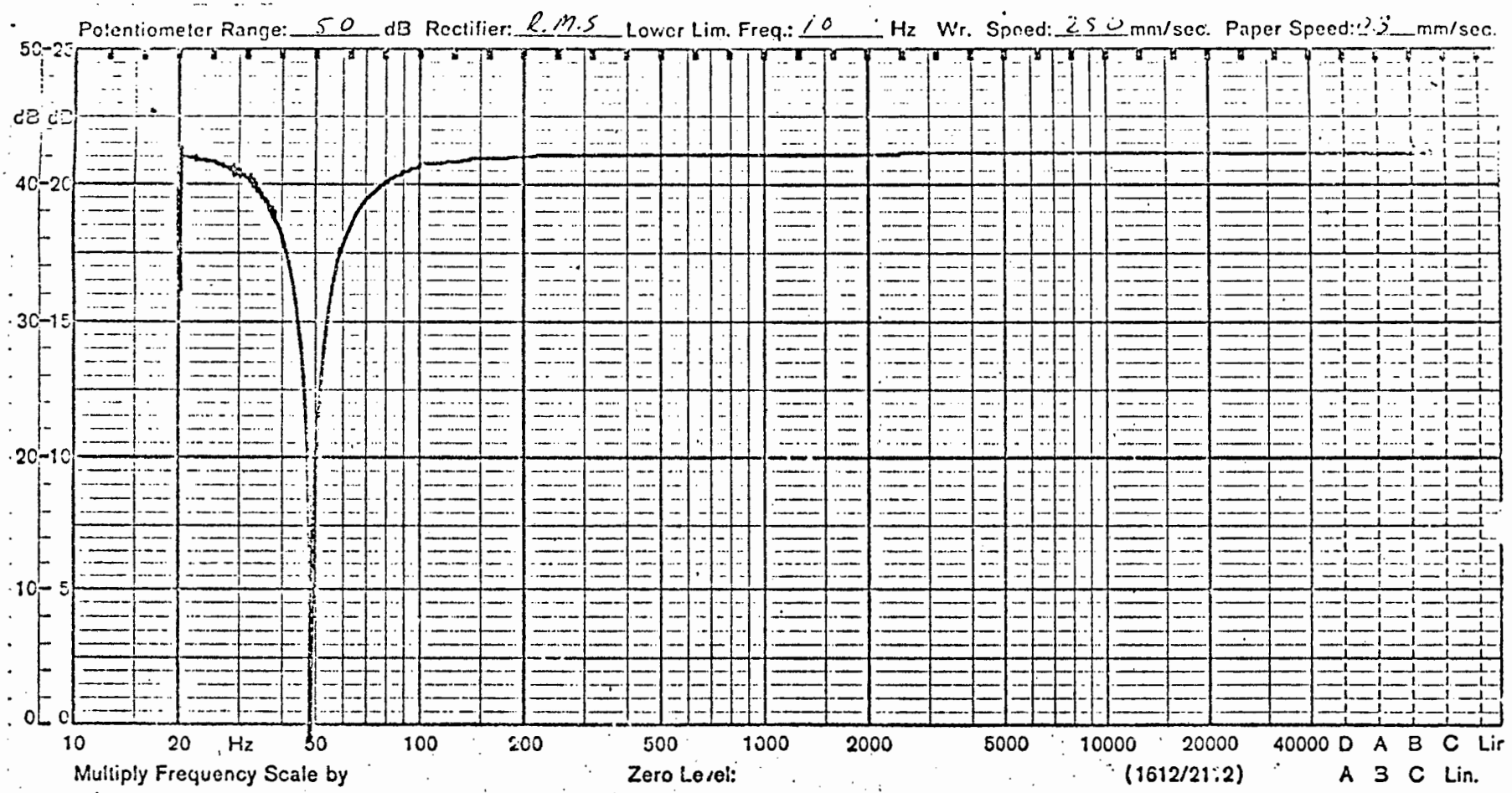

DIAGRAM 1.8

that off-line processing of the data could be done to test theories and develop control schemes.

The format of this disc file and the operating instructions to the programs associated with accessing the file is described in N.I.M. memos (Ref. 5). These programs were used on the plant computer as well as the in-house computer to determine where on the file the data for each day was located, and to access, condense and plot selected data channels.

It was infeasible to install instrumentation for gathering operating condition data as the instrumentation and recording ability of the working computer system could be used. It was decided to use computer magnetic tape for transporting the data as this form of data storage is common to most computers. The disc system used on the Nova is not common to other computers and paper tape would be too bulky for data storage.

The data was read from the disc and transformed into minute records, each giving Date, Time, section number, then the average values of each of the 25 operating conditions logged over the previous minute. This data was transformed to ASCII character and written onto magnetic tape. Each tape block held just over one minute record.

The operating conditions data was thus restricted to a resolution of one minute samples. As described in Appendix 6, only certain data was relevant and the values logged on some channels were not direct measurements but values calculated from direct measurements with certain assumptions made.

CHAPTER 2.

ANALYSIS TECHNIQUE

This chapter describes the techniques used for analysis of the collected data records, and the theory relevant to the analysis which may not be assumed to be common knowledge. The techniques used are largely the application of classical techniques (Refs. 2 and 3) which are relevant to the analysis of the collected data.

The equipment used in applying these techniques varied with the data format, but the techniques are the same.

The chapter is divided into:

1. Individual Record Analysis.
2. Cross Record Analysis.

2.1 INDIVIDUAL RECORD ANALYSIS

Data gathered from physical phenomenon must be classified before analysis techniques can be applied. This classification is part of the analysis and is necessary as further analytical techniques are only valid with certain types of data.

Data can be classified as shown in the flow chart in Diagram 2.1. The first step is establishing whether data is

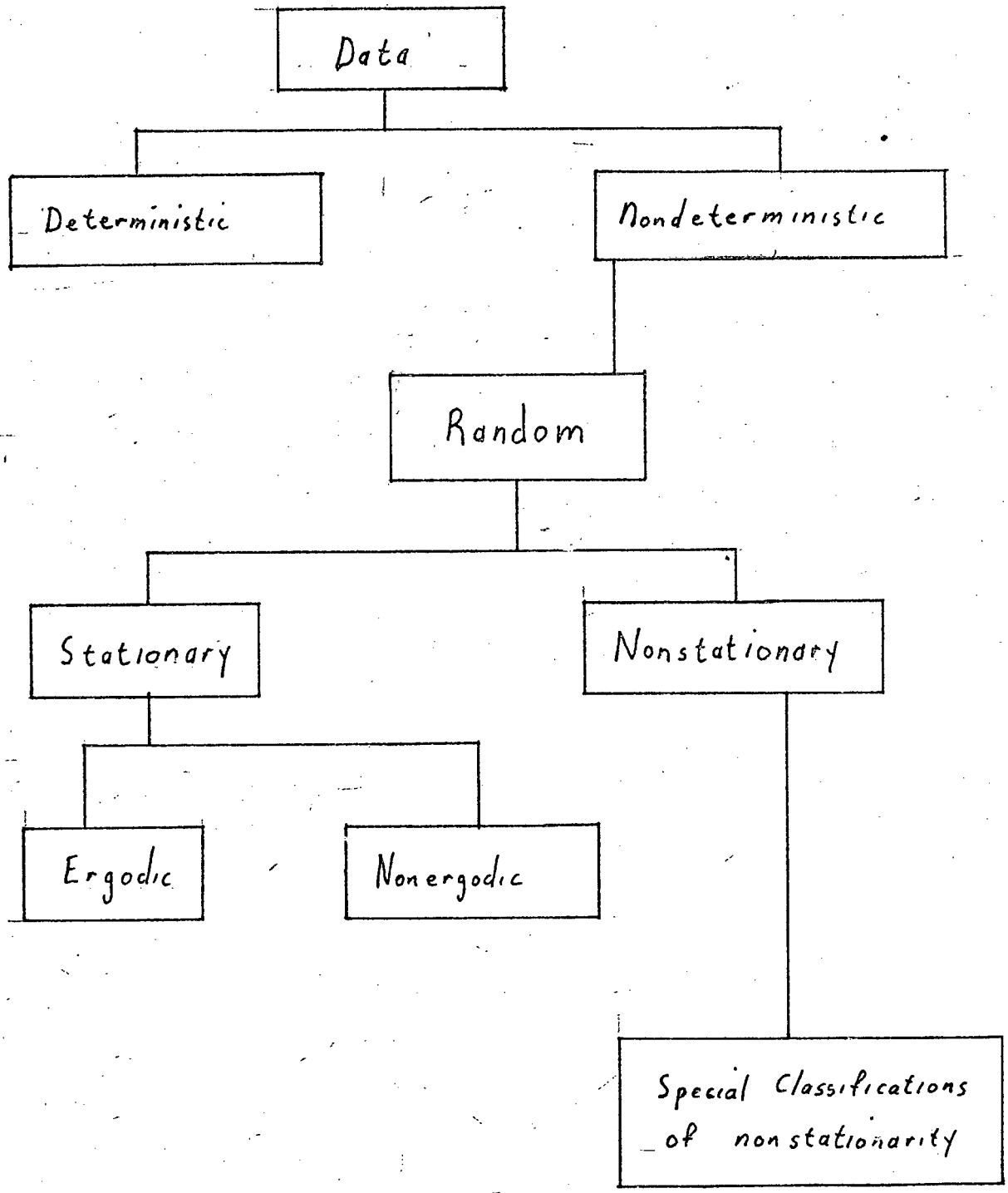
Data
Deterministic
Nondeterministic
Random
Stationary
Nonstationary
Ergodic
Nonergodic
Special Classifications of nonstationarity

DIAGRAM 2.1

deterministic or non-deterministic. Deterministic data can be described by an explicit mathematical relationship and can be periodic or non-periodic. Non-deterministic data cannot be described by explicit mathematical relationships and the exact value at a future instant in time is not predictable. These data are random in character and must be described in terms of probability statements and statistical averages rather than explicit equations.

Data Qualification

The correct procedure for analyzing random data, as well as interpreting the analyzed results, are strangely influenced by certain basic characteristics which may or may not be exhibited by the data. The three most important of these basic characteristics, are the stationarity of the data, the presence of periodicities in the data, and the normality of the data.

Stationarity is of concern, because the analysis procedures required for non-stationary data, are generally more complicated than those which are appropriate for stationary data.

Periodicites in the data should at least be identified to avoid erroneous interpretation of later results. The validity of an assumption that the data (excluding periodicities) have a Gaussian probability, density function should be investigated since the normality assumption is vital to many analytical applications for random data.

The sections following describe the techniques used to investigate the basic characteristics mentioned above.

The sections are:

(a) Classification of Random Data

(b) Detection of Periodicities.

(c) Testing for Normality.

(a) CLASSIFICATION OF RANDOM DATA

Random data may be divided into two categories, stationary and non-stationary. Stationary random data can again be either Ergodic or Non-ergodic and Non-stationary data can be classified into specific types of Non-stationarity.

The above classification is important in that the analysis is determined by the class into which the Random Data falls.

Stationary Random Processes.

The concepts of stationarity and ergodicity are important and are defined in Appendix 7. For the purpose of this analysis these concepts were applied to sample records, in the following manner:

Stationarity as defined in Appendix 7 relates to ensemble averaged properties of a random process. An ensemble being a collection of sample functions forming a random process. A

sample function (or sample record in the case of a finite time interval) is a single time history representing a random phenomenon.

In practise stationarity or non-stationarity can describe individual time history records of a random phenomenon. When a single history record is referred to as being stationary, it is generally meant that the properties computed over short time intervals do not vary "significantly" from one interval to the next. The word significantly is used here to mean that observed variations are greater than would be expected due to normal statistical sampling variations.

To help clarify this point, consider a single sample record $x_k(t)$ obtained from the kth sample function of a random process $\{x(t)\}$. Assume a mean value and autocorrelation function are obtained by time averaging over a short interval T with a starting time of t_1 as follows.

$$\mu_x(t_1, k) = \frac{1}{T}\int_{t_1}^{t_1+T} x_k(t)\,dt$$

$$R_x(t_1, t_1+\tau, k) = \frac{1}{T}\int_{t_1}^{t_1+T} x_k(t)\,x_k(t+\tau)\,dt \qquad \ldots\ldots\ldots 2.1$$

For the general case where the sample properties defined in Equation 2.1 vary significantly as the starting time t_1 varies, the individual sample record is said to be non-stationary. For the special case where the sample properties defined in Equation 2.1 do not very significantly as the starting time

t_1 varies, the sample record is said to be stationary. Furthermore, sample records from most physically interesting non-stationary random processes will be non-stationary. Hence, if an ergodic assumption is justified (as it is for most actual stationary physical phenomena), verification of stationarity for a single sample record will effectively justify an assumption of stationarity and ergodicity for the random process from which the sample record is obtained.

Non-Stationary Random Processes

Non-stationary random processes include all random processes which do not meet the requirements for requirements for stationarity defined in Appendix 7. Unless further restrictions are imposed, the properties of a non-stationary random process are generally time-varying functions which can be determined only by performing instantaneous averages over the ensemble of sample functions forming the process. In practice, it is often not feasible to obtain a sufficient number of sample records to permit the accurate measurement of properties by ensemble averaging. This fact has tended to impede the development of practical techniques for measuring and analyzing non-stationary random data.

In many cases, the non-stationary random data produced by actual physical phenomena can be classifed into special categories of non-stationarity which simplify the measurement and analysis problem. For example, some types of random data might be described by non-stationary random process $y(t)$ where each sample function is given by $y(t) = A(t)x(t)$. Here,

x(t) is a sample function from a stationary random process x(t) and A(t) is a deterministic multiplication factor. In other words, the data might be represented by a non-stationary random process consisting of sample functions with a common deterministic time trend. If non-stationary random data fit a specific model of this type, ensemble averaging is not always needed to describe the data. The various desired properties can sometimes be estimated from a single sample record, as is true for ergodic stationary data.

Record Lengths in Stationarity Considerations.

When data is classified as being 'stationary' one must take into account the restriction that the data record used for testing is of a finite length. The lowest frequency component in the data, including a non-stationary mean must have a period much less than the record length, otherwise the record length is not large enough to classify the data.

The sample of data must also be collected such that it will reflect any non-stationary character of the random process.

Stationarity can be evaluated by considering the physics of the phenomenon creating the data. If the basic factors creating the phenomenon are time invariant stationarity can be accepted. In the present case of the acoustic noise produced by a submerged arc furnace the factors creating the acoustic noise are unknown. (An untested hypothesis on the cause of this noise is included in Appendix 8). Stationarity of the acoustic noise could

only be assumed over very long periods of time of the order of weeks, provided no large change is made to the furnace which could affect the Acoustic Noise. This assumption has no value as the lengths of the data records collected have a maximum of two days.

The following test, called the Run Test was used for evaluating the stationarity of data. (Ref. 2, Section 4.7 and Section 7.4.2).

Test for Stationarity

The data given should fulfill the following assumptions:

1. Any given sample record will properly reflect the non-stationary character of the random process in question.

2. Any given sample record is very long compared to the lowest frequency component in the data, excluding a non-stationary mean. In other words, the sample record must be long enough to permit non-stationary trends to be differentiated from the random fluctuations of the time history.

Beyond these basic assumptions, it is convenient (but not necessary) to assume further that any non-stationarity of interest will be revealed by time trends in the mean square value of the data. There are of course, non-stationary random processes with a stationary mean square value, but this is unusual in practice, because it is highly unlikely for non-stationary data to have a

time varying autocorrelation function at any time displacement τ without the value at $\tau = 0$ varying. Since the autocorrelation at $\tau = 0$ (R(0)) is equal to the mean square value (ψ^2), the mean square value will usually reveal a time varying autocorrelation. A similar argument applies to higher order properties.

The stationarity of random data can be tested by investigating a single record x(t) as follows:

1. Divide the sample record into N equal time intervals where the data in each interval may be considered independent.

2. Compute a mean square value (or mean value and variance separately) for each interval and align these sample values in time sequence, as follows:

$$\overline{x_1^2}, \quad \overline{x_1^2}, \quad \overline{x_3^2}, \quad \ldots\ldots\ldots, \quad \overline{x_N^2}$$

3. Test the sequence of mean square values for the presence of underlying trends or variations other than those due to expected sampling variations.

The final test may be accomplished in many ways, but a non-parametric approach which does not require a knowledge of the sampling distributions of data parameters is more desirable. The Run Test fulfills these requirements, and is applied as follows; Let it be hypothesized that the sequence of sample

mean square values

$$\overline{x_1^2},\ \overline{x_2^2},\ \overline{x_3^2},\ \ldots\ldots\ldots,\ \overline{x_N^2}$$

are each independent sample values of a random variable with a mean square value of ψ_x^2. If this hypothesis is true, the variations in the sequence of sample values will be random and display no trends. Hence the number of runs in the sequence relative to, say, the medium value, will be as expected for a sequence of independent random observations of the random variable, as presented by Table A.6. If the number of runs is significantly different from the expected number given in Table A.6, the hypothesis of stationarity would be rejected. Otherwise, the hypothesis would be accepted. Note that the above testing procedure does not require a knowledge of either the frequency bandwidth of the data or the averaging time used to compute sample mean square values, or any other parameter estimate. Furthermore, it is not necessary for the data under investigation to be free of periodicities. Valid conclusions are obtained even when peiodicities are present, as long as the fundamental period is short compared to the averaging time used to compute sample values. Examples of the application of Run Test can be found in Chapter 3.

Application of Table A.6

For the acceptance of the Run Test hypothesis at a significance level α, the number of runs (r_n) generated by using 2n=N data points must fulfil the following requirements

$$r_{n;\,1-\alpha/2} < r_n < r_{n;\,\alpha/2}$$

The values of $r_{n;}$ are given in Table A.6 (Ref. 2).

Table A.6

Percentage Points of Run Distribution

Values of $r_{n;\alpha}$ such that Prob $[r_n > r_{n;\alpha}] = \alpha$, where $n = N_1 = N_2 = N/2$

	α					
$n = N/2$	0.99	0.975	0.95	0.05	0.025	0.01
5	2	2	3	8	9	9
6	2	3	3	10	10	11
7	3	3	4	11	12	12
8	4	4	5	12	13	13
9	4	5	6	13	14	15
10	5	6	6	15	15	16
11	6	7	7	16	16	17
12	7	7	8	17	18	18
13	7	8	9	18	19	20
14	8	9	10	19	20	21
15	9	10	11	20	21	22
16	10	11	11	22	22	23
18	11	12	13	24	25	26
20	13	14	15	26	27	28
25	17	18	19	32	33	34
30	21	22	24	37	39	40
35	25	27	28	43	44	46
40	30	31	33	48	50	51
45	34	36	37	54	55	57
50	38	40	42	59	61	63
55	43	45	46	65	66	68
60	47	49	51	70	72	74
65	52	54	56	75	77	79
70	56	58	60	81	83	85
75	61	63	65	86	88	90
80	65	68	70	91	93	96
85	70	72	74	97	99	101
90	74	77	79	102	104	107
95	79	82	84	107	109	112
100	84	86	88	113	115	117

(b) THE DETECTION OF PERIODICITIES

Periodicities in data are broughtout in many analysis techniques. Strong periodic components are visible as delta functions in the power spectrum, but can be confused with narrow-band contributions. The two can be distinguished by narrowing the resolution of the filter bandwidth

in which case the indicated bandwidth of the peak will always be equal to the bandwidth of the analyser filter frequence. This will not work unless the resolution bandwidth of the analyzer filter is smaller than the bandwidth of possible narrow band random data.

The amplitude probability density functions for sinusoidal and random data are different as shown in diagram 2.2. The problem with this technique is that data with many periodic components could look like pure random data, and that in the case of a single single sinusoid, identification is difficult unless the variance of the sine wave is less than the variance of the random part of the data. Diagram 2.3 shows the probability density function of furnace acoustic noise. This plot does not show periodicities in the data because of the large amount of periodic components present.

The autocorrelation is another method of detecting sinusoids. Random data without periodicities will have an autocorrelation which has a value approaching the square of the mean value as the time displacement becomes large. The autocorrelation function of a sinusoid or collection of sinusoids will continue to oscillate no matter how large the time displacement becomes. Diagram 3.7 shows these autocorrelograms and diagram 2.5 shows the autocorrelogram of typical furnace noise.

The autocorrelation function oscillates at the same frequencies as the periodic components in the data. The fourier transform of the autocorrelation function gives the spectral density function. This gives no new information but presents the infor-

Probability Density Functions

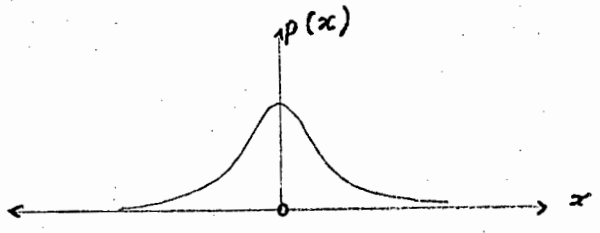

a) Narrow Band Random Noise

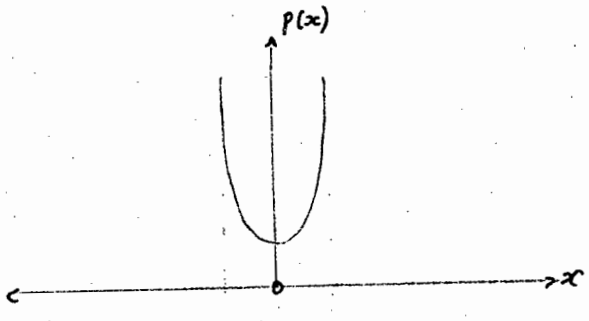

b) Sine Wave

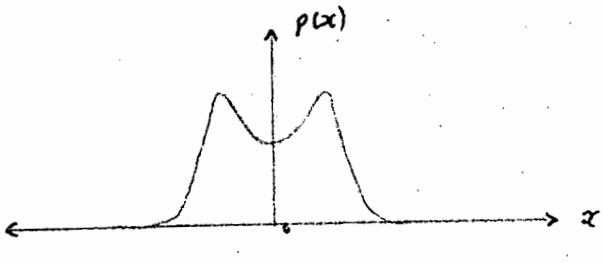

c) Sine Wave Plus Random Noise

DIAGRAM 2.2

PROBABILITY DENSITY FUNCTION OF FURNACE ACOUSTIC NOISE.

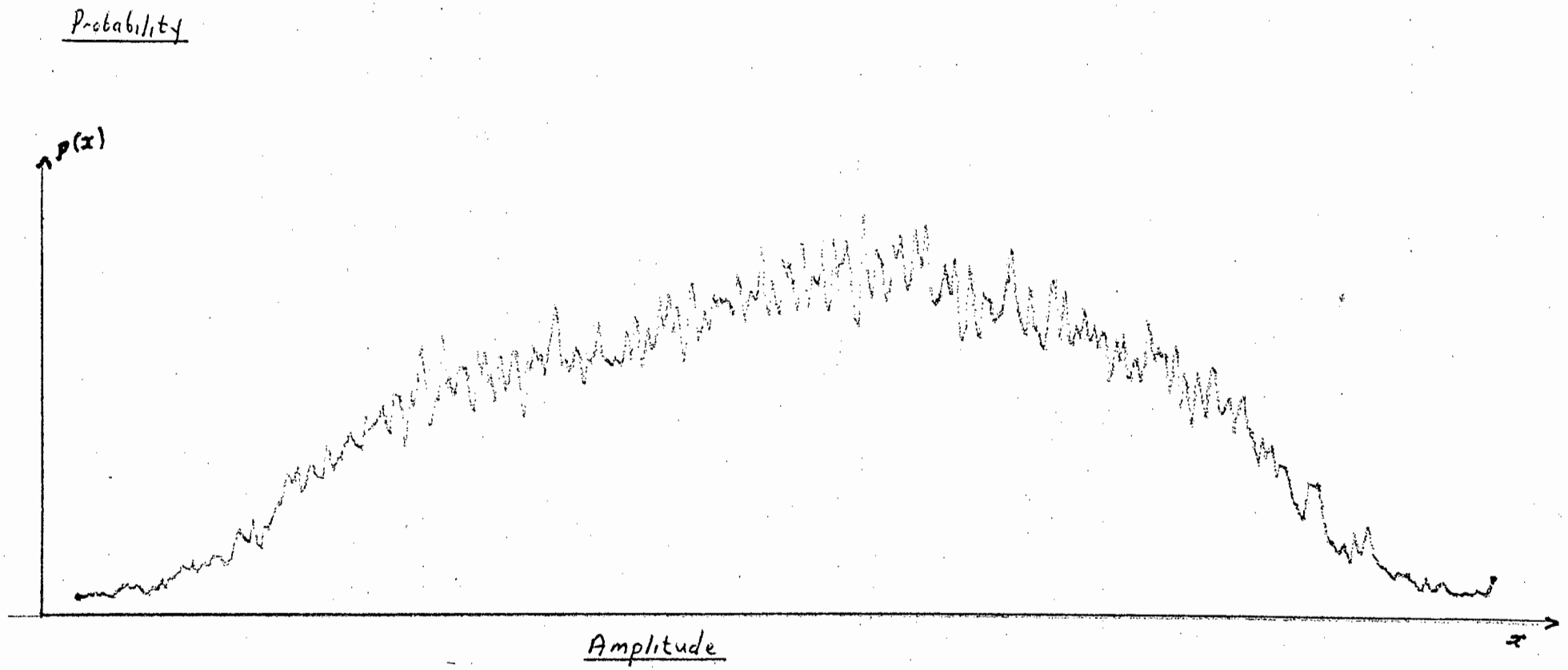

DIAGRAM 2.3

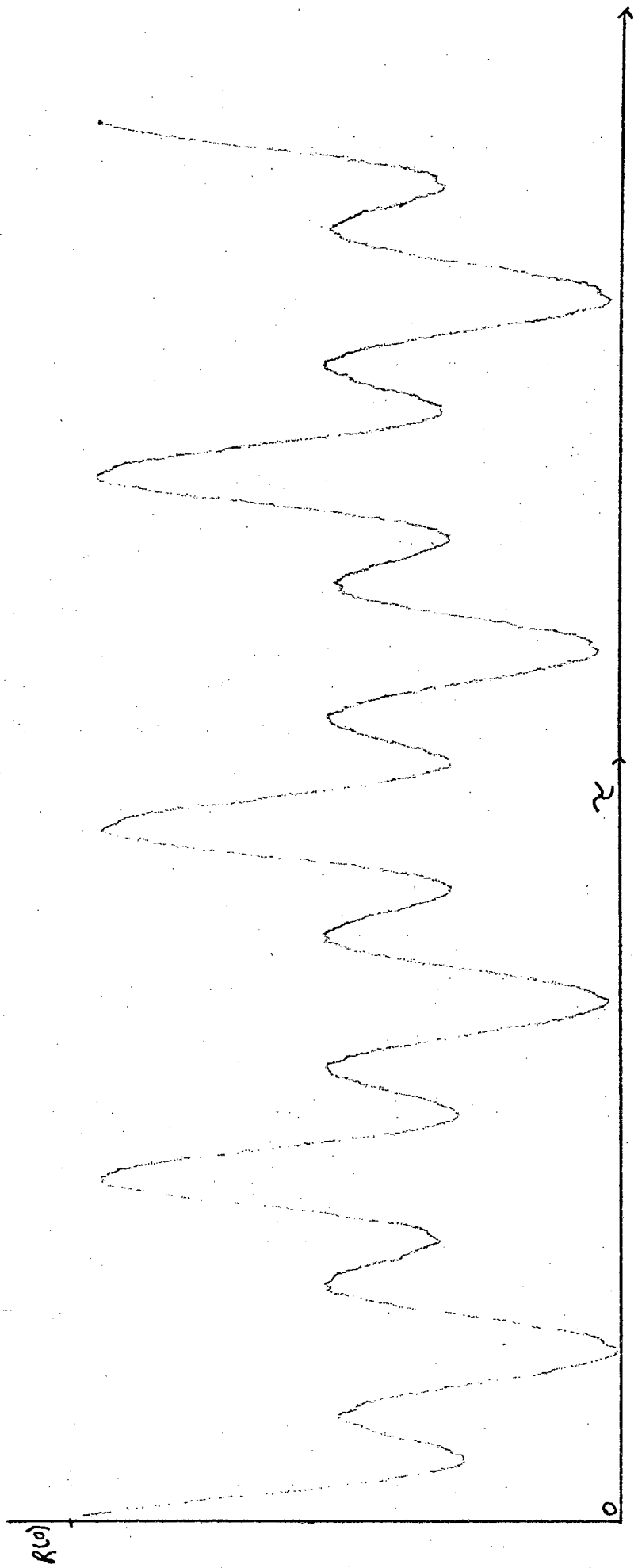

DIAGRAM 2.5

mation in the autocorrelation function in a different form. Diagrams 2.6 and 2.7 show the log spectral density plots of furnace noise. Diagram 2.6 shows the log spectral density plot produced by a real time analyser and ensemble averager using actual recorded furnace noise. Diagram 2.7 shows the Fourier transform of the autocorrelation function into the real time analyzer and using an ensemble averager.

The long displacement autocorrelation function of periodic components removes random noise and leaves only periodic components. The value of the autocorrelation function at $\tau = o$ gives the mean square value of the data.

The autocorrelation function and its Fourier transform was the main technique used to detect and identify periodicities in the data. The mathematical definition of the auto-correlation function is given by:

$$R_x(\tau) = \lim_{T\to\infty} \frac{1}{T} \int_0^T x(t)\, x(t+\tau)\, dt$$

where

$$R_x(-\tau) = R_x(\tau)$$

and

$$R_x(0) \geq |R_x(\tau)| \qquad \text{for all } \tau$$

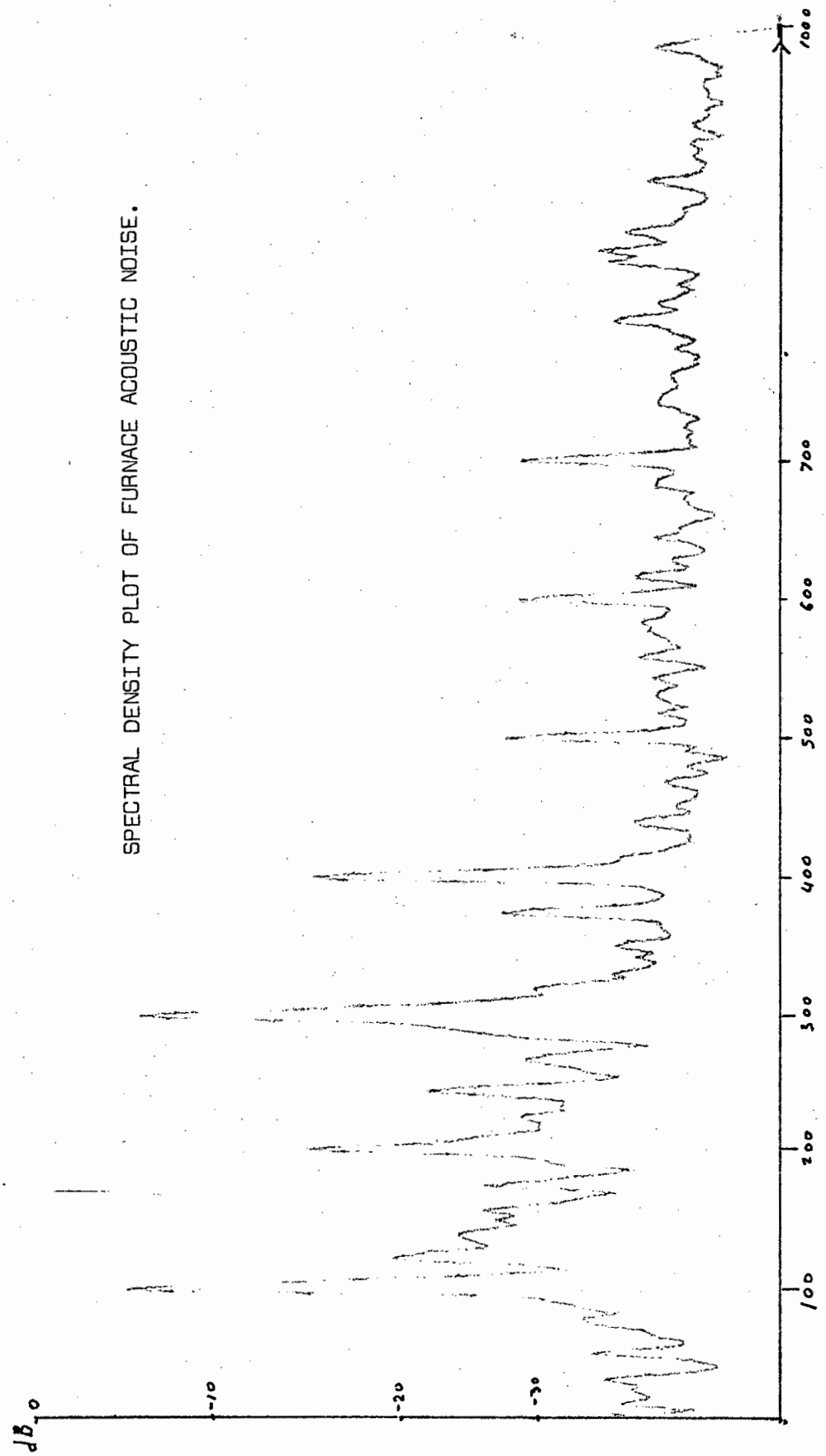
SPECTRAL DENSITY PLOT OF FURNACE ACOUSTIC NOISE.
dB
0
-10
-20
-30
100
200
300
400
500
600
700
1000
Frequency Hz.

DIAGRAM 2.6

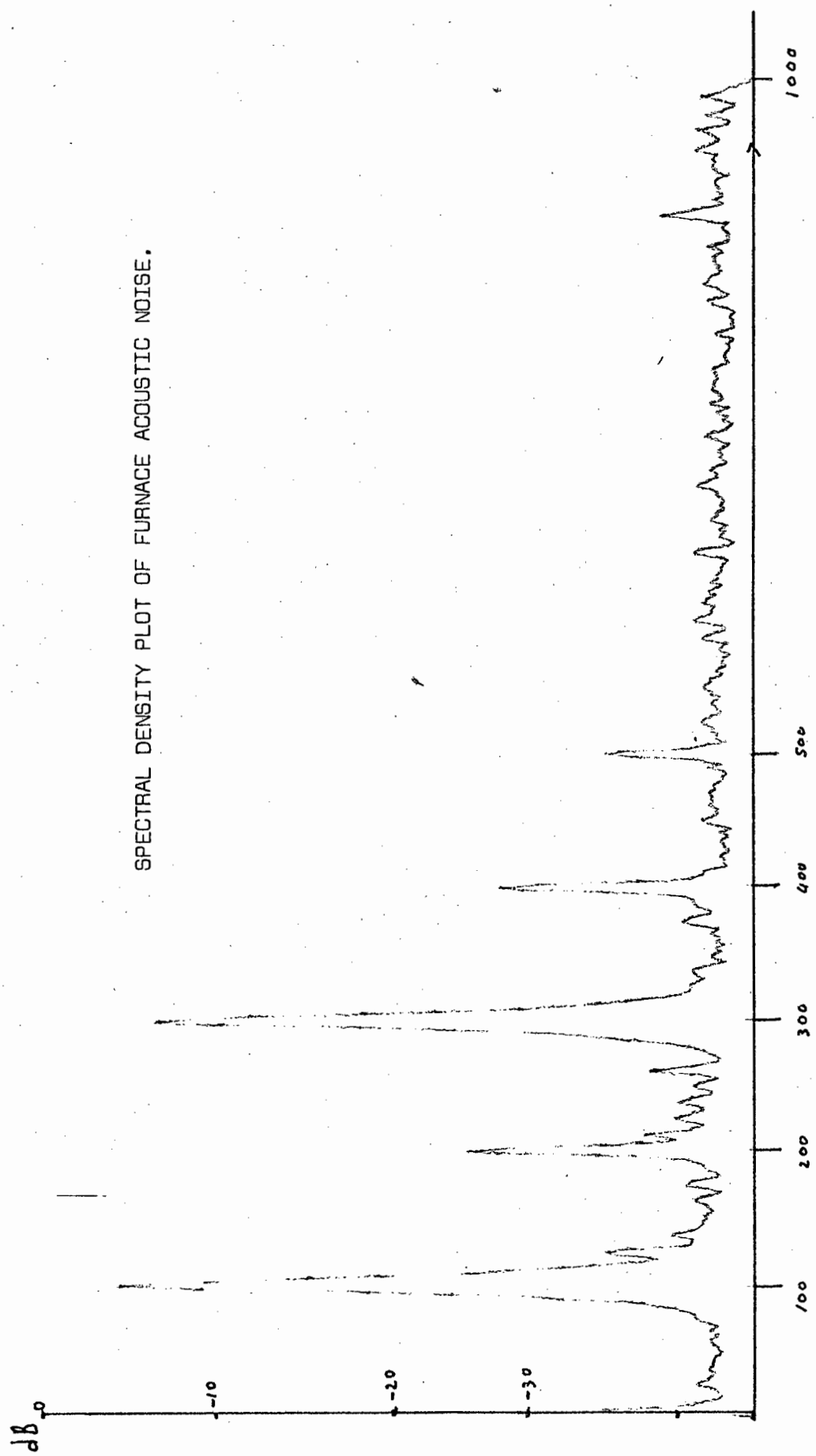
SPECTRAL DENSITY PLOT OF FURNACE ACOUSTIC NOISE.
dB
0
-10
-20
-30
100
200
300
400
500
1000
Frequency Hz

DIAGRAM 2.7

(c) TESTING FOR NORMALITY

The obvious method of testing data for normality is to measure the probability density function of the data and compare this to the theoretical normal distribution. In the case of where the probability density function is not easily available a non-parametric test called the Chisquare goodness-of-fit test can be applied. This test requires discrete samples of the data and is suited towards digital processing. This test which is described in section 4.6 of Ref. 2 was not required in the analysis.

2.2 CROSS RECORD ANALYSIS

After the individual records have been applied, cross analysis can be performed to detect similarities in a collection of data records.

The individual record analysis is necessary to validate the data for cross analysis. An example of meaningless analysis is the correlation of a single pulse with a record made up of many pulses with different pulse lengths. The cross correlation function has many peaks which are all significant, but, give no meaningful information.

The individual record analysis classifies the data and describes its characteristics. The characteristics of individual records are then visually compared before cross analysis. This gives an insight to the true meaning of the cross analysis.

The function used for cross analysis is the cross correlation

function which describes the dependence of the values of one set of data on the other. For two time history records x (t), y(t) the exact cross correlation function.

$$R_{xy}(\tau) = \lim_{T\to\infty} \frac{1}{T} \int_0^T x(t)\, y(t+\tau)\, dt$$

$R_{xy}(\tau)$ is always a real-valued function which may be positive or negative. $R_{xy}(\tau)$ need not have a maximum at $\tau = o$ nor is $R_{xy}(\tau)$ an even function as was true for the autocorrelation function.

The position of the cross correlation peak gives the delay time between the signals if the system is linear. The cross correlation function of two periodic signals with the same frequency, will be a periodic function having the same frequency. In this case there are many positive and negative peaks in the cross correlation function and the determination of relevant time delays, and whether the correlation is positive or negative is difficult.

The Fourier transform of the cross correlation function is another way of presenting the information contained in the cross correlation function. The function produced is called the cross spectral density plot which is very useful in detecting frequency components common to both signals.

ACOUSTIC NOISE ANALYSIS

The analysis follows a sequence which is most easily described by the flow chart in Diagram 3.1. The first data records to be analysed were the recordings of continuous noise. Recordings from Electrode 3 were chosen as its noise varied more than that of Electrode 2, and the top position was preferred due to the larger signal produced. The lower position opposite Electrode 2 was not considered. (See Appendix 10 describing the instrumentation check).

The recordings used were on tape 7 and had a 0 - 10 kHz bandwidth.

3.1 STATIONARITY OF THE ACOUSTIC NOISE SIGNAL

From inspection of the waveform it was decided that the noise as a whole can be considered as being stationary. This was confirmed by applying the Run Test to mean square values averaged over eight seconds.

As described earlier the value of the autocorrelation function at lag time zero is equal to the mean square value of the data. Using the SAI - 43A Correlation and Probability Analyzer, the autocorrelation function was calculated seventeen times, once every eight seconds, using 16 x 1024 summations per calculation. Their values at τ = o, being the mean square values, were

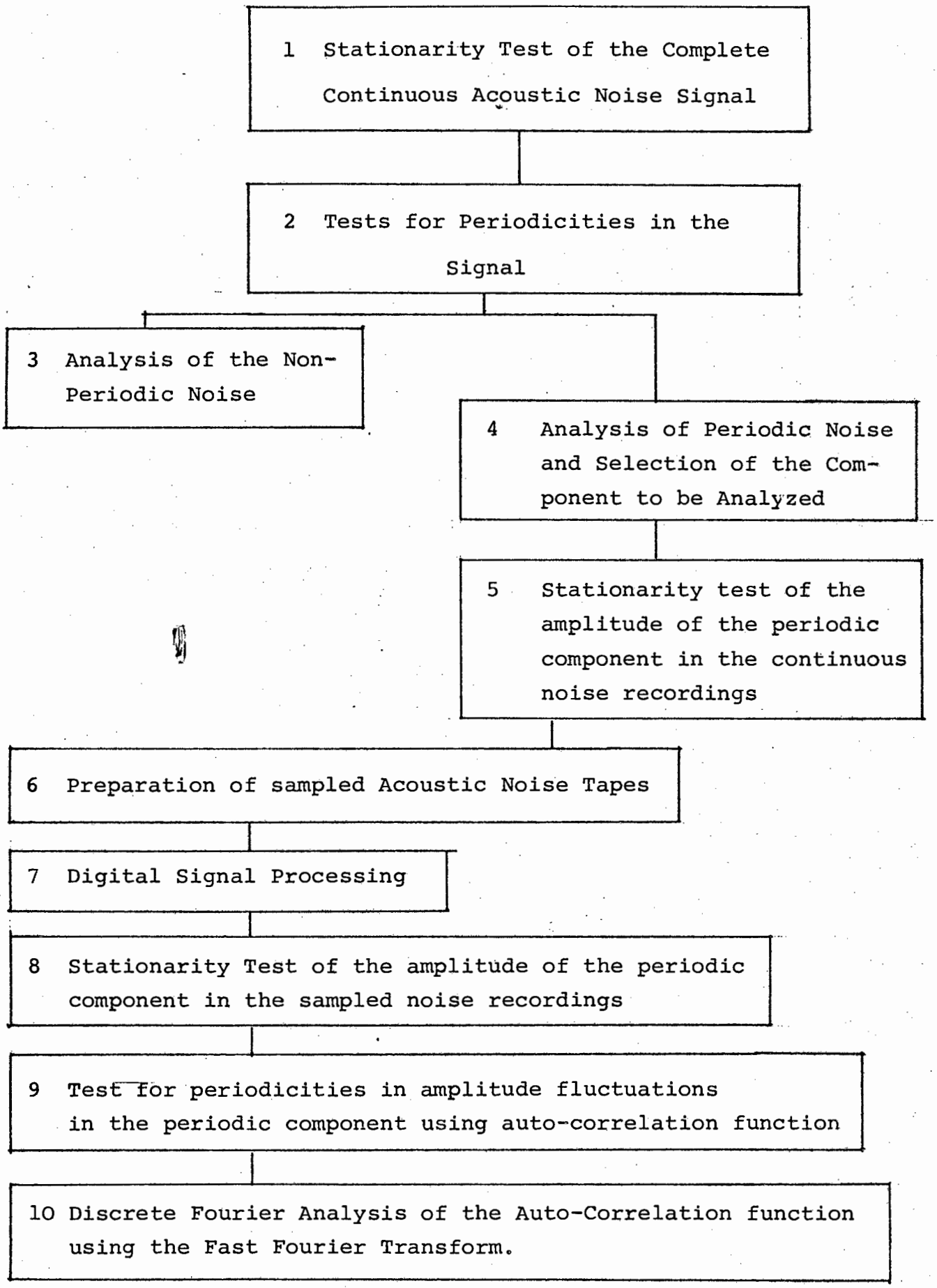
1 Stationarity Test of the Complete Continuous Acoustic Noise Signal
2 Tests for Periodicities in the Signal
3 Analysis of the Non-Periodic Noise
4 Analysis of Periodic Noise and Selection of the Component to be Analyzed
5 Stationarity test of the amplitude of the periodic component in the continuous noise recordings
6 Preparation of sampled Acoustic Noise Tapes
7 Digital Signal Processing
8 Stationarity Test of the amplitude of the periodic component in the sampled noise recordings
9 Test for periodicities in amplitude fluctuations in the periodic component using auto-correlation function
10 Discrete Fourier Analysis of the Auto-Correlation function using the Fast Fourier Transform.

DIAGRAM 3.1

displayed on a digital voltmeter and recorded. The Run Test (as described previously), was applied to this set of mean square values. The mean square values and median line are shown in diagram 3.2. The number of points = 17 and the number of runs = 8. For the hypothesis to be accepted at the $\alpha = 0.05$ level of significance the number of runs must be between 5 and 12. (From Table A.6). The hypothesis that the mean square value of the data is stationary was accepted at the $\alpha = 0.05$ significance level.

3.2 PERIODICITIES IN THE ACOUSTIC NOISE SIGNAL

The second step in analysis is the detection of periodicities in the noise. The equipment used was a Spectral Dynamics SD301C Real Time Analyzer with the SD302C ensemble averager (RTA), and a Honeywell Correlator and Probability Analyzer.

The frequency spectrum of the acoustic noise was investigated using the RTA. As the maximum frequency of the recording is 10 kHz and the RTA was set with a 0 - 10 kHz range. Diagram 3.3 shows the plot obtained using 512 ensembles. The majority of the noise lies between 0 and 1 kHz. Around 5 kHz the noise is 35 dB down on the noise in the 0 and 1 kHz band. The conclusion drawn was that significant noise is more likely to occur in the 0 - 1 kHz band. Diagram 3.4 shows a plot with a bandwidth of 1 kHz. This plot indicates periodic components which are harmonics of 100 Hz along with wide band random noise. 256 ensembles were used to produce the plot shown.

In order to distinguish the periodic components from what might

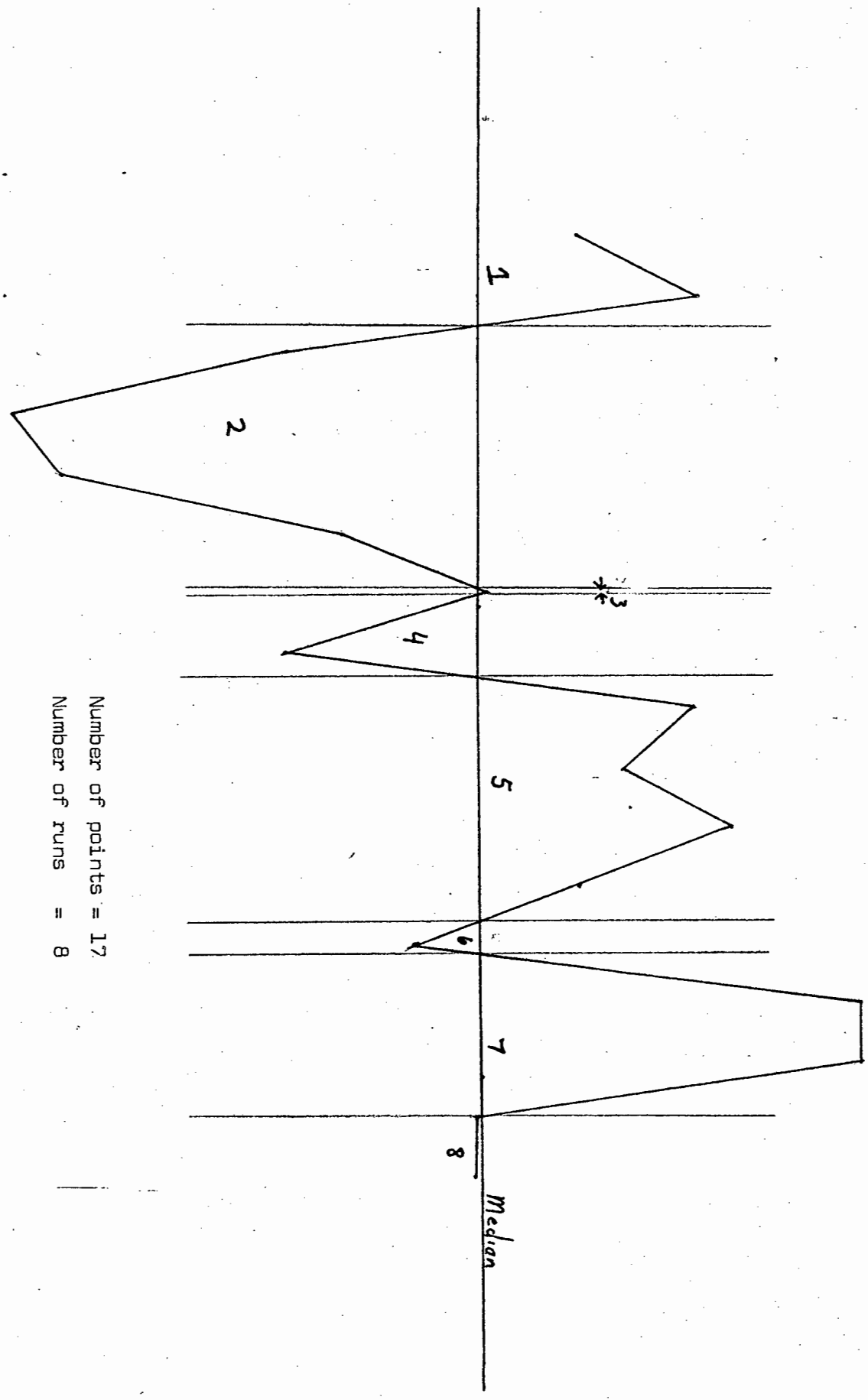
RUN TEST FOR STATIONARITY.
Number of points = 17
Number of runs = 8
1
2
3
4
5
6
7
8
Median

DIAGRAM 3.2

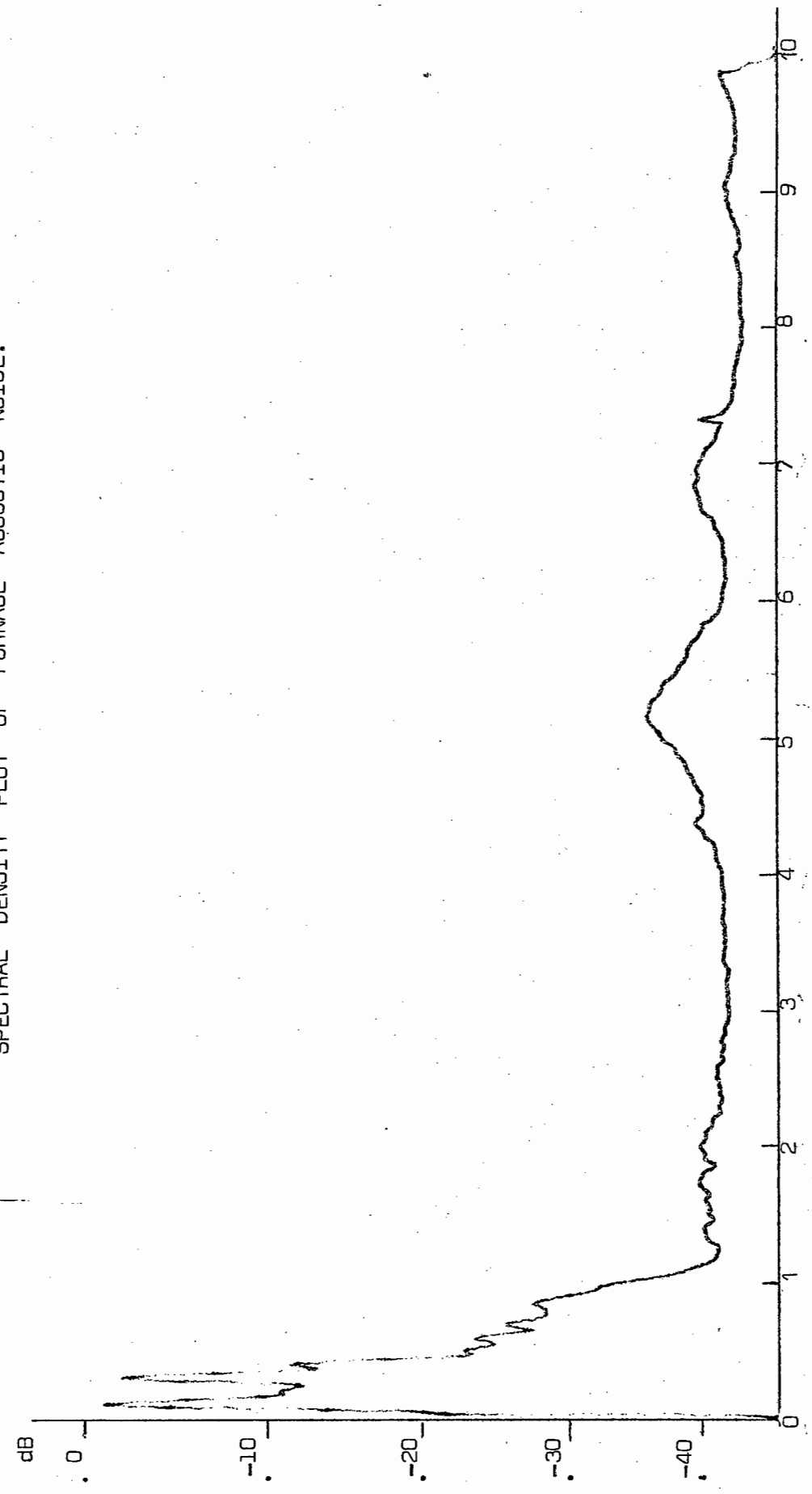
SPECTRAL DENSITY PLOT OF FURNACE ACOUSTIC NOISE.
dB
0
-10
-20
-30
-40
0
1
2
3
4
5
6
7
8
9
10
Frequency kHz

DIAGRAM 3.3

SPECTRAL DENSITY PLOT OF FURNACE ACOUSTIC NOISE.

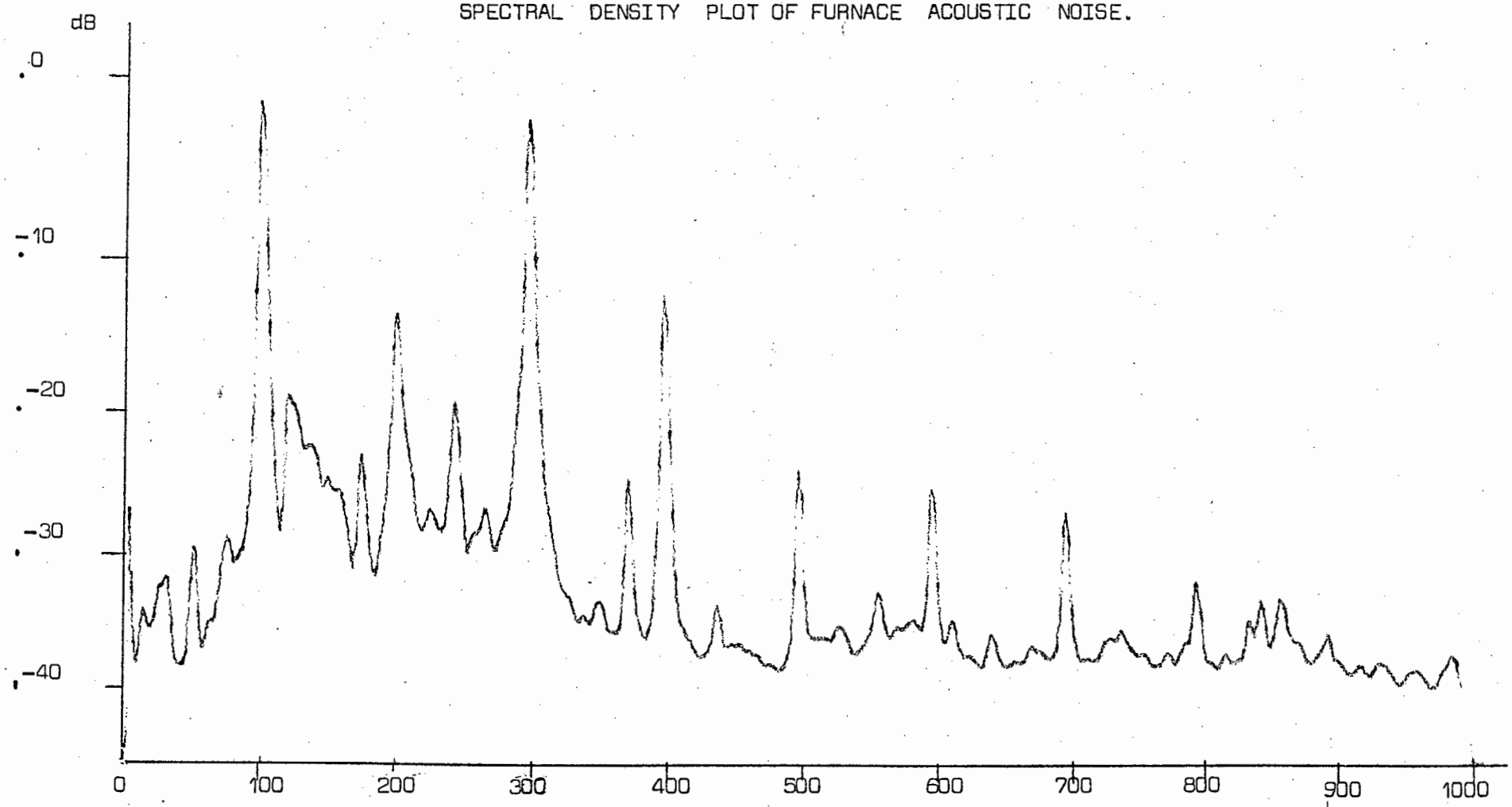

DIAGRAM 3.4

be narrow band random noise, the correlator and probability analyzer were used. The probability density function is shown in diagram 2.3. It conveys no meaningful information about periodicities as many periodic components are present. Diagram 3.5 shows the autocorrelation function of the acoustic noise. The correlator used a sampling interval of 0.2 m.sec. and 32 x 1024 summations were performed. The autocorrelation plot (autocorrelogram) confirms that more than one periodic component is present and that the components are harmonics. The Fourier transform of the autocorrelation function was performed and a plot of the periodic components without the random background noise was obtained (See Diagram 3.6).

This spectral density plot shows harmonics of 100 Hz. After 400 Hz the harmonics are -35 dB and were considered insignificant when compared to the tape recorder's 32 dB signal-to-noise ratio.

The Fourier transform of the autocorrelation function cannot be obtained by feeding the autocorrelation function into the RTA. The autocorrelation function is made up of 400 discrete d.c. levels in the correlator memory which appear sequentially at the correlators function output. The output is continuous with the 400 points being repeated every 40 m.sec. If this is fed into the RTA one gets a comb effect caused by the discontinuities between the end of the 50 m.sec. period and the beginning of the repetition of the period. This effect is similar to the window effect experienced when using the Fast Fourier Transform (FFT) in digital analysis which is explained more fully in a later section.

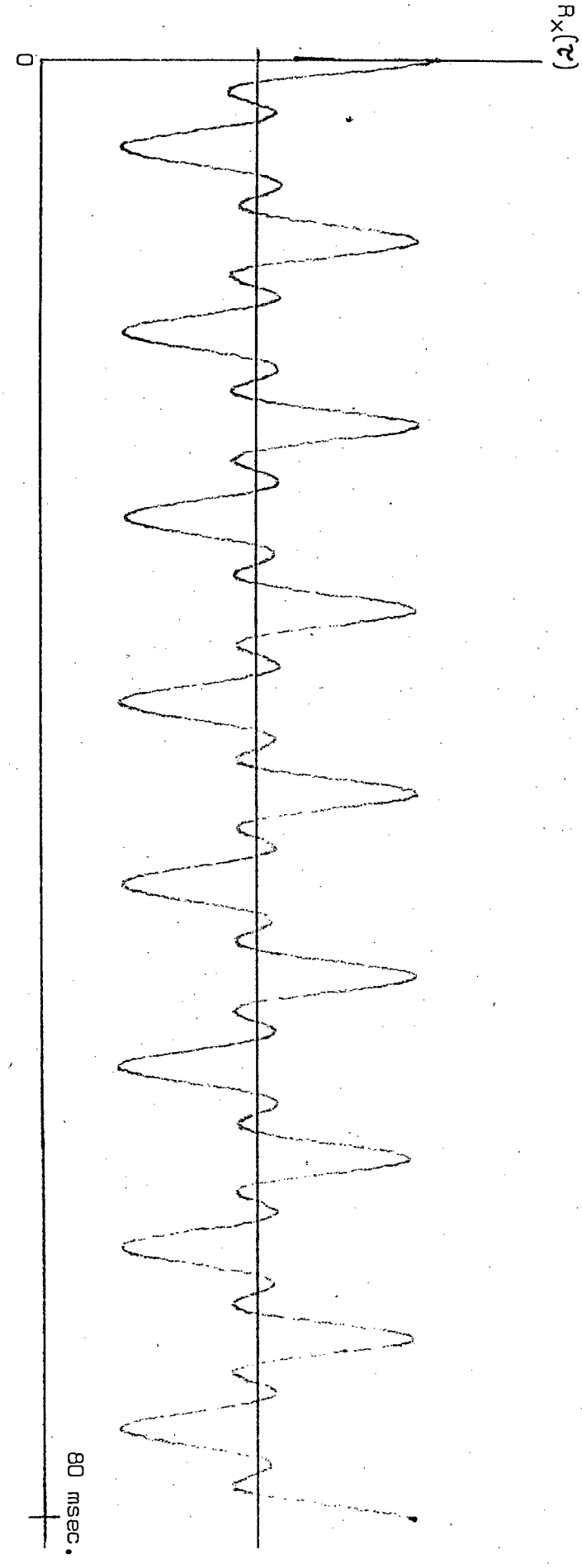

AUTOCORRELATION FUNCTION OF FURNACE ACOUSTIC NOISE.

DIAGRAM 3.5

dB
FREQUENCY SPECTRUM OF ACOUSTIC NOISE AUTOCORRELATION FUNCTION.
0
-10
-20
-30
-40
0
100
200
300
400
500
600
700
800
900
1000
Frequency Hertz

DIAGRAM 3.6

This effect can be avoided by choosing a sampling frequency which reduces the discontinuity between the beginning and end of the autocorrelation function. The RTA then sees the autocorrelation function as being continuous and the error is eliminated. In this case, as the autocorrelation is periodic, the sampling interval was chosen so that the autocorrelation (shown in Diagram 3.5) function appeared to be continuous. The effect of the slight discontinuity is visible in Diagram 3.6 as the small peaks occuring at fixed intervals between the harmonics.

The problem can also be overcome by 'clocking' the single block containing the autocorrelation function into the RTA memory.

The analyzer will then consider the autocorrelation function as the complete signal. Unfortunately, the RTA and correlator are not directly compatible in this way and an interface which was not available is required.

In both methods a multiplication factor must be calculated and the RTA bandwidth must be adjusted to take into account the difference between real time and the correlator output sweep time.

The detection of periodicities was applied to acoustic noise recorded at various times, and the conclusion drawn was that the acoustic noise has large periodic components, whose amplitudes vary in time. These components are harmonics of 100 Hz.

The acoustic signal can be described as random noise, as yet uninvestigated , and specific harmonics of 100 Hz. The sequence of analysis as described in the flow chart divides into two

paths. The analysis of the harmonics, and the analysis of the periodical components.

3.3 THE NON-PERIODIC NOISE

The periodic components, being 100 Hz and its harmonics dominate the acoustic noise signal.

The importance of the remaining noise in conveying useful information to the operator is considered below:

The autocorrelation function of a signal containing random noise and a periodic component can be made up of the autocorrelation functions of the periodic component and that of the random noise. Diagram 3.7 shows this. A single sinewave with a period T, has and autocorrelation function which is a cosine wave with period T.

As seen from Diagram 3.7b

$$R_{xx}(o) = R_{xx}(nT) \qquad \text{..... 3.3.1}$$

$$n = 0, 1, \ldots, \infty$$

For a non-periodic signal (Diagram 3.7a)

$$R_{xx}(o) = \frac{1}{N} \sum_{i=1}^{N} x_i^2 \qquad \text{..... 3.3.2}$$

and

$$R_{xx}(\infty) = \left(\frac{1}{N} \sum_{i=1}^{N} x_i \right)^2 \qquad \text{..... 3.3.3}$$

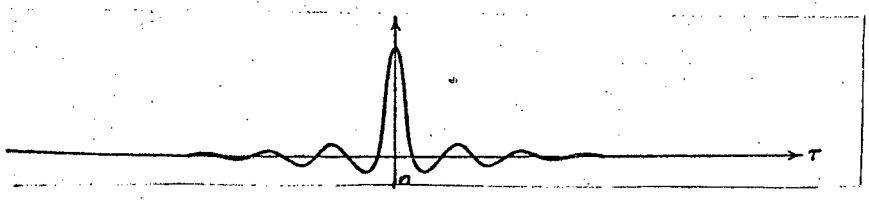

a

Random Noise

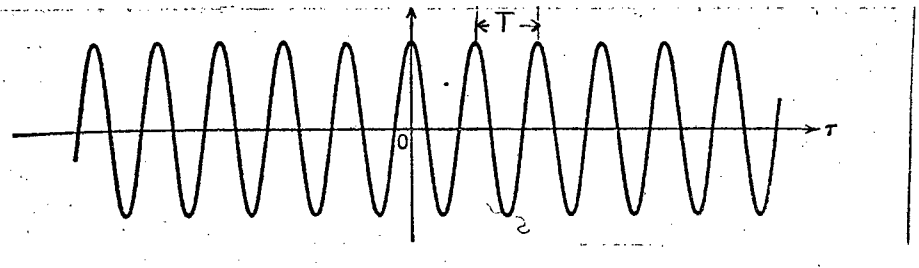

b

Periodic Component

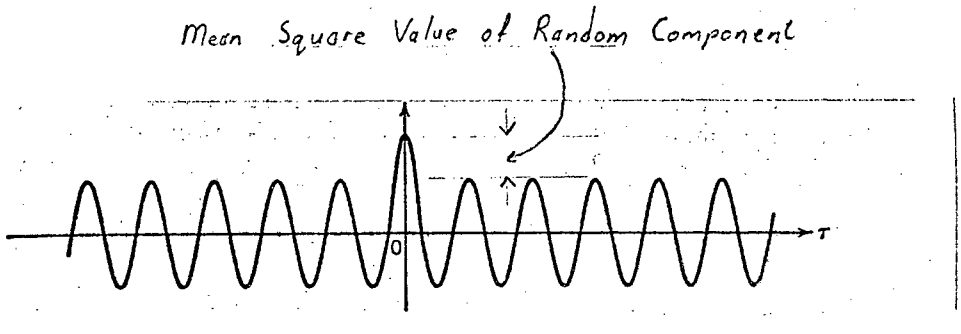

c

Random Noise plus Periodic Component

DIAGRAM 3.7

where x_i is the value of the ith sample of a total of N samples making up the data record. This is provided that N is large.

In this case the autocorrelation function gives the mean square value of the data and its mean value squared.

The mean square value of the random noise in a signal also containing a periodic component is

$$R_{xx}(o) - R_{xx}({}_nT) \quad \ldots\ldots\ldots 3.3.4$$

Where n is large and the mean value of the data can be arranged to be zero by a.c. coupling the signal (See Diagram 3.7).

If the signal contains a periodic component with its harmonics the same priciple applies provided that T is the period of the fundamental component.

In this way the contribution of the random noise to the total signal can be considered.

Diagram 3.8 shows the autocorrelation functions of the acoustic signals recorded from the positions near the top of the furnace opposite electrodes 2 and 3. It an be seen from the autocorrelograms that the signals contain periodicities. The autocorrelograms are plotted with $\tau = o$ at the centre and a time scale of $\pm$ 20 m.sec. The correlator was a.c. coupled to the signal to ensure a zero mean value. The random noise component of the autocorrelation function reaches its final value (the squared mean value = o) before 10 m.sec. of delay time. As

AUTOCORRELATION FUNCTION OF ACOUSTIC NOISE AT ELECTRODE 2.

AUTOCORRELATION FUNCTION OF ACOUSTIC NOISE AT ELECTRODE 3.

DIAGRAM 3.8

described aboye the mean square value of the periodic components can be separated from the mean square value of the total signal. From Diagram 3.8 it was calculated that for the signal from electrode 3 only 16% of the total mean square value was due to random noise and the signal from electrode 2 had a random noise contribution of 9% of the total mean square value.

In order to record the random noise signal without swamping the dynamic range of the tape recorder with the 100 Hz signal and its harmonics, a set of notch filters was used to condition the signal before recording. Diagrams 3.9 and 3.10 show the power spectra of the filtered signals collected opposite electrodes 2 and 3.

At the time of recording the exact structure of the acoustic signal was unknown and the set of notch filters removed 100, 150, 200, 300, 400, and 500 Hz components. These active filters were designed using Siliconix application note AN74-6 (Ref.6). The design parameters and characteristic of the 50 Hz Notch is shown in Appendix 5. The numerous filters tended to attenuate the interharmonic noise but as seen in Diagrams 3.3 the majority of the random noise is wide band with increasing amplitude in the 0 - 1250 Hz band. Diagram 3.4 shows the unfiltered acoustic signal which shows the random noise at least 30 dB lower that the 200 Hz component.

The full unfiltered signal is approximately 3 mV while the filtered signal is 200 μV, both referred to the accelerometer output. This indicates that the filtered signal is 23 dB down on the total signal.

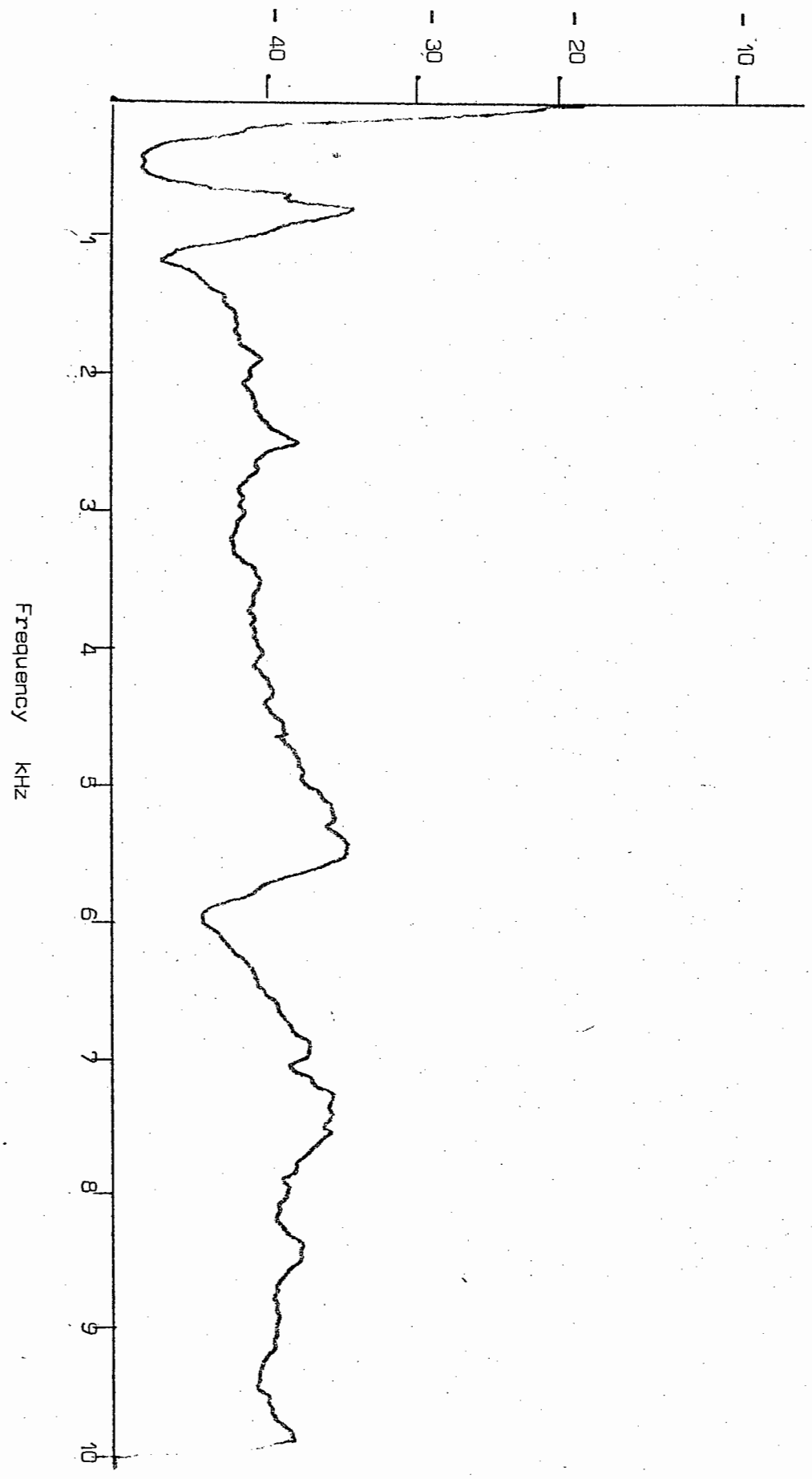

FREQUENCY SPECTRUM OF FILTERED ACOUSTIC NOISE SIGNAL FROM ELECTRODE 2.

DIAGRAM 3.9

FREQUENCY SPECTRUM OF FILTERED ACOUSTIC NOISE SIGNAL FROM ELECTRODE 3.

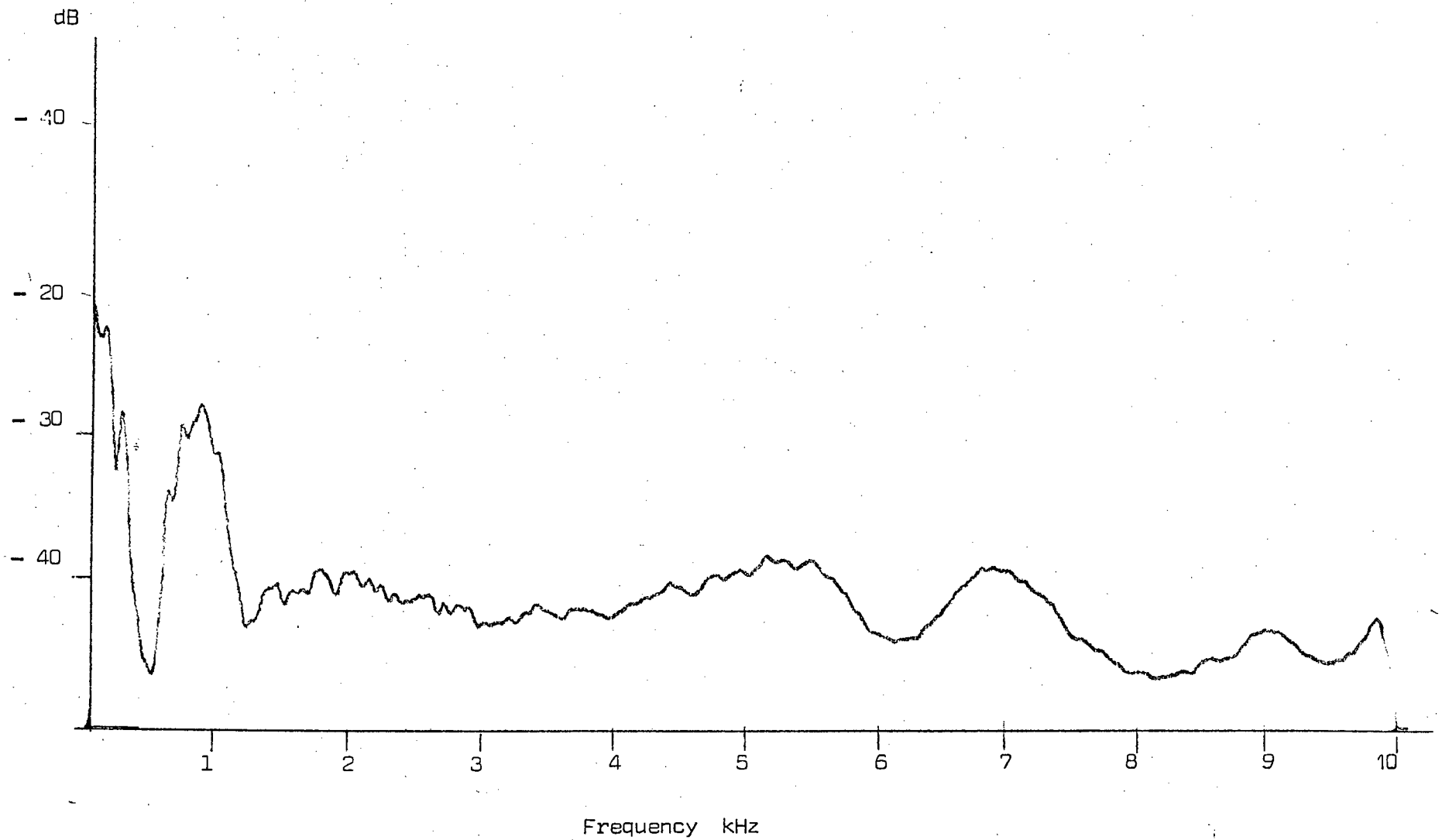

DIAGRAM 3.10

The above considerations take into account the level of the random component compared to the total signal in both the time and frequency domain. This project originated with the ideas that the acoustic noise provided information to the operators via their ears and via instrumentation. To investigate fully the significance of the non-periodic noise the hearing ability of the ear must also be considered.

The instrumentation for gathering the acoustic noise signals was designed to follow the characteristic of the ear as far as possible. The limit of the instrumentation was the dynamic range of the tape recorder being approximately 30 dB, while the ear can detect a pure tone 60 dB down in noise. The use of pre-filtering diminished this limitation and allowed small signals to be recorded. A feature of the human ear not found in instrumentation is the phenomenon of 'Masking'.

In this case the background furnace noise is masked by loud pure tones. (Masking by pure tones, as described more fully in Appendix 11, cause the threshold of audibility to be raised for noise at frequencies higher than the masking tone. The curves of masking of a pure tone by another tone are shown and explained in Appendix 11).

The sound level in the vicinity of the operating room measured with a sound level meter using the 'A' scale was of the order of 85 - 90 dB. From the mean square estimates of the random noise as compared with the 100 Hz signal and its harmonics, and observing power spectrum of the total signal it was assumed that a large amount of the noise was made up of pure tones.

From the curves shown in Appendix 11 it can be seen that pure tones with large amplitudes will raise the threshold of audibility for tones of higher frequencies.

In the case of furnace noise the large 100, 200 and 300 Hz components could cause the threshold of audibility to be raised by 20 to 70 dB for frequencies higher than 100 Hz. The curves shown in Appendix 11 refer to masking of pure tones by pure tones, but will largely affect the masking of higher frequencies by pure tones.

On taking into account the low noise levels of the non-periodic noise and the masking effect by the pure tones on higher frequencies, it was decided that information on furnace operation detected by the operators was more likely to be carried by the periodic components.

The random noise in the 1 - 10 kHz band could be caused by bubbling and movement in the furnace, but it is very unlikely that changes in these random components could be heard by the operators.

This decision was also influenced by the only other work in this field done by Higgs (Ref. 1) and his team.

Higgs in his work 'Noise Statistics in an Electric Arc Furnace' used the same type of instrumentation as was used in this project. His intrumentation differed in that he fed his signals directly from a furnace wall mounted accelerometer into an on-plant processing computer. He used the computer via digital filtering to

remove his periodic components being 60 Hz and its harmonics and conducted analysis on the remaining noise in the frequency band 500 - 1250 Hz. His work was aimed at creating signatures of furnace noise for different operating stages occurring in a scrap furnace. He concluded that his furnace generated noise in a random fashion on the decibel scale, and that his signatures changed with furnace lining quality and/or thickness.

3.4 THE PERIODIC NOISE

As mentioned previously the only other work done on the analysis of noise in arc furnaces is by Higgs (Ref. 1), who developed signatures of the random noise occurring between the harmonics of 60 Hz. The following analysis of the periodic noise follows the opposite approach.

The 100 Hz component and its harmonics are related to the electrical power driving the furnace. This was easily proved by investigating the noise at periods when the furnace was briefly switched off.

The submerged arc furnaces has no set operating cycles apart from four-hourly metal tappings. The process is continuous and is controlled by lowering and raising the electrodes and controlling the power supplied to the furnace.

As the operating parameters are linked to the power source of the furnace and the same power produces the 100 Hz component and its harmonics it was decided to pursue the analysis of the periodic components.

The difference between this approach and that of Higgs (Ref. 1) is that Higgs had set stages in his process which caused random noise. He formed noise signatures of initial arcing, pooling and other characteristics which occur in the process. In considering the periodic components in the noise signal one is investigating noise related to electrical parameters which in themselves give indications of "good" or "bad" operation of the furnace.

"Good" and "bad" operation of the furnace is difficult to define, but furnace operation resulting in a large power input to the furnace normally gives good metal yields and erratic operation with difficulties in power input normally reduces the metal yield.

An untested hypothesis on the cause of the 100 Hz signal and its harmonics in the acoustic noise is described in Appendix 8.

The periodic noise consists of diminishing harmonics of 100 Hz. The levels of the 100, 200 and 300 Hz signals in the full acoustic signal collected from the transducer mounted at the top position opposite electrodes 2 and 3 were investigated. Harmonics higher than 300 Hz tended to be frequently at a very low level and were not investigated. Then analysis was done using the Real Time Analyzer (RTA) in the manual mode, as a narrow band pass filter with an output rectifier, and feeding the resultant time varying d.c. signal to a chart recorder.

This initial 'pre-analysis' indicated that the level of the 300 Hz noise had more variations than the other two harmonics.

Another 'pre-analysis' technique was performed by plotting the level of the harmonics with the hoist position of the nearby electrodes against time. The only visible correlation between the parameters occurred for data from both electrodes when the level of the 300 Hz signal and the hoist positions were compared. These plots are shown in Diagram 3.11 and 3.12.

From initial pre-analysis as described above it was found that the 100 Hz and the 200 Hz components had few variations and had no visible correlations with hoist position. For these reasons it was decided to concentrate analysis on the amplitude of the 300 Hz component.

3.5 STATIONARITY OF THE AMPLITUDE OF THE 300 Hz COMPONENT INVESTIGATED OVER A 3 HOUR PERIOD

The level of the 300 Hz signal varies with time as established previously. The longest continuous recordings of furnace noise covered a time period of just under three hours.

From observation of the rectified 300 Hz signal plotted over 3 hours it was suspected that the signal was not stationary over this period. The plot indicated that the record length included the lowest frequency component in the signal, but this was not conclusive.

It was decided to apply the 'Run Test' to test the stationarity

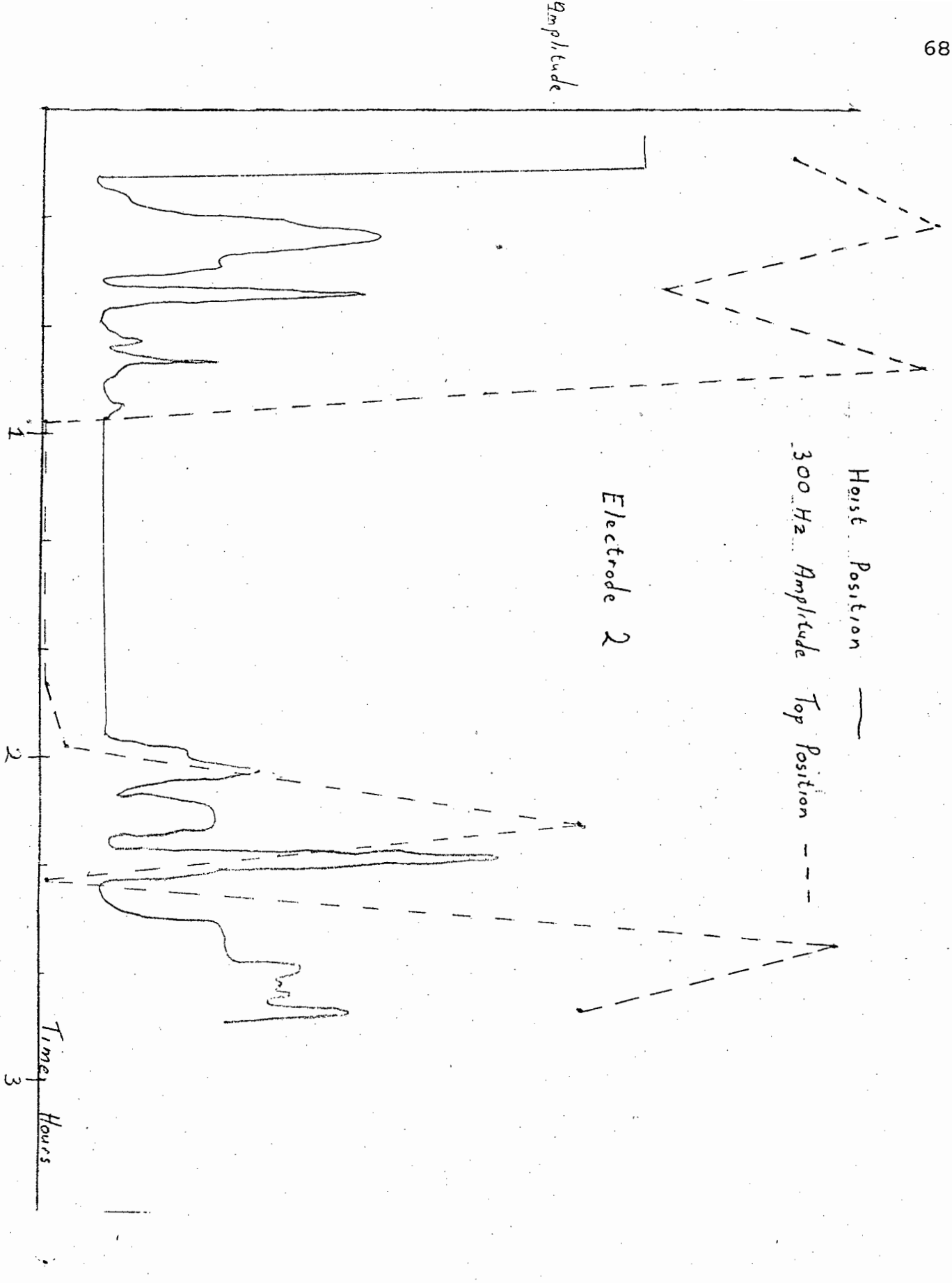
Amplitude
Hoist Position ——
300 Hz Amplitude Top Position - - -
Electrode 2
1
2
3
Time Hours

DIAGRAM 3.11

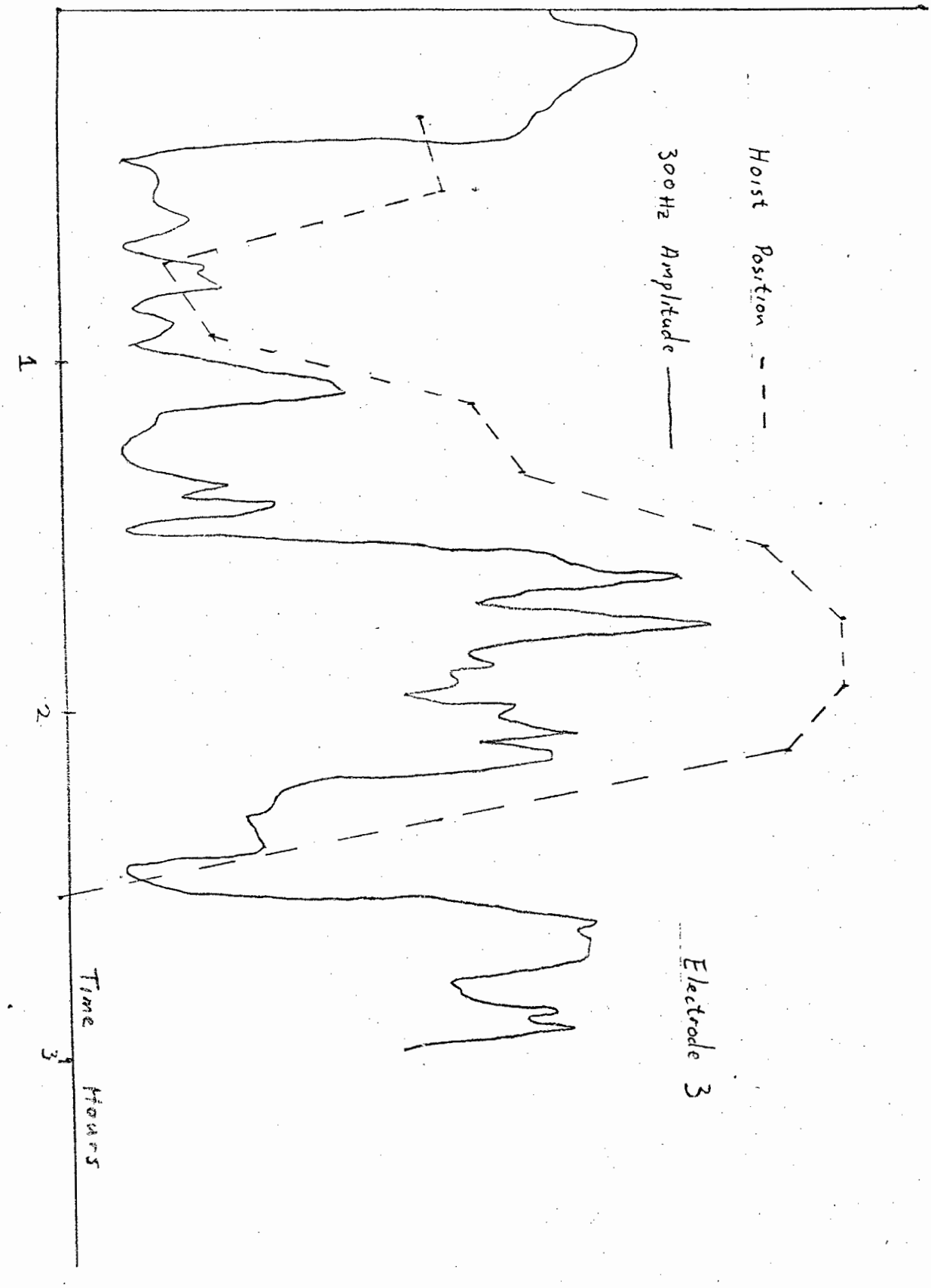

DIAGRAM 3.12

of the mean square. The application and theory of this test is described previously in Chapter 2.

The test requires that the data record be divided into equal sections and the mean square value be calculated for each section.

This was accomplished by calculating the autocorrelation function for each section and using the expression:

$$R_{xx}(o) = \psi^2 = \text{mean square value} \quad \ldots 3.5.1$$

The sampling rate of the Honeywell correlator was set to 1 m.sec. and 128 x 1024 summations were performed. This setting caused an autocorrelation function to be calculated every 66 seconds.

The data came from a three hour continuous tape of furnace noise recording, and the noise data used was collected opposite electrode three near the top of the furnace wall.

The tape was recorded at 3¾"/second but was played back for analysis at 32"/second giving a frequency multiplication factor of 8 (and a tape playing time of 22 minutes) The RTA was used (in the manual mode) as a 2400 Hz band pass filter and rectifier. The rectified time varying d.c. signal was connected to the input of the correlator.

The value of BIN o in the correlator ($R_{xx}(o)$) in this case) was noted after the autocorrelation function for each section of the data was completed. The noted values formed a sequence of

20 mean square values which were tested using the Run Test. The Run Test plot is shown in Diagram 3.13. The number of points = 20 and the number of runs = 4. From Table A.6 in Chapter 2 the number of runs required to accept the hypothesis of stationarity of the mean square at the $\alpha = 0.05$ significance level must lie between 6 and 15. At this significance level the hypothesis of stationarity of the mean square of the level of the 300 Hz signal, over a period of 3 hours is rejected.

The above test for stationarity of the mean square of the level of the 300 Hz component was performed on a data record of only 3 hours. From earlier considerations on record lengths influencing stationarity tests, it is possible that the mean square value of the level of the 300 Hz component may be stationary if longer data records are investigated.

3.6 PREPARATION OF SAMPLED DATA TAPES

In order to investigate the level of the 300 Hz signal over long time spans sampled data was used. As explained in earlier sections on data collection, the tape recorder was operated by an on-off timer which switched on the tape recorder for 44 seconds every ten minutes. The tape recorder bandwidth was 0 - 1250 Hz. The longest uninterrupted span of sampled data covered 46 hours 52 minutes and was recorded on Tape 9.

Signal processing techniques can be applied to data using different forms of equipment. Diagram 3.14 shows the different equipment options. In the analysis so far the processing

RUN TEST FOR STATIONARITY.

Points = 20
Runs = 4

DIAGRAM 3.13

equipment has been by analog devices. The analysis instruments being the 'Honeywell SAI - 43 Correlator and Probability Analyzer' and the 'Spectram Dynamics Real Time Analyzer and Ensemble Averager', are both special purpose instruments requiring analog inputs.

The sampled data records are not in a form where they can be analyzed by the above special purpose instruments. These instruments expect continuous analog inputs and will not operate on sampled analog data records.

From the analysis so far the indications are that the level of the 300 Hz component varies very slowly in time. Neither of the above instruments can analyse very low frequency variations without preparation of the data.

Preparation of data is a procedure common to signal processing, where data is converted to a format acceptable by the analysis equipment. It was not required in the analysis of the continuous noise signal as the data was already in a format acceptable to the analog analysis equipment.

The sampled data records require preparation before analysis by either digital or analog equipment. The preparation required to format the data for analog analysis is complex and the resultant data records would have frequencies out of the range of the analog equipment. For these reasons the analysis equipment used for analysing the sampled tapes was a digital VARIAN 620 L minicomputer with a 12 bit Analog to Digital converter.

3.7 DIGITAL SIGNAL PROCESSING

A digital computer is a versatile analysis tool. The computer can perform the function of dedicated analog instruments when programmed with the required softwave. Digital analysis is not as straightforward as Analog analysis and can create errors which are not found in Analog equipment.

The Analog-to-Digital converter samples a continuous analog signal and forms a data record consisting of a sequence of numbers representing the value of the analog signal at the instant of sampling. This digitizing procedure can cause the following types of errors.

(a) The sampling theorem requires that for full digital representation of an analog signal the digital sampling frequency must be at least twice the frequency of the highest component present in the signal. If the sampling frequency is too low, confusion of the low and high frequency components occurs. This causes an error not found in analog signal processing called the aliasing or folding error. This error is avoided by low pass filtering the analog signal and selecting a sampling frequency greater than twice the bandwidth filter.

(b) The sampled data is quantized to a discrete number of levels. The accuracy of the quantization depends on the number of quantization levels. For ideal conversion the quantizing error will have a uniform probability distribution with a standard deviation of $0.29\,\Delta x$ where Δx is the quantizing increment (Ref. 2 Section

7.3.1). The VARIAN A to D converter is a 12 bit converter having 4096 levels. The standard deviation $= 0.29\Delta x$ is the rms value of the quantization error, which can be considered as rms noise on desired signals. This gives a peak signal to rms noise ratio of:

$$20 \log \left(\frac{4096\,\Delta x}{0.29\,\Delta x} \right) = 83 \text{ dB}$$

With this A to D converter quantization error can be ignored provided the analog signal occupies a reasonable portion of the A to D's input range.

(c) Other infrequent errors which can occur are 'Jitter', arising from the fact that the time interval between samples can vary slightly in some random manner, and 'Aperture error', due to the sample being taken over a finite period of time rather than instantaneously. These errors can be eliminated by sampling faster than is necessary and averaging over a few points.

The actual A to D conversion was done in the following manner:

The tape recorder was run at 32"/sec giving a frequency multiplication of x8. This reduced the amount of computer time required The 300 Hz component was removed from the total signal and rectified to produce a time varying d.c. level proportional to the 300 Hz component. This was done by HP model 302 A wave analyzer set to 2400 Hz. The wave analyzer has an out-of-band rejection of -80 dB at $\pm$ 70 Hz bandwidth.

The recorder output was used to obtain the rectified filtered signal.

The d.c. signal which was adjusted to vary between 0 - 10 volts, was connected to one of the channels of the A to D converter. The sampling frequency of the A to D converter was set at 8 Hz, giving a sampling rate of 1 Hz when taking into account the x8 speed-up of the tape recorder.

The language used for the digital signal processing was BASIC. This language is an interpreter language which, although being slow, is suitable for varying analysis techniques necessitating frequent program changes. The maximum sampling rate of the A to D converter when using BASIC is 5 kHz, which is quite adequate.

The BASIC subroutine ADC1, X, Y initializes A to D conversion, the parameters X and Y determine the analog input channel number and the number of blocks of digital data required. The digital data blocks are magnetic tape blocks each containing 576 data values. Using this subroutine analog tapes were digitized and the digital data was stored on magnetic tape.

As the analog signals digitized were actually sampled analog signals made up of 44 second sections, the digital data was split into these sections. From the tape recorder specifications (Apendix 4) it was observed that the tape start time and stop time took a total of 5 seconds. The data on the tape during these five seconds is not of value and was discarded by dividing the digitized data record into 39 element intervals, and discarding the five elements between each section.

The tape recorder recorded a switch-on spike when switched on,

which was easily visible in the digital data and indicated the beginning and end of each section.

A pre-processing program was written which collected the 39 elements in each section, and outputted their mean value to the teletype in the following format:

N Data XXXXX

where N is the line number and XXXXX is the data value.

The teletype was selected as the output device as BASIC language on the VARIAN, can only write data to magnetic tape via the A to D converter and data can only be read from the teletype or magnetic tape.

When outputting mean values, the teletype punch was switched on and a paper tape data record, in the format necessary for use in a BASIC program was created by the pre-processing program.

The data values contained 'line numbers' and were acceptable as data lines in further analysis programs. This involved pre-processing was done to save time, as the procedure of reading data from magnetic tape and calculating mean values before applying analysis techniques took up a significant amount of processing time. In the case of many records on the same magnetic tape, the access time is even larger due to the computer having to read through the tape to find the required record.

3.8 LONG TERM STATIONARITY OF THE AMPLITUDE OF THE 300 Hz COMPONENT

The data record whose preparation is described above, consisted of 250 averaged samples of the amplitude of the 300 Hz component in the acoustic noise. The sampling rate is once per 10.75 minutes. Diagram 3.15 is a plot of the level of the 300 Hz component against time for a period of approximately 47 hours. This plot indicates that visually the data is stationary and that the failure of the previous test for stationarity of the mean square amplitude of the 300 Hz component could be due to an insufficient record length.

A computer program was written which calculated 12 mean square values each value calculated from 20 data points. These values were applied to the Run Test to test for the stationarity of the mean square. The plot of mean square values along with the median value was plotted on the computers Visual Display Unit (VDU) and is reproduced in Diagram 3.16.

As seen from Diagram 3.16 the number of runs = 6 for the 12 point plot. From Table A.6 (Chapter 2) the stationarity of the mean square of the data is accepted at the $\alpha = 0.05$ significance level.

3.9 INVESTIGATION FOR PERIODICITIES

The data used in this investigation is the 250 element data record used in the stationarity test. This data record represents a very slowly varying signal and covers a time period of 44¾ hours.

EQUIPMENT OPTIONS FOR DATA ANALYSIS.

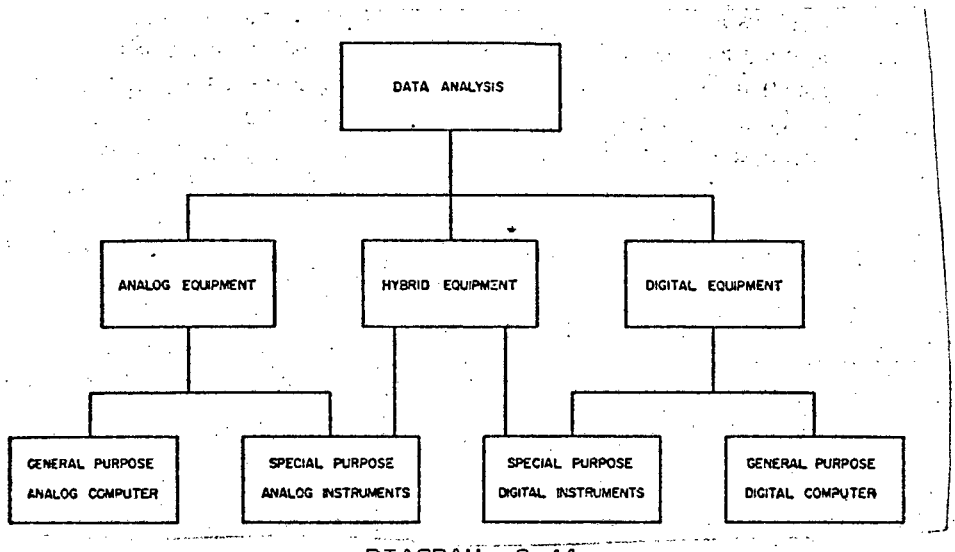

DIAGRAM 3.14

Amplitude fluctuations of 300 Hz component of the Acoustic Noise Signal over a period of 47 hours.

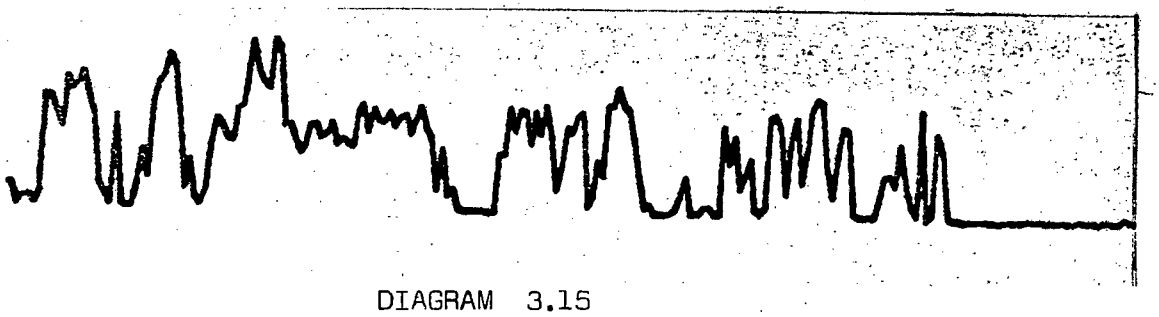

DIAGRAM 3.15

Run Test for stationarity of the mean square of the amplitude of the 300 Hz component in the acoustic noise over a period of 47 hours.

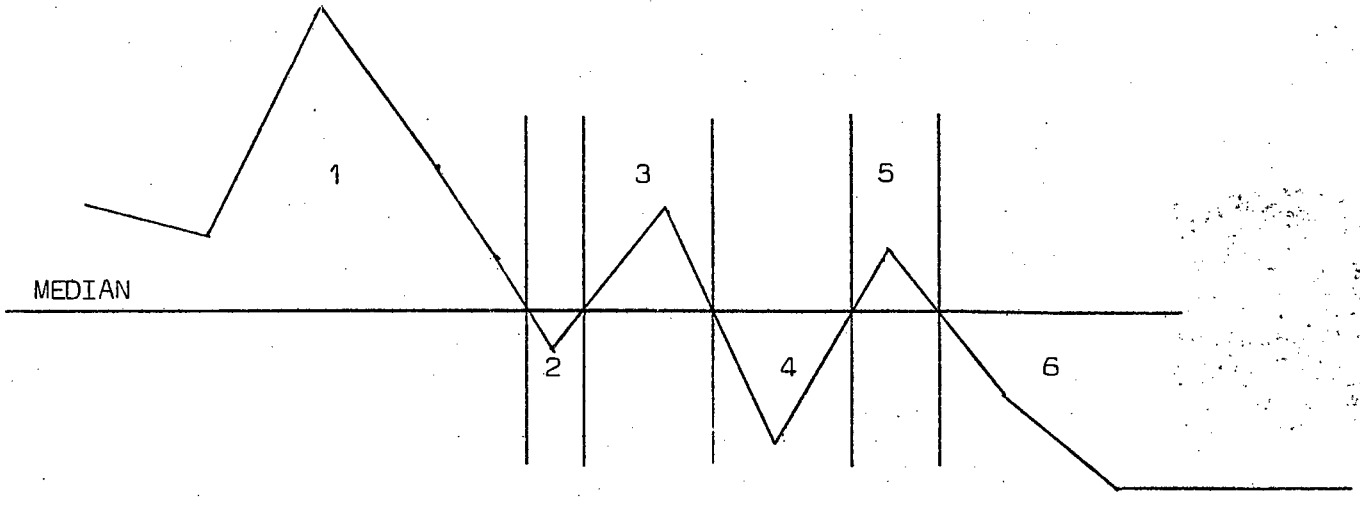

POINTS = 12

RUNS = 6

DIAGRAM 3.16

The sample autocorrelation function was used to investigate the data record for periodicities. Using digital signal processing, only estimates of the true autocorrelation function can be calculated.

The sample autocorrelation function for a data record $\{x_n\}$ where n = 1,2 ..... , N. as given by Ref. 2 is:

$$R_x(rh) = \frac{1}{N-r} \sum_{n=1}^{N-r} x_n \; x_{n+r} \; .... \quad 3.9.1$$

$$r = 0, 1, 2, \; ..... \; m.$$

where r is the lag number, m is the maximum lag number and h is the sampling interval of the data.

Another definition valid for $m \ll N$ is given by (Ref.2).

$$R_x(rh) = \frac{1}{N} \sum_{n=1}^{N-r} x_n \; x_{n+r} \; ..... \quad 3.9.2$$

$$r = 0, 1, ... , \; m.$$

The expression used in the analysis was

$$R_x(rh) = \frac{2}{N} \sum_{n=1}^{N/2} x_n \; x_{n+r} \; ..... \quad 3.9.3$$

where $r = 0, 1, 2, \; ..... \; N/2$

which is a sample autocorrelation valid for $r \leq \frac{N}{2}$

The autocorrelation function consisted of N/2 points calculated from N data points. The variance is the same for each point unlike the function generated by expression 3.9.1 where the

variance of the individual points vary with r. Expression 3.9.2 was not suitable as it is only valid for $m \ll N$.

The BASIC program written removed the mean value from the data record and using expression 3.9.3, calculated and plotted the sample autocorrelation function. The 250 element data record has the 125 point autocorrelation function shown in Diagram 3.17. The sample autocorrelation function which covers 22 hours 21 minutes does not approach zero for large r.

This is due to an error E in the calculated mean value which is an estimate of the true mean value, in which case the autocorrelation function should approach E^2 for large r.

The function in this case does not approach any set value but varies about zero. This is indicative of periodic components in the signal, which cause periodicities in the autocorrelation function. The periodicities in the autocorrelation function are visually difficult to identify due to the functions' limited lag time, and resolution.

The periodicites can be identified by calculating the Fourier Transform of the sampled autocorrelation function to give the sampled spectral density function of the original data record. As explained in the section describing signal processing techniques, the Fourier transform of the autocorrelation function excludes the random noise which is present in the Fourier transform of the original data record. The Fourier transform provides no new information, but presents the information in the autocorrelation function in a different form.

AUTOCORRELOGRAM OF THE AMPLITUDE OF THE 300 Hz COMPONENT IN THE ACOUSTIC NOISE.

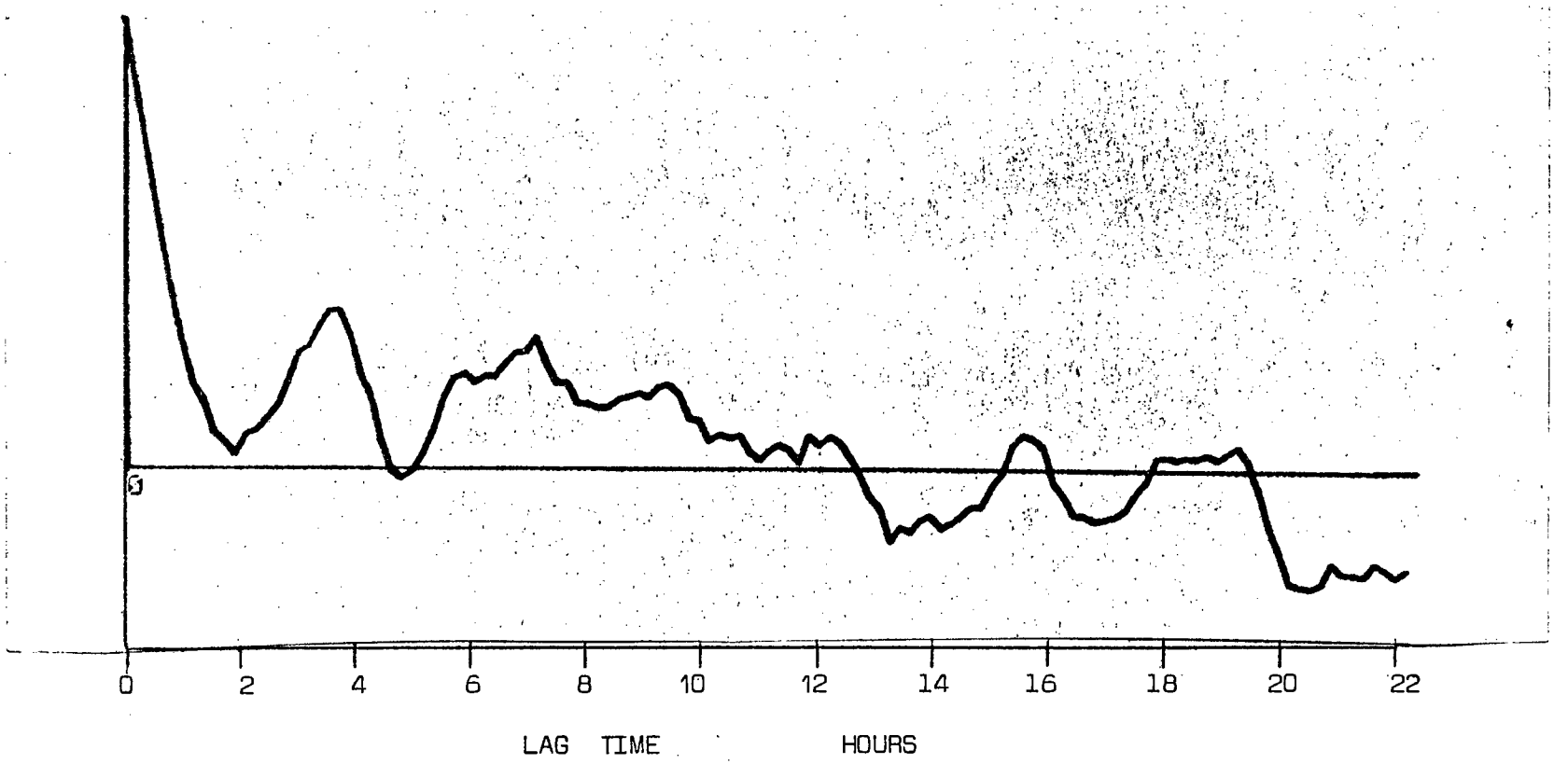

DIAGRAM 3.17

3.10 THE DISCRETE FOURIER TRANSFORM

The digital Fourier transform called the Discrete Fourier Transform, is calculated by a Fast Fourier Transform Routine. There are many Fast Fourier Transform routines available in different computer languages and most of these are simple to implement.

The function produced is an estimate of the spectral density function and can contain significant erroneous information. Appendix 12 compares the Discrete Fourier Transform with the Continuous Fourier Transform and arrives at the following conditions for equivalence of the two transforms.

(a) The time domain function h(t) to be transformed must be periodic.

(b) h(t) must be band limited and the sampling rate must be at least twice the largest frequency component of h(t). This prevents aliasing errors.

(c) The truncation function x(t) being the data record period must satisfy

$$x(t) = nh(t) \qquad n = 1, 2, 3 \ldots\ldots$$

Condition C is not satisfied in general, causing errors in the spectral density plot. The most serious error being 'leakage'.

Leakage, as explained more fully in Appendix 12, is the interference between the side lobes of the sinx/x functions. The sinx/x function (Diagram 3.18) is the Fourier Transform of the truncation

DIAGRAM 3.18

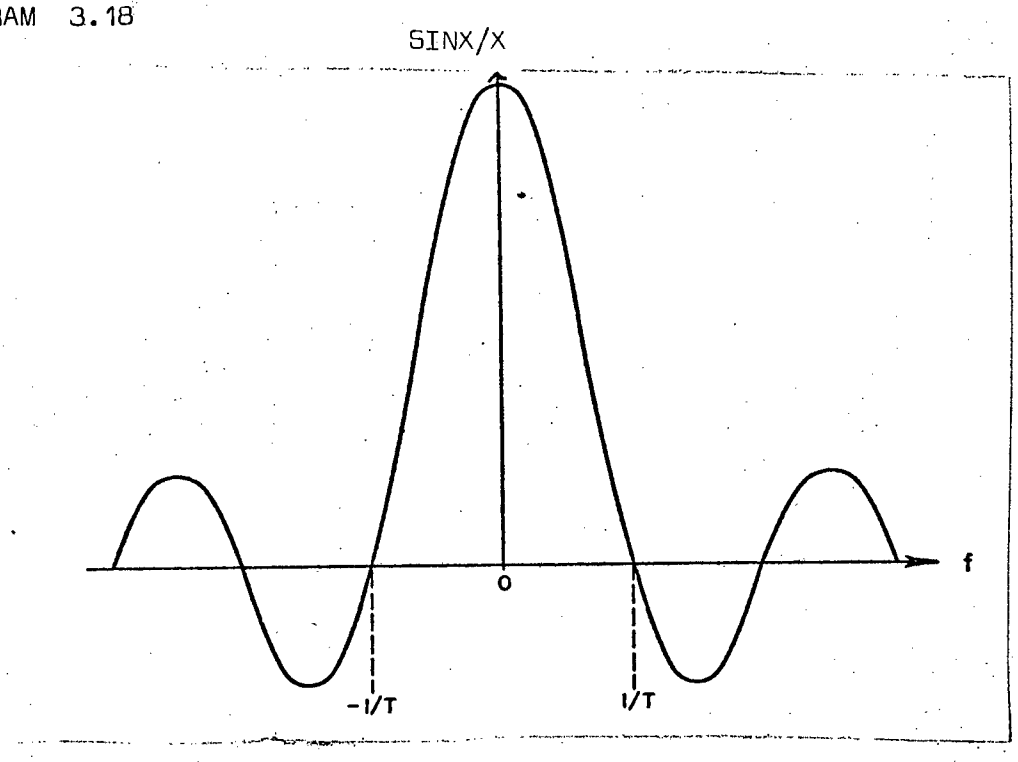

DIAGRAM 3.19

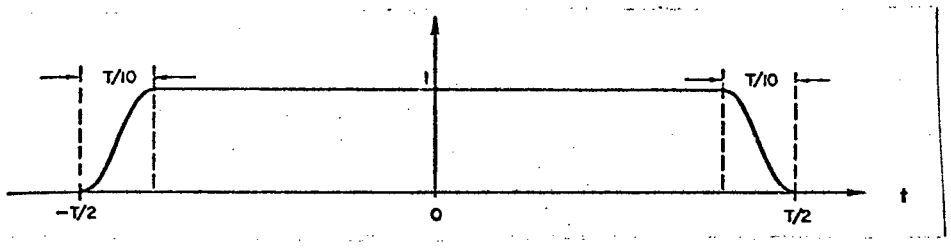

DIAGRAM 3.20

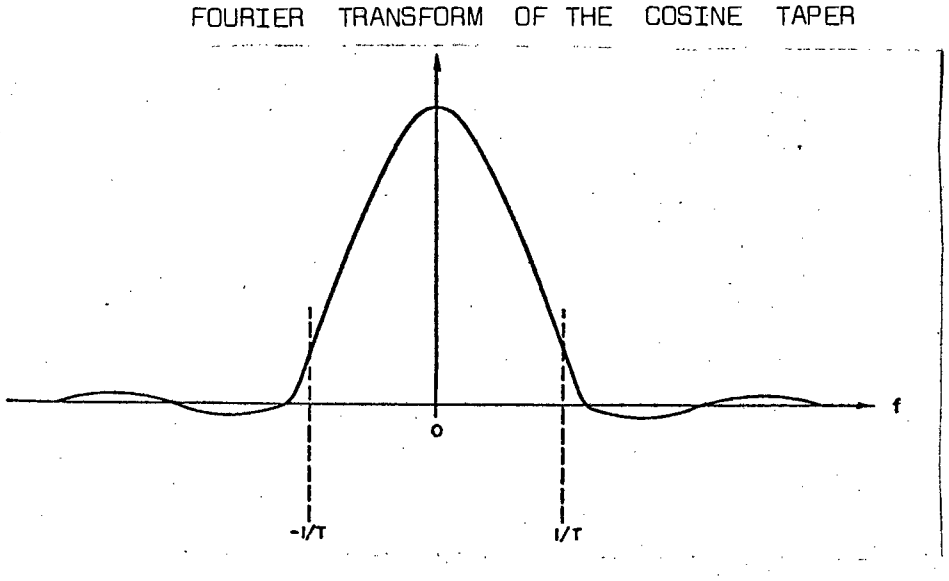

function x (t). If $x(t) \neq nh(t)$ $n = 1, 2, 3 \ldots$ then side-lobe interference occurs.

Leakage can be reduced to a suitable level by applying a cosine taper to the ends of the truncation function x(t). The resulting function as shown in Diagram 3.19 has a Fourier transform (Diagram 3.20) with reduced side lobes. The cosine taper is applied to first and last tenths of x(t). Other truncating functions, e.g. the Hamming and Hanning windows can be used to prevent leakage, but the cosine taper was most suitable.

The Fast Fourier Transform (FFT) used was acquired by Dr. Swingler (Electrical Engineering Department, UCT) who translated it from FORTRAN to BASIC and made it available for use on the VARIAN minicomputer. The adapted FFT program used for this signal processing analysis is reproduced in Appendix 13.

The autocorrelation function in Diagram 3.17 is only one side of the full even function. The full function includes a mirror image of the present function about the $\tau = o$ axis. The FFT performs a 256 point transform on 128 points of data in complex notation. The imaginary parts of the data are all zero as the autocorrelation function is real.

The adapted FFT program read the one-sided autocorrelation function, removed its mean value and created a mirror image to form the full even autocorrelation function. This function was then symmetrically truncated to 128 points, and the cosine taper was applied to the truncated ends. The FFT of the function was

then calculated, reformated and plotted.

Diagram 3.21 shows the plot of the FFT of the autocorrelation function in Diagram 3.17. The plot is symmetrical about 0 Hz and has a full-scale frequency range of $\pm$ 1/2h Hz with a sample resolution of 1/128hHz, where h is the lag time between autocorrelation function samples.

The program scaled the plot to the maximum value in spectral density function. The mean value, if it had not been removed would have appeared as a large 0 Hz (d.c.) value which would increase the amplitude scale and dominate the plot.

The spectral density plot (Diagram 3.21) indicates the following:

No mean value is present as expected.

The largest amplitude has a period of 128h which is the truncating period. This is an error created by the Discrete Fourier Transform (DFT). The DFT assumes a continuous signal consisting of the repeated data block. The truncated double sided autocorrelation function data block, when repeated forms a function, with a long period equal to the truncating period (Diagram 3.19). This error is an effect other than 'leakage' which is caused by unsatisfactory fulfilment of condition C.

The remainder of the spectral density is a valid presentation of the frequencies of the periodic components in the auto-

FFT OF THE AUTOCORRELATION FUNCTION OF THE AMPLITUDE OF THE 300 Hz COMPONENT IN THE ACOUSTIC NOISE.

(SPECIAL DENSITY PLOT)

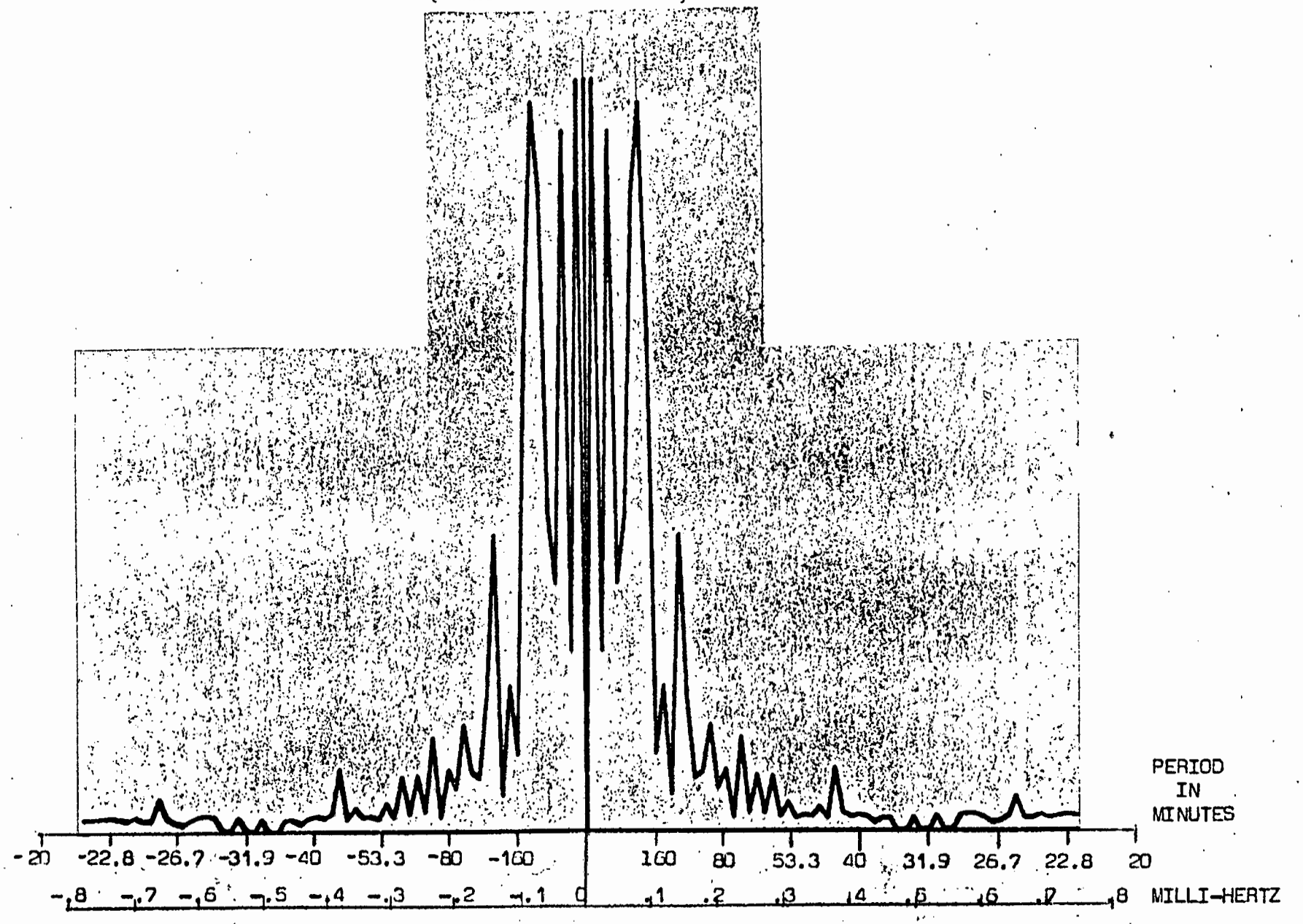

DIAGRAM 3.21

correlation function.

The plot shown in Diagram 3.21 is made up of 128 points joined by straight lines. If a frequency component is present which is not a multiple of 1/128h Hz it is not accurately shown in the plot on both the time and frequency axis. Instead the nearest multiple of 1/128h has a peak whose amplitude is less than the true peak. This error caused by sampling in the frequency domain is described in Appendix 12.

The three dominant components in the plot are at frequencies of approximately 3/128h, 7/128h, and 11/128h. Thesefrequencies have periods of 7 hours 38 minutes, 3 hours 16 minutes and 2 hours five minutes.

The variation of the amplitude of the 300 Hz component of the acoustic noise, is adequately described by the above analysis. It can now be 'cross analyzed' with data describing Furnace Operating Conditions.

CHAPTER 4.

FURNACE OPERATING CONDITIONS ANALYSIS

4.1 DECODING: OF OPERATING CONDITIONS DATA

The magnetic tapes containing the data dealing with the operating conditions were loaded on the UNIVAC and VARIAN computer systems and attempts were made to read the data. The reading of the tape was found to be not straightforward and translation programs were written. A description of the problems encountered and the operation of the programs written follows below. The UNIVAC computer was chosen due to its ability to work with large amounts of data and the ability of its ASCII FORTRAN compiler to access the magnetic tapes.

Translation of the Tape to usable form on the UNIVAC

The program FURN.DATA2 reads the tape and transfers the data into a UNIVAC data file which is readily accessible to analytical programs written for the UNIVAC.

The problems encountered in translation were:

1. The tape has one ASCII character (8 bits + 1 parity) written perpendicular to tape motion which must be read into a UNIVAC word containing 36 bits.

   In this way 4½ ASCII characters fit into a UNIVAC word. To avoid splitting characters Q format was used in reading the tape. Q format reads four 8 bit words into a 36 bit

word leaving a zeroe to the left of each ASCII character.

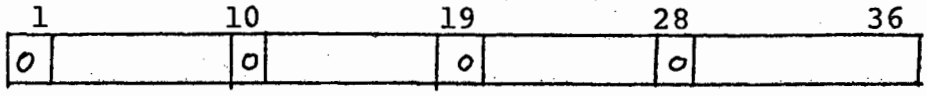

This word containing 4 ASCII characters is split into 4 words using a DECODE statemat.

2. The tape is written in blocks each containing 129 UNIVAC words or 516 ASCII characters. The last two characters are ASCII NULL characters and scattered within the block are four carriage return ASCII characters which were inserted while translating the data from disk to tape. The program must search for the carriage return characters in each block, delete them and shift the rest of the characters up to take up the empty space.

3. The data recorded every minute gives the Date, Time and Sector Number followed by 25 values. Unfortunately, this piece of information can be spread across two blocks. The program has to search for the completeness of a minute data record, which can involve collecting data from two blocks.

4. The minute data record is written to a data file. This data file must be manipulated by the EDIT processor in order to convert the ASCII characters to field data used by the UNIVAC.

A second program FURN.FIND searches for any given data and time and notes the position on the tape. This position allows FURN. DATA2 to skip blocks and save time, when reading data. Unfortu-

nately, the Condat file often has gaps in the time record corresponding to breakdowns on the plant computer. This restricts FURN.FIND's capabilities.

4.2 ANALYSIS OF THE FURNACE OPERATING CONDITIONS

The list of operating conditions logged is shown in Appendix 6. The secondary current and hoist position were chosen for analysis, as both these parameters are related to the power input to the furnace via the electrodes. The secondary current is calculated by the computer from the value of the current measured in the primary circuit and is a minute average of the current flowing.

The electrodes hoist position data is made up of minute averages of directly measured data. The furnace operation is controlled by varying the vertical position of the individual electrodes via their hoists.

The data records available restricted the sampling frequency to a maximum of 1/60 Hz. This factor influenced the decision in the previous section to concentrate analysis on low frequency amplitude fluctuations of periodic components.

As the data is in digital form, digital signal processing is indicated.

The analysis techniques are the same as those described in Chapter 3, Sections 8, 9 and 10 of the analysis of the acoustic noise, and their description will not be repeated.

The preparation of the data and the analysis results are described below.

Preparation of Furnace 'Operating Conditions' Data

The VARIAN was chosen for digital signal processing of the current and hoist position data as the analysis programs already written could be used. The cross-analysis between operating conditions and acoustic noise required that all sets of data be available on the same computer. The UNIVAC is unable to digitize the acoustic data, for this reason all analysis was performed on the VARIAN.

Although facilities do exist for transfer of data from the UNIVAC to the VARIAN, the software required to read this data into BASIC analysis programs was not available.

It was found that the amount of data to be transferred did not justify this software being written.

The data required covered the same time period as the recorded sampled acoustic noise signal.

Using the programs FURN.FIND and FURN.DATA 2 the relevant data was located and printed.

From this data a new data record was manually prepared with a 10.75 minute sampling period. The new data points were averages of the 3 minute-averaged points at the 10.75 sampled interval. The sampled points were time sychronized with the sample points

of the acoustic data.

This new data record was manually entered into the computer and stored on paper tape in the same format as the acoustic noise data. This enabled the digital analysis techniques described previously to be used on the current and hoist position data.

4.3 STATIONARITY OF CURRENT AND HOIST POSITION DATA OF ELECTRODE 3

Using the Run Test the hypothesis of stationarity of the mean square of the hoist position and the current relating to electrode 3 of the furnace, was accepted at the $\alpha = 0.05$ significance level.

Diagram 4.1 shows the plots of mean square values as required by the Run Test.

Results:

	Current	Hoist Position
No. of points	20	13
Runs	7	5
Run Acceptance region $\alpha = 0.05$	6 - 15	3 - 12

(From Table A.6)

4.4 DETECTION OF PERIODICITIES IN CURRENT AND HOIST POSITION DATA

The hoist position and current data were analyzed with the techniques used in analyzing the amplitude of the 300 Hz component. The autocorrelation functions are shown in Diagrams 4.2 and 4.3.

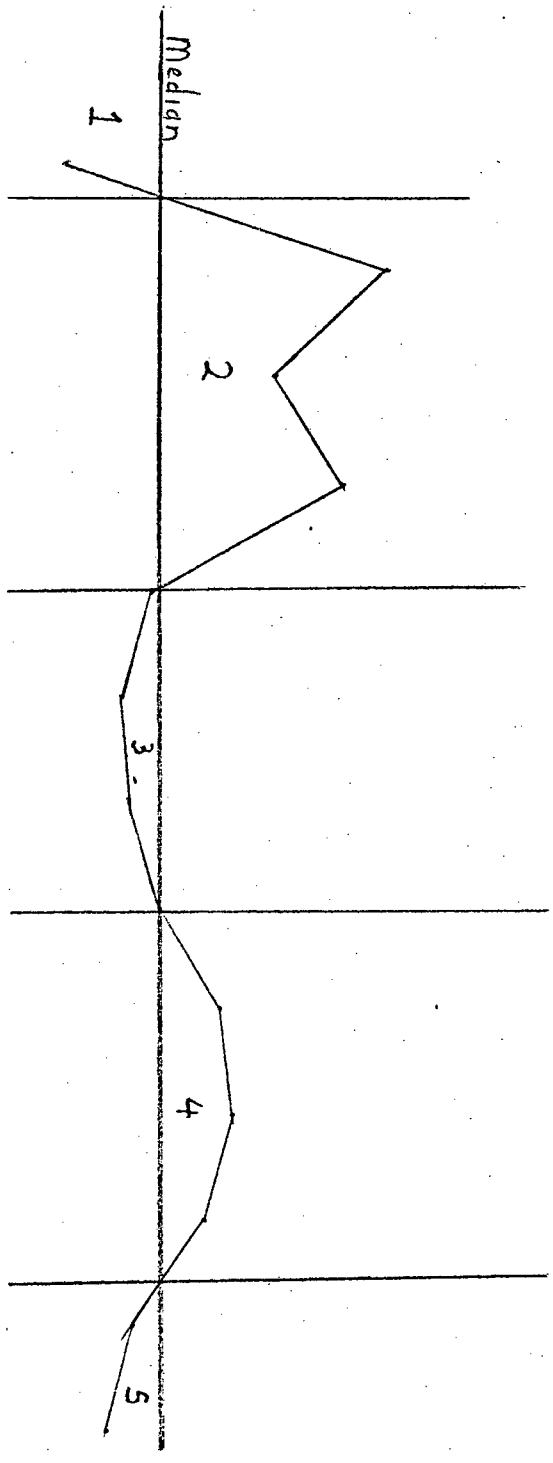

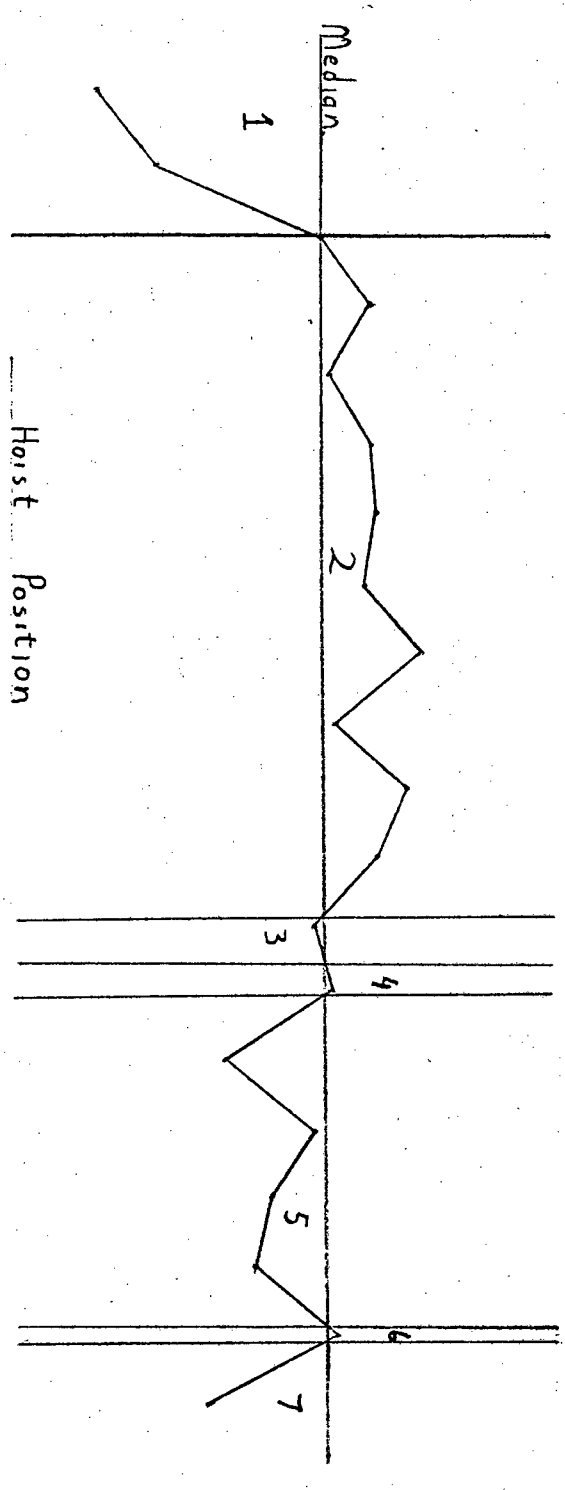

RUN TESTS FOR STATIONARITY OF THE MEAN SQUARE

DIAGRAM 4.1

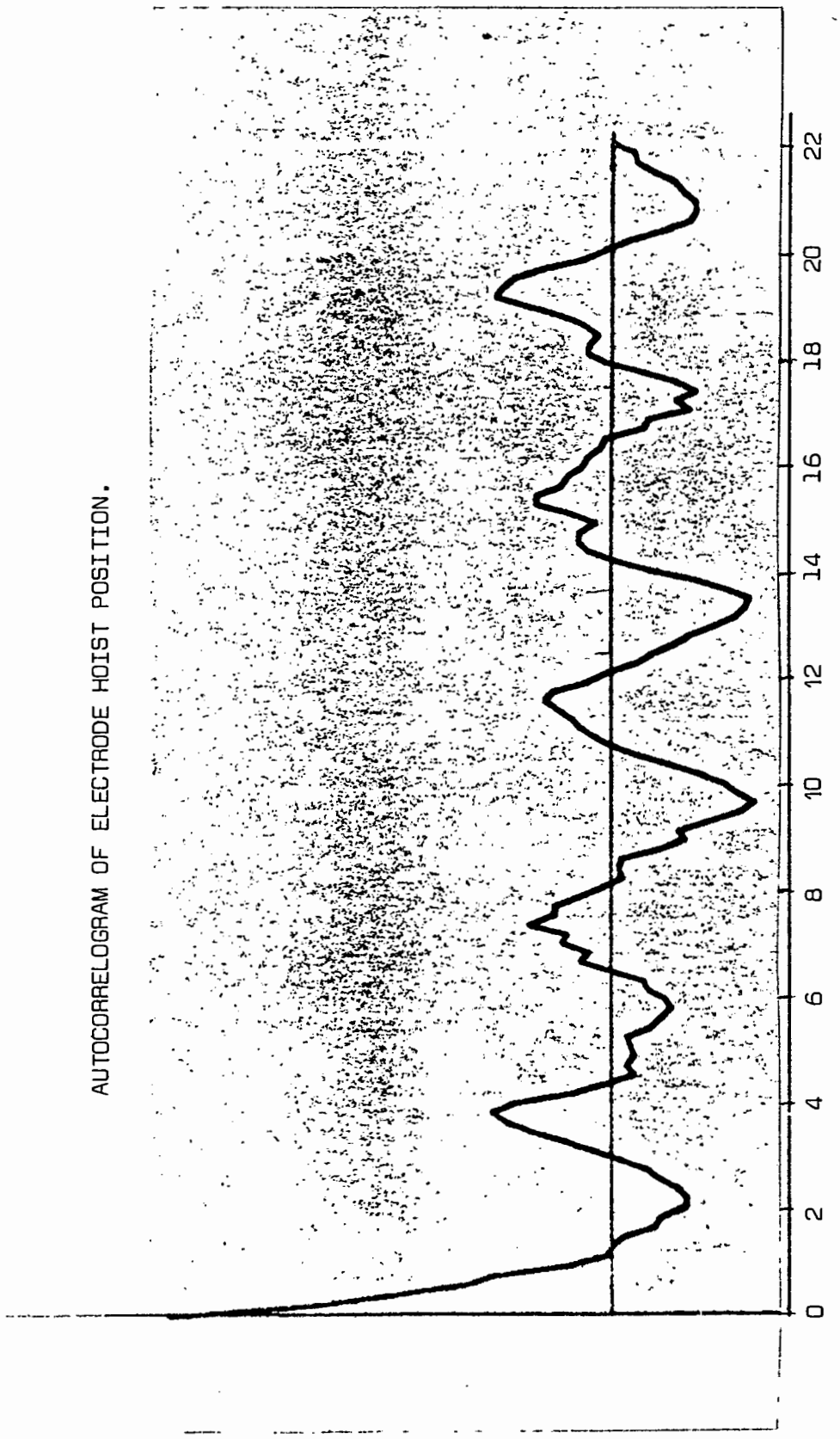
AUTOCORRELOGRAM OF ELECTRODE HOIST POSITION.
0
2
4
6
8
10
12
14
16
18
20
22
LAG TIME HOURS

DIAGRAM 4.2

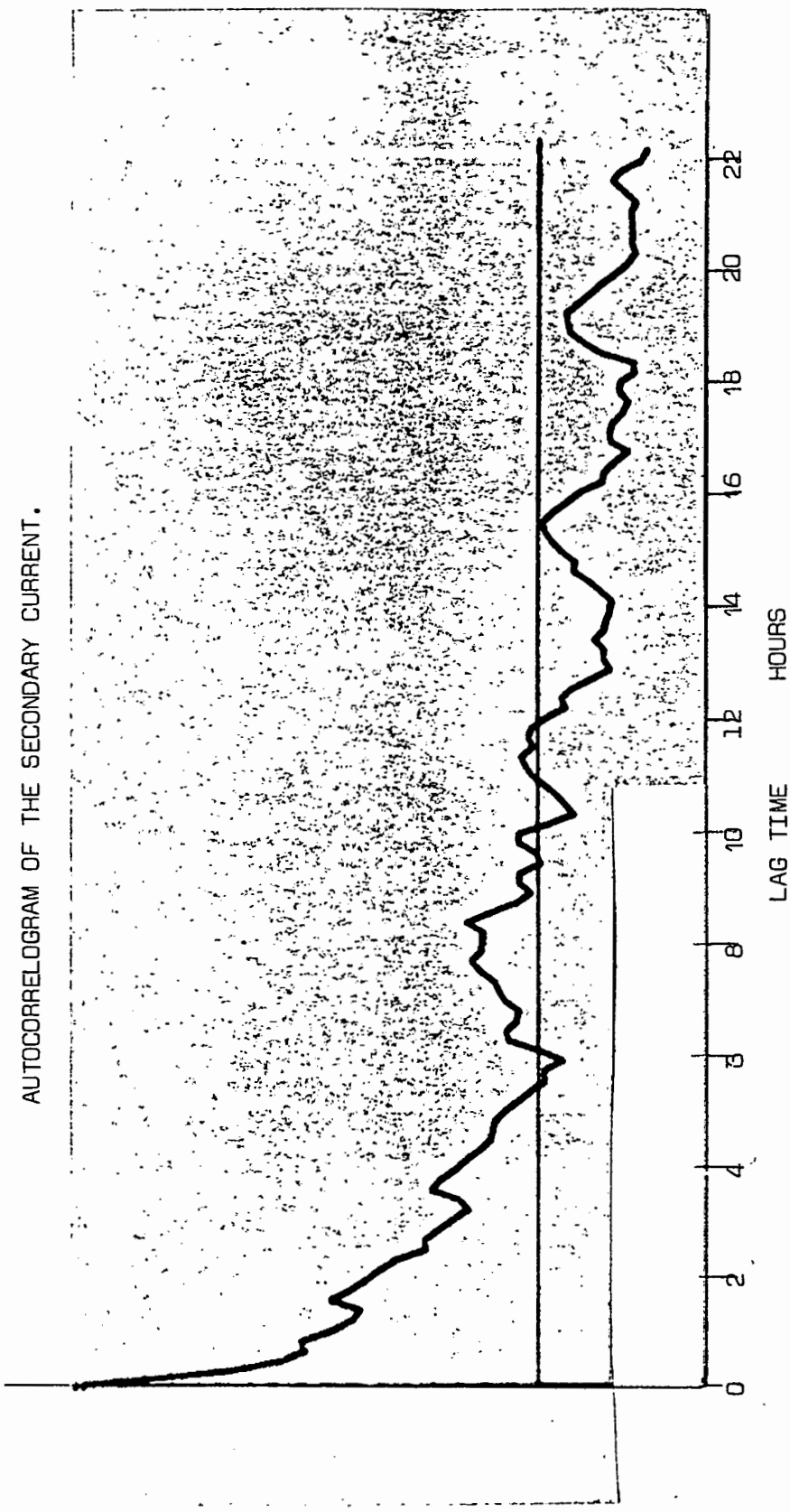
AUTOCORRELOGRAM OF THE SECONDARY CURRENT.
0
2
4
6
8
10
12
14
16
18
20
22
LAG TIME HOURS

DIAGRAM 4.3

The autocorrelation function of the hoist position data clearly indicates periodicities. These periodicities are clearly visible in the spectral density plot (Diagram 4.4) of the autocorrelation function. The dominant periodic component has a period of approximately 3 hours 48 minutes. Its second harmonic is -11 dB and its third harmonic is -15 dB. A very low frequency component occurs between the dominant component and the error peak (discussed previously) at 1/128h.

The autocorrelation function of the current data shows periodicities, which are not as dominant as those in the hoist position data. For large lag time the function value is less than zero due to a depressed mean caused by inaccuracies in the calculation of the mean value of the data. The error in the mean value calculation is due to short periods in the data when the current is zero. Diagram 4.5 shows the spectral density function of the autocorrelation function. The dominant peak is the error peak caused by the FFT. The periodic component has a period of approximately 3 hours 48 minutes. The remainder of the spectrum could contain 1st and second harmonics but this is not conclusive from the plot.

The above analysis adequately describes the Hoist Position and Current Data. The periodicities detected are of smaller frequencies to those found in the amplitude of the 300 Hz component in the acoustic noise.

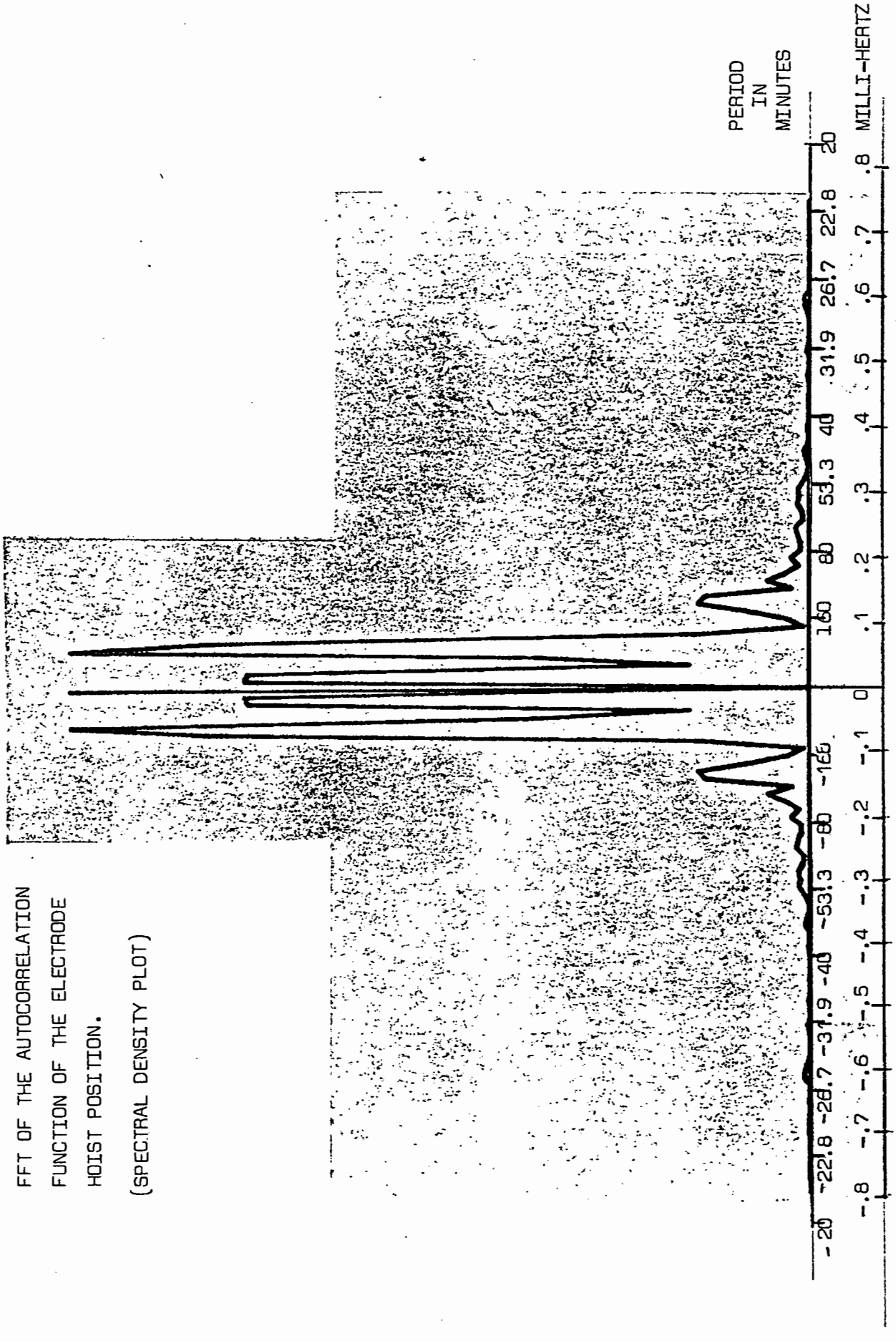
FFT OF THE AUTOCORRELATION
FUNCTION OF THE ELECTRODE
HOIST POSITION.
(SPECTRAL DENSITY PLOT)
PERIOD
IN
MINUTES
MILLI-HERTZ
-20 -22.8 -26.7 -31.9 -40 -53.3 -80 -160 0 160 80 53.3 40 31.9 26.7 22.8 20
-.8 -.7 -.6 -.5 -.4 -.3 -.2 -.1 0 .1 .2 .3 .4 .5 .6 .7 .8

DIAGRAM 4.4

FFT OF THE AUTOCORRELATION FUNCTION OF
THE ELECTRODE SECONDARY CURRENT.
(SPECTRAL DENSITY PLOT)

DIAGRAM 4.5

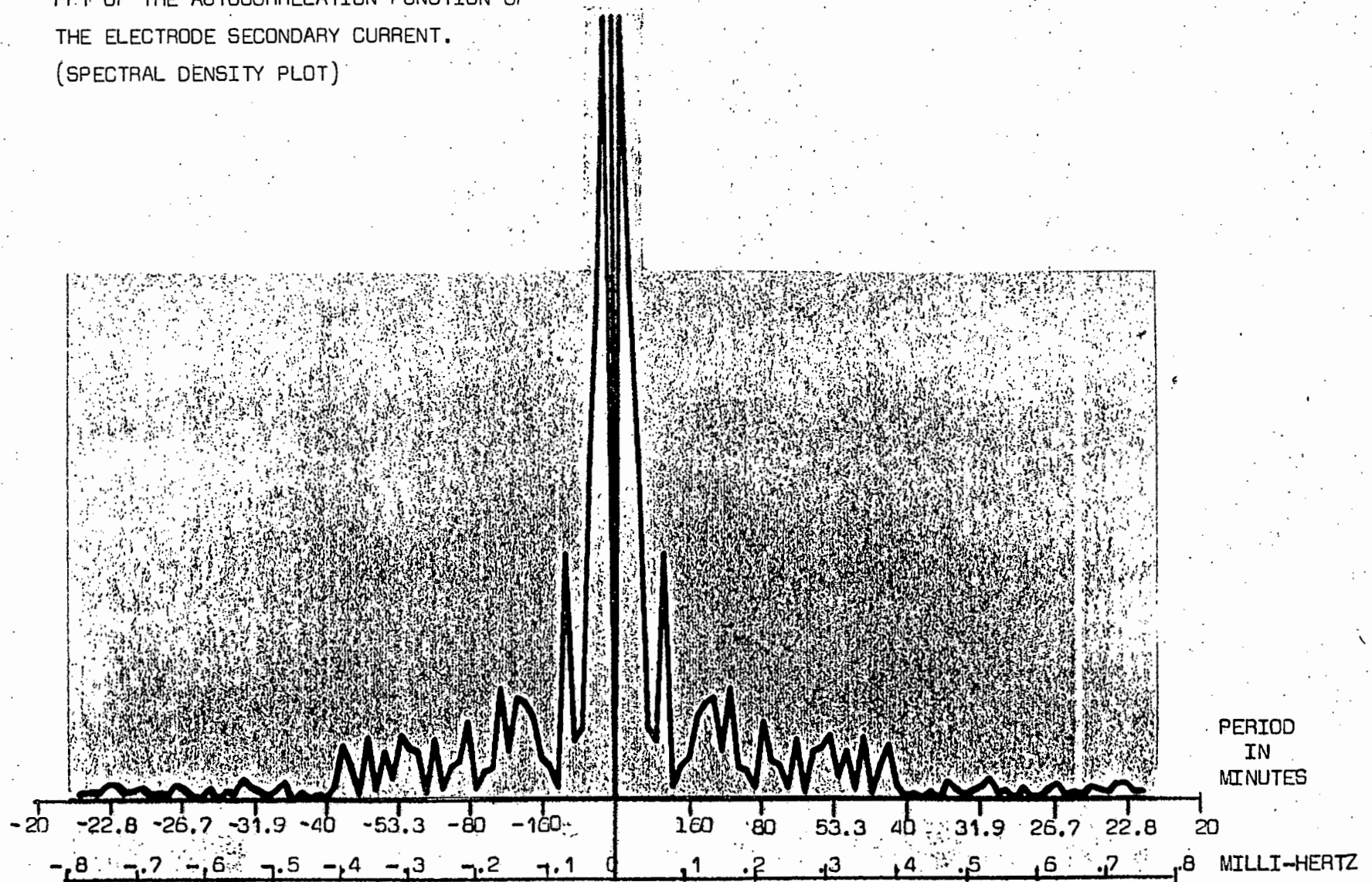

CHAPTER 5.

CONCLUSIONS ON ANALYSIS OF ACOUSTIC NOISE AND FURNACE OPERATING CONDITIONS

In previous sections the amplitude of the 300 Hz signal in the acoustic noise and the current and hoist position data of the related electrode have been analyzed. These analysis terminated with spectral density plots indicating periodicities of large time periods. The resolution of the plots was not sufficient to determine with any accuracy the actual frequencies of the peaks.

This resolution can be doubled by using an effect know as 'adding zeroes'. The data block to be transformed has a block of equal length filled with zeroes added serially to it. The cosine taper is till only applied to the initial block, and the mean is calculated and subtracted from the non-zero data. The FFT is performed on double the resolution.

This resolution was not applied as the FFT was limited to 256 points. The resolution could have been doubled by halving the number of data points then adding zeroes and applying the FFT, but this procedure was also rejected as it reduced the number of data points to the low value of 64 which would not fully represent the data.

Further analysis on these parameters was not necessary as the

parameters were adequately specified by the above analysis. The following analysis concentrates on detecting common properties in the data records. These properties are already visually apparent from the pre-analysis plots in Diagrams 3.11 and 3.12 and from observations of the spectral density plots of the individual parameters.

CHAPTER 6

ANALYSIS RESULTS USING DIFFERENT DATA RECORDS

To confirm the findings of the analysis of the amplitude of the 300 Hz component, the analysis was repeated using date recorded over a different time interval. The data relating to the hoist position and current over the same interval were analyzed. The data records shown in diagrams consisted of 88 points as compared with the 250 points of the previous records.

The same data preparation and analysis preocedures used on the previous data records were applied, the only difference being the record lengths.

All three data records were tested for the stationarity of their mean squares. Diagrams 6.1, 6.2 and 6.3 show the mean square plots required for the Run Tests. All three data records had stationarity of their mean squares at the $\alpha = 0.05$ significance level.

The autocorrelation functions were calculated for all three data records. (Diagrams 6.4, 6.5 and 6.6). The maximum lag number (r) was 44 and each point on the plot was calculated from 44 multiplications resulting in a limited accuracy. The autocorrelation function of the hoist position data showed a single meaningful periodic component which is dominant on the spectral density plot (Diagram 6.7). The frequency of this component is

RUN TESTS FOR THE STATIONARITY OF THE MEAN SQUARE OF:

The electrode current

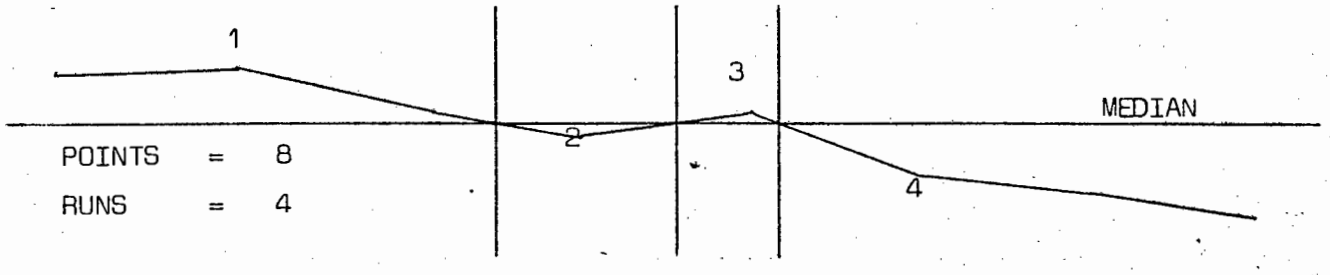

DIAGRAM 6.1

The electrode hoist position

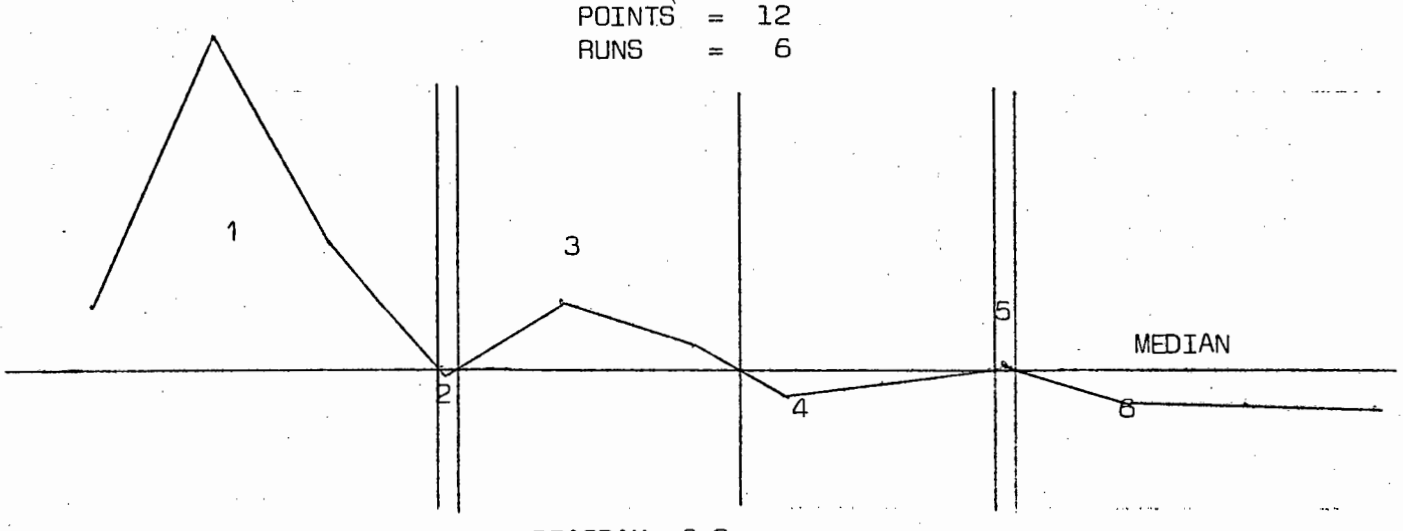

DIAGRAM 6.2

The amplitude of the 300 Hz component in the acoustic noise.

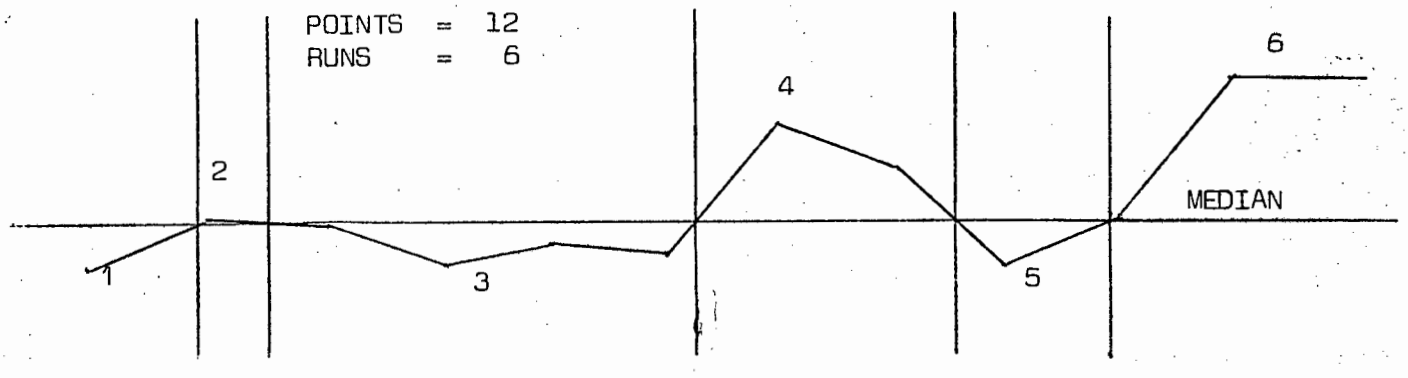

DIAGRAM 6.3

44 POINT AUTOCORRELOGRAM OF THE SECONDARY CURRENT.

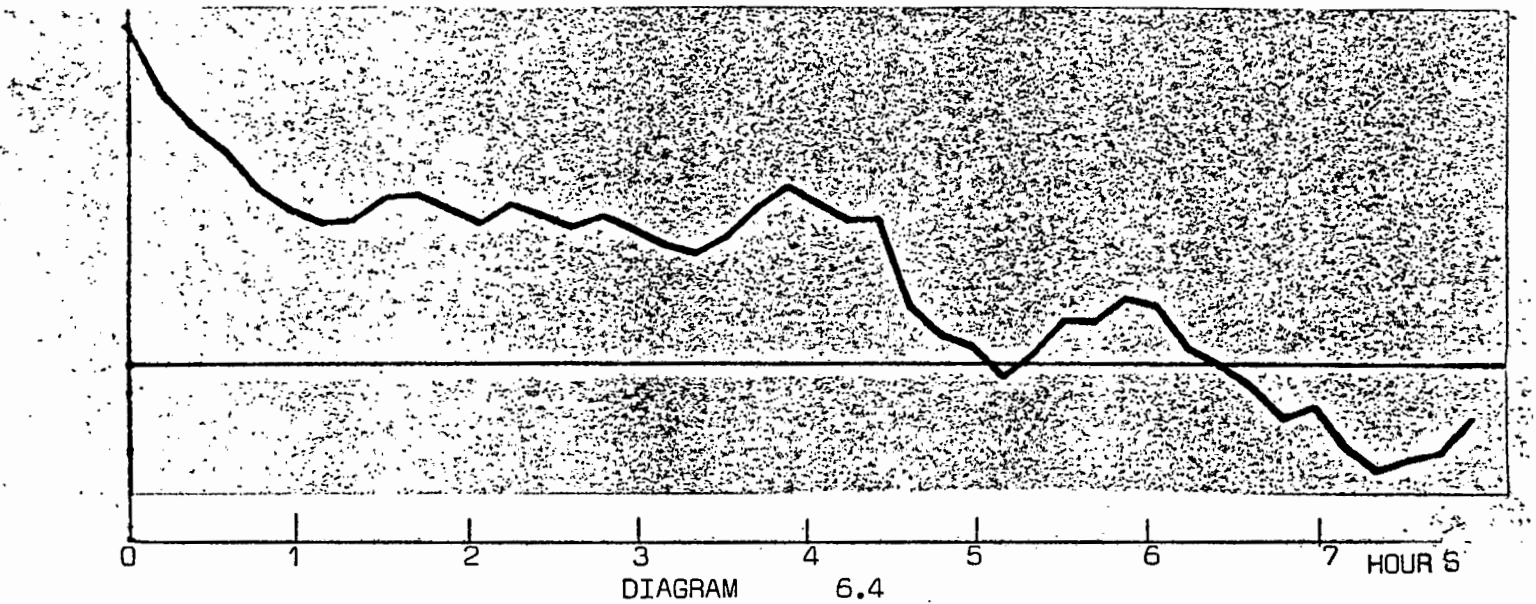

DIAGRAM 6.4

44 POINT AUTOCORRELOGRAM OF THE ELECTRODE HOIST POSITION.

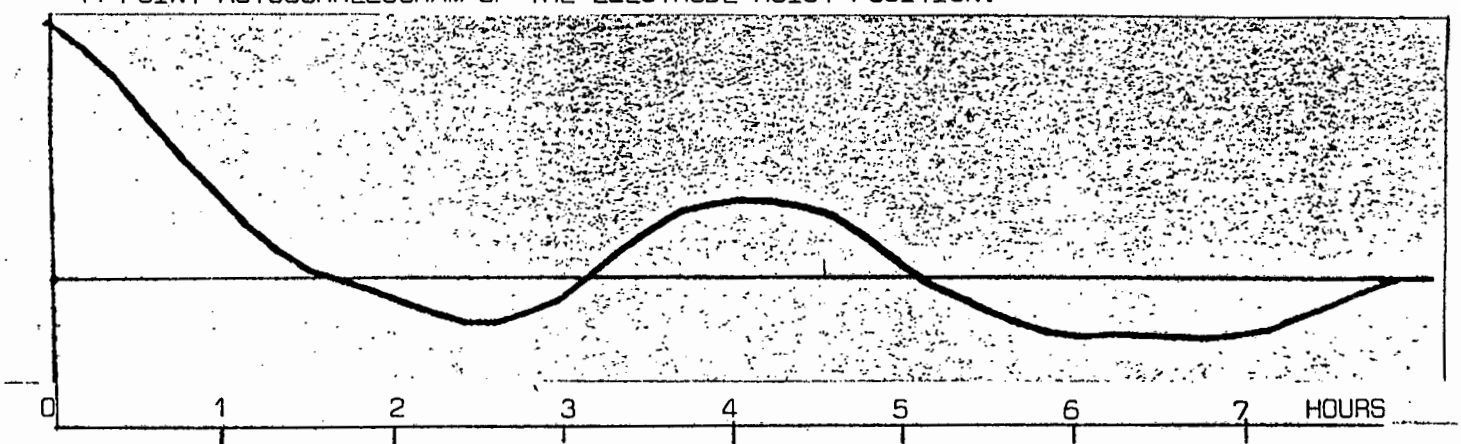

DIAGRAM 6.5

44 POINT AUTOCORRELOGRAM OF THE AMPLITUDE OF THE 300 Hz COMPONENT IN THE ACOUSTIC NOISE.

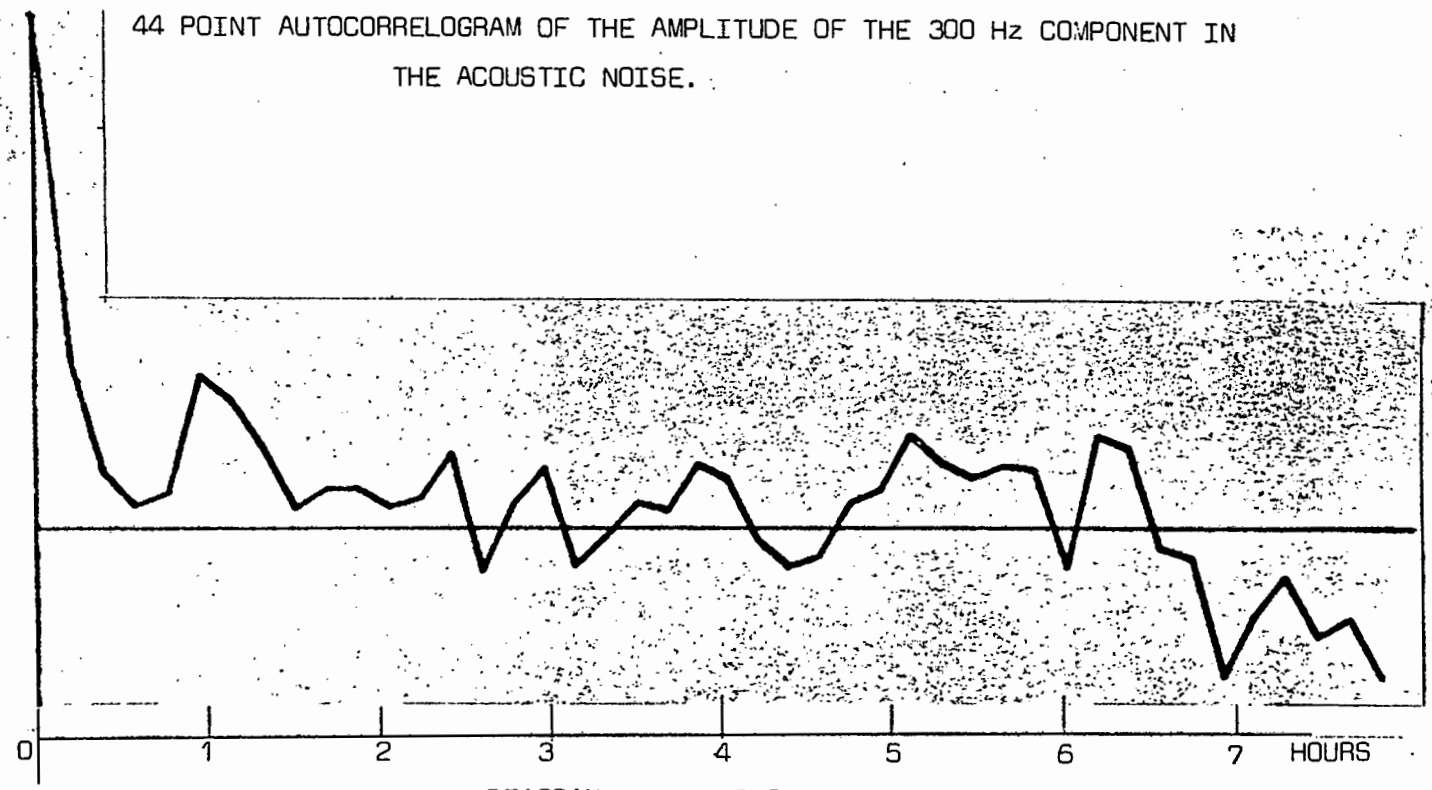

DIAGRAM 6.6

FFT OF AUTOCORRELATION FUNCTION
OF THE ELECTRODE HOIST
POSITION.
(SPECTRAL DENSITY PLOT)

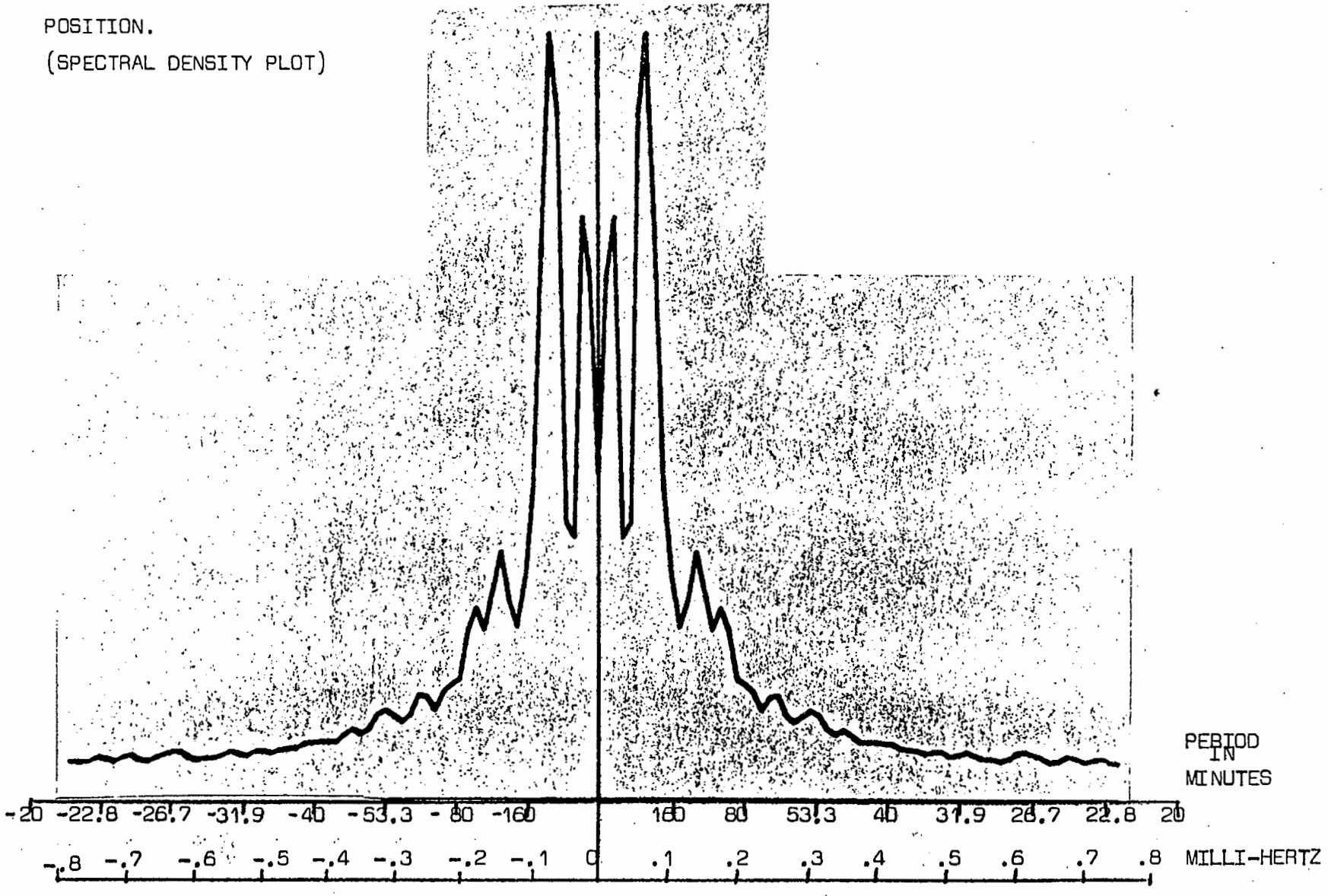

DIAGRAM 6.7

the same as the dominant component in the previous hoist position data record analyzed.

The autocorrelation functions of the current and the amplitude of the 300 Hz component indicate periodicities but do not have the accuracy required for meaningful discrete Fourier analysis.

These data records were cross-analyzed, the results and conclusions are described along with those of the other 'time period' data set, in the Cross Analysis section.

CHAPTER 7.

7.1 FURTHER ACOUSTIC NOISE ANALYSIS

In the previous analysis of the acoustic noise data records it was decided that the periodic components in the noise signal were likely to be affected by furnace operating conditions. The 300 Hz component was chosen for analysis from indications found in the pre-analysis. The other large periodic components are the 100 and 200 Hz components. For the sake of completeness the analysis of these components follows:

The formation of the data records followed the same procedure as that of the 300 Hz component. The wave analyzer was tuned to give a d.c. value proportional to the amplitude of the 100 and 200 Hz components respectively. The conversion procedure of the analog signals into sampled digital records having a sample interval of 10,75 minutes is as described previously.

Tests for stationarity of the mean square value of these data records were applied. The results of the Run Tests are shown in Diagrams 7.1 and 7.2. Both data records were found to be stationary at the $\alpha = 0.05$ significance level.

The autocorrelation functions of the data records were calculated in the same manner as described previously. The autocorrelograms which have a time axis of r = 63 are shown in Diagrams 7.3 and 7.4. These plots indicate that there are no large periodic components in the data.

The spectral density plot for the 200 Hz data was not calculated

RUN TESTS FOR STATIONARITY OF THE MEAN SQUARE OF :

The amplitude of the 100 Hz component in the acoustic noise.

POINTS = 20

RUNS = 10

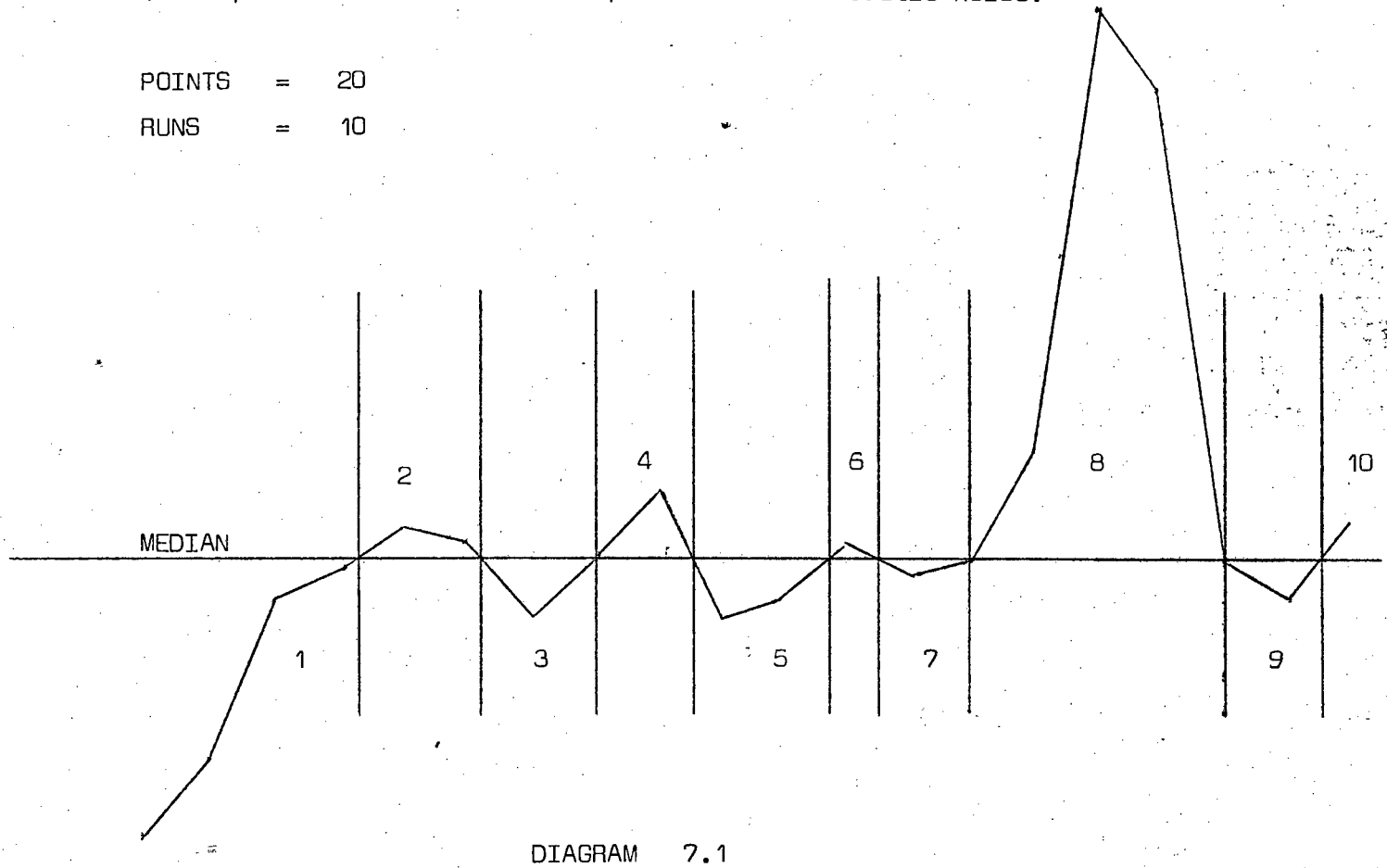

DIAGRAM 7.1

The amplitude of the 200 Hz component in the acoustic noise.

POINTS = 20

RUNS = 6

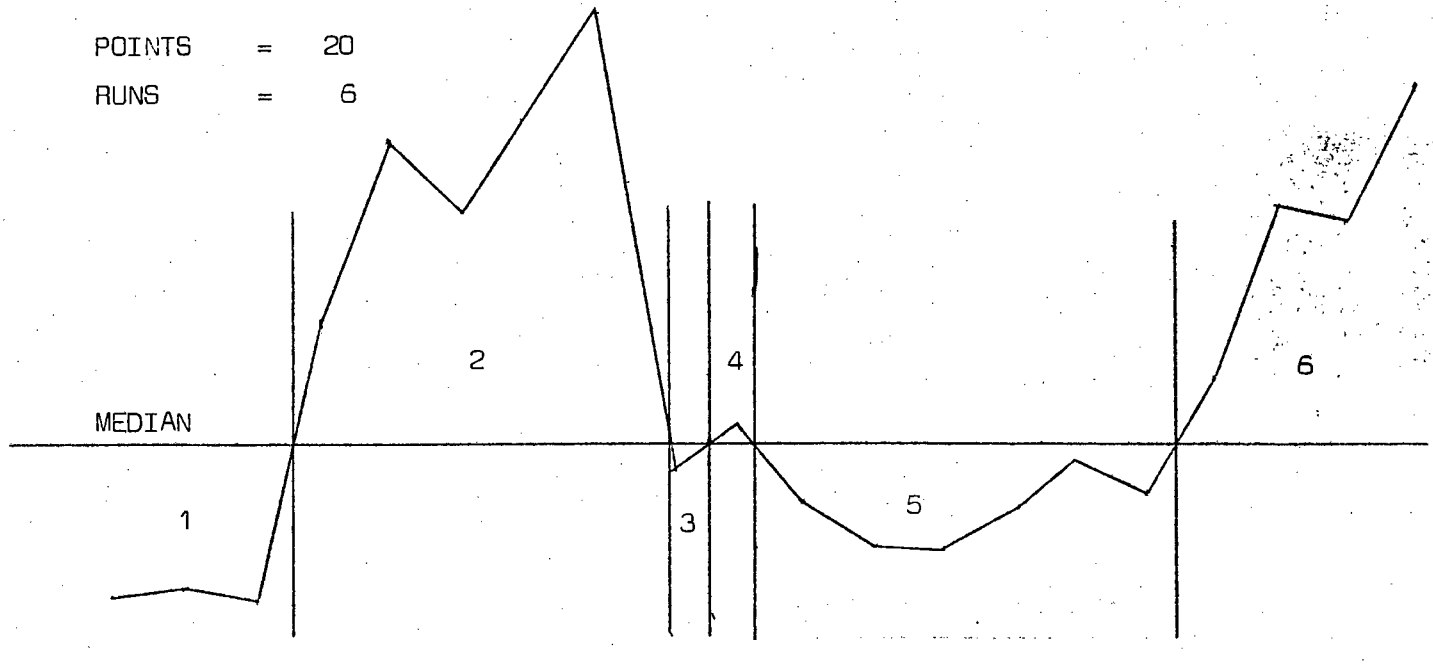

DIAGRAM 7.2

AUTOCORRELOGRAM OF THE AMPLITUDE OF THE 100 Hz COMPONENT IN THE ACOUSTIC NOISE.

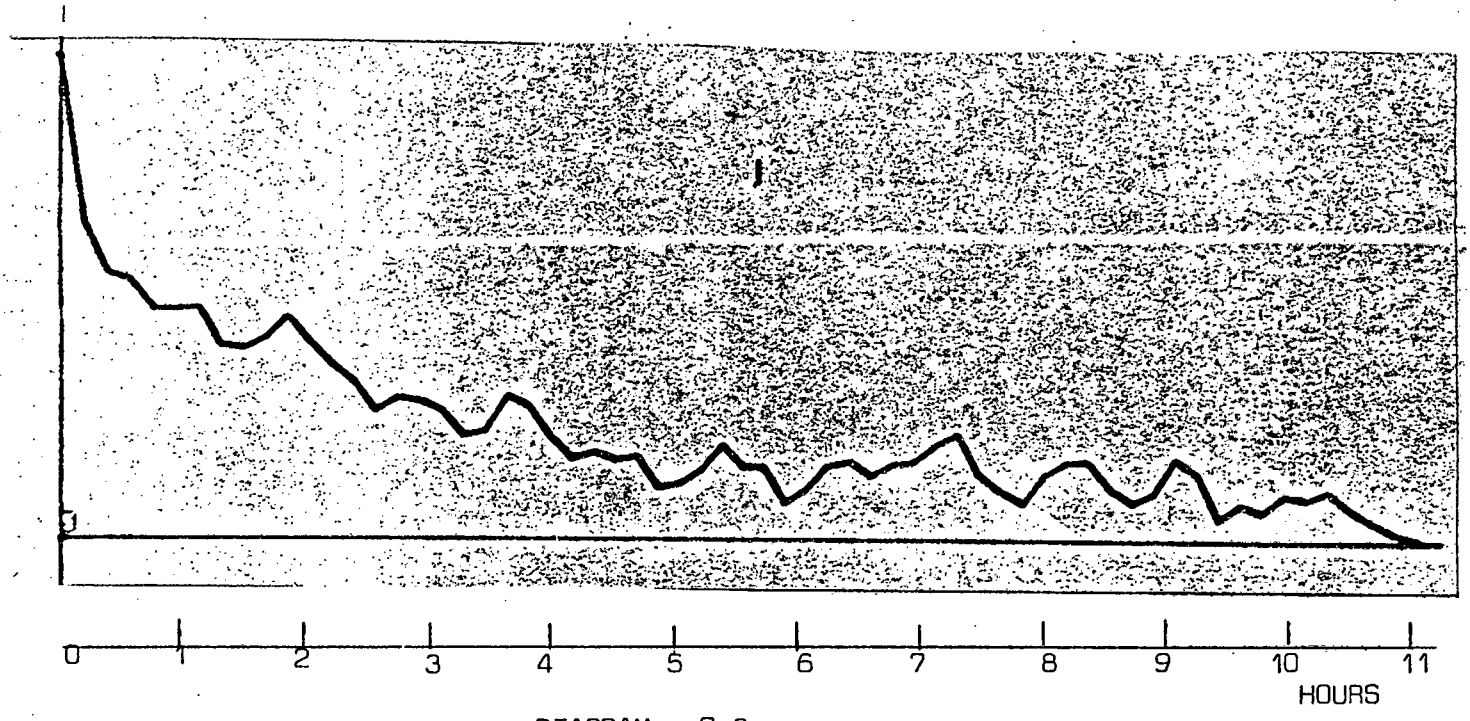

DIAGRAM 7.3

AUTOCORRELOGRAM OF THE AMPLITUDE OF THE 200 Hz COMPONENT IN THE ACOUSTIC NOISE.

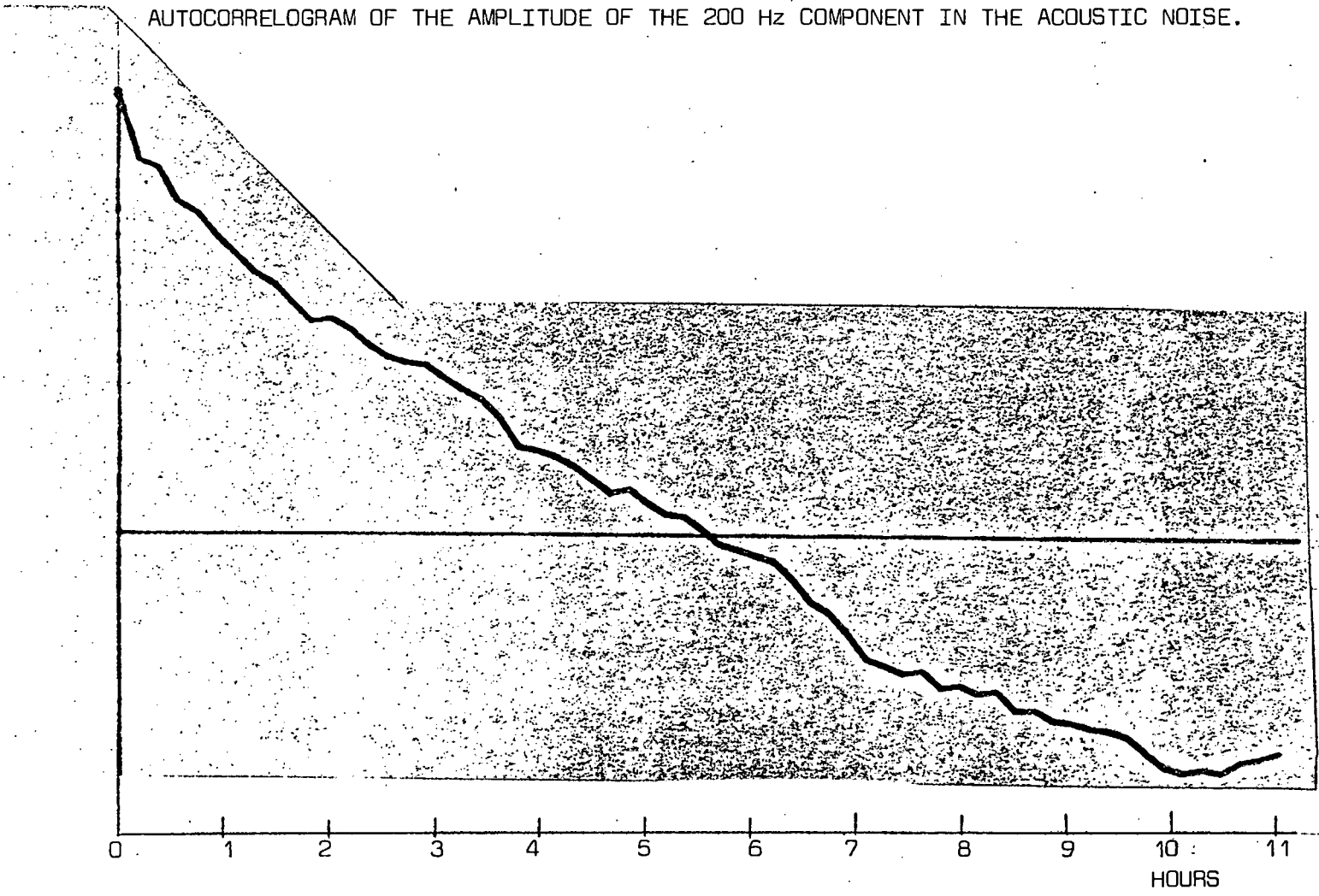

DIAGRAM 7.4

as the autocorrelation function does not fulfil the requirements for discrete Fourier analysis. Diagram 7.3 showing the autocorrelation function of amplitude of the 100 Hz component shows some slight periodic fluctuations. These are displayed in the spectral density plot (Diagram 7.5) and are shown to be of a low level. The large components on the plot close to zero are errors of the discrete Fourier transform.

This analysis indicates that the amplitude of the 200 Hz periodic component varies very slowly with time and that possible periodic components will only be detected over larger time periods.

The amplitude of the 100 Hz periodic component has a few low frequency low amplitude periodicities, but is largely random.

FFT OF THE AUTOCORRELATION FUNCTION
OF THE AMPLITUDE OF THE 100 Hz
COMPONENT IN THE ACOUSTIC NOISE.

(SPECTRAL DENSITY PLOT)

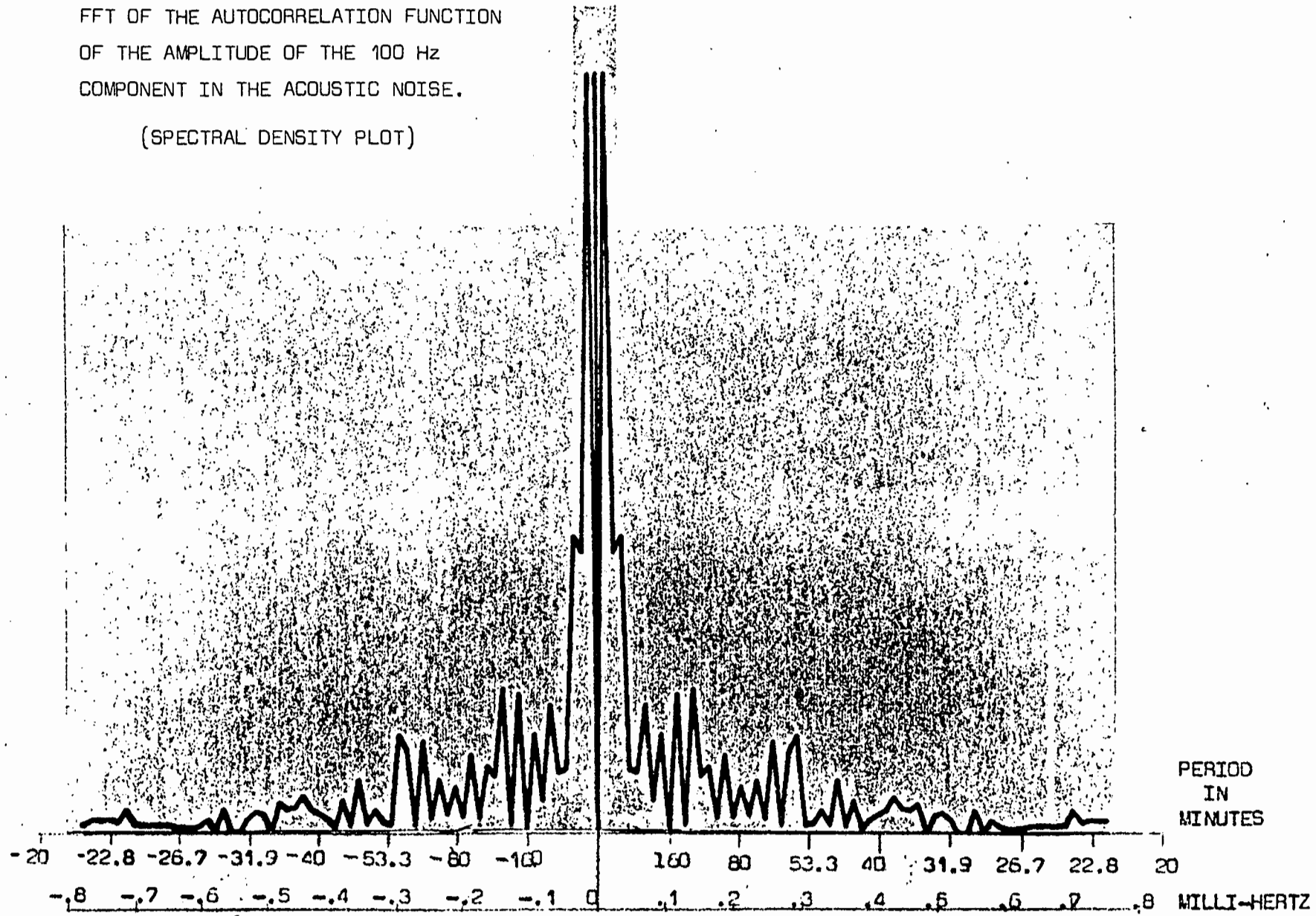

DIAGRAM 7.5

CHAPTER 8.

8.1 CROSS ANALYSIS

Cross analysis involves the detection of similarities between data records. In this case, the amplitude of the 300 Hz component in the acoustic noise was compared with the current flowing in the nearby electrode and its position.

The technique used for the analysis is the cross-correlation function. This is similar to the autocorrelation function, but it compares two separate data records.

$\{x_n\}, \{y_n\} \quad \bar{x}, \bar{y} = 0$

$$n = 1, 2 \ldots\ldots\ldots\ldots N$$

The cross-correlation function used is given by

$$R_{xy}(rh) = \frac{2}{N} \sum_{1}^{N/2} x_{\frac{N}{4}+n-1} \, y_{n+r} \quad \ldots\ldots \text{8.1.1}$$

or

$$R_{yx}(rh) = \frac{2}{N} \sum_{1}^{N/2} y_{\frac{N}{4}+n-1} \, x_{n+r} \quad \ldots \text{8.1.2}$$

$$r = N/4 \ldots\ldots\ldots 0 \ldots\ldots\ldots + N/4$$

where r is the lag number and h is the sampling interval.

This expression requires N data points per record to give a N/2 cross-correlation function. This expression was chosen from other equally valid expressions for the same reasons that the similar autocorrelation function was chosen (See Section 3.9).

The cross-correlation function shows correlation between data records and the lag time of one record behind the other.

The cross-correlation function can be normalized to $\pm$ 1 by dividing the function by $\sqrt{\overline{x^2}\,\overline{y^2}}$

8.2 CROSS ANALYSIS BETWEEN CURRENT AND AMPLITUDE OF 300 Hz COMPONENT IN THE ACOUSTIC NOISE SIGNAL

The cross-correlation function of these parameters was calculated and plotted by the VARIAN minicomputer. The expression 8.1.1 described above was used with x_n the current data and y_n the amplitude of the 300 Hz component.

Diagram 8.1 shows the cross-correlation plot, the number of points = N/2 = 125.

Diagram 8.2 shows another cross-correlation plot using different data collected with the same instrumentation. This plot has N/2 = 44 points as the original data record has only 88 points.

The 125 point plot shows that there is no unique peak in the cross-correlation function. This is because both data records contain periodic components of similar frequencies giving a cross-correlation function very similar to the autocorrelation function of a periodic component. The peak close to the $\tau = 0$ axis indicates that the noise lags behind the current. The noise lag time is approximately 10 minutes.

The 44 point plot agrees with the 125 point plot, but shows only one peak due to the short record length. The noise lag time

CROSS CORRELATION FUNCTIONS OF ELECTRODE SECONDARY CURRENT AGAINST AMPLITUDE OF THE 300 Hz COMPONENT IN THE ACOUSTIC NOISE.

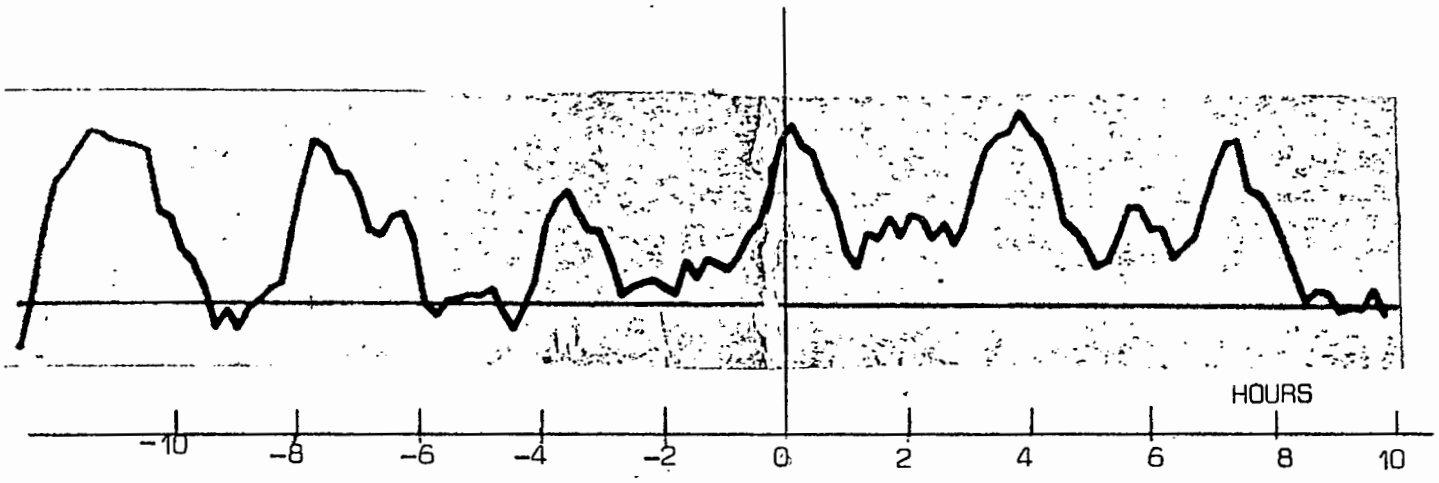

DIAGRAM 8.1

CURRENT LAGS 300 Hz COMPONENT

CURRENT LEADS 300 Hz COMPONENT

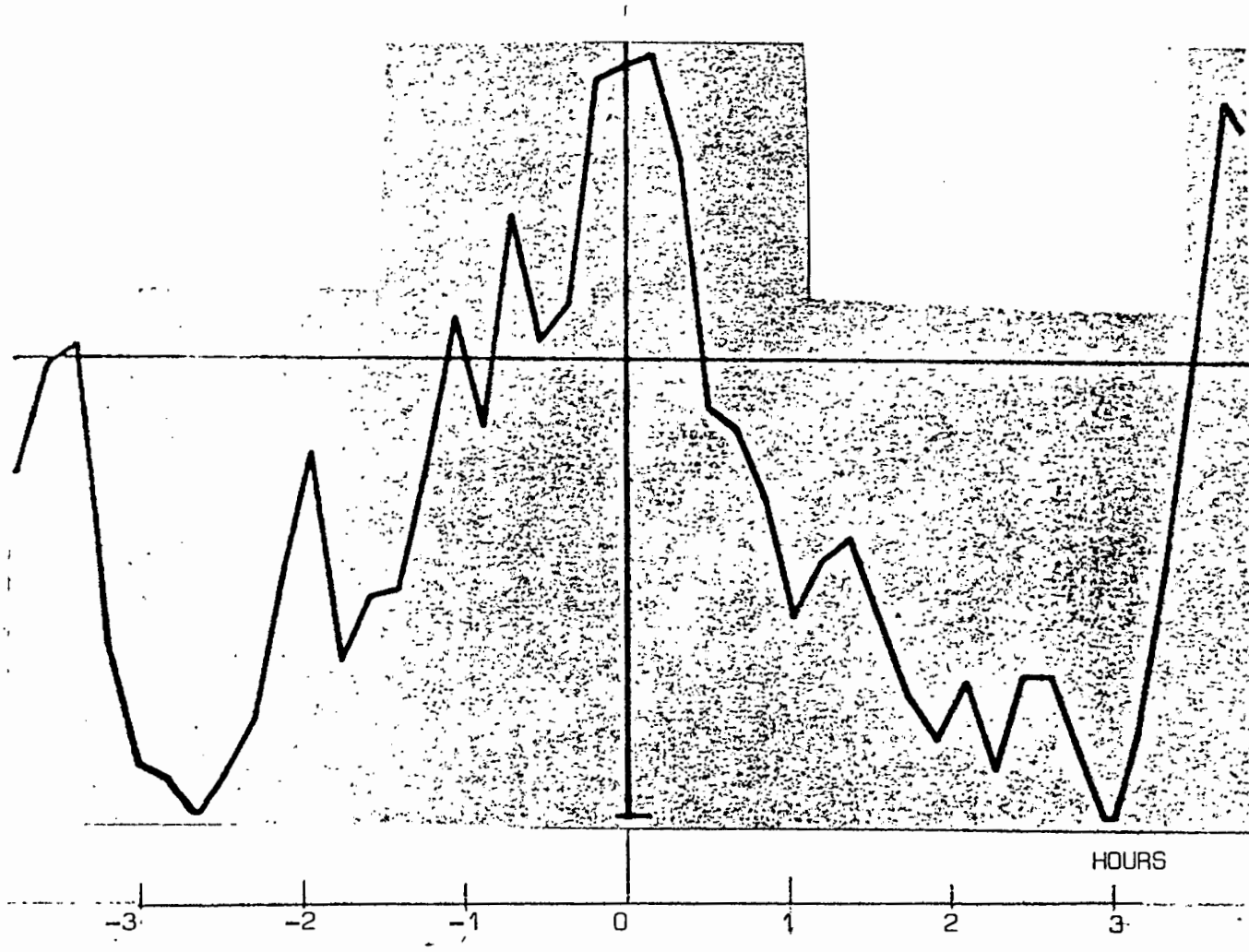

DIAGRAM 8.2

is also approximately 10 minutes.

8.3 CROSS ANALYSIS BETWEEN ELECTRODE HOIST POSITION AND AMPLITUDE OF THE 300 Hz COMPONENT IN THE ACOUSTIC NOISE SIGNAL

The cross-correlation function was calculated in the same manner as above, using expression 8.1.1 with x_n the electrode hoist position data and y_n the amplitude of the 300 Hz component. Diagram 8.3 shows the cross-correlation plot, the number of points = N/2 = 125.

Diagram 8.4 shows another cross-correlation plot, using independent data from the same data collection instrumentation. This plot contains N/2 = 44 points.

After taking into account the different scales it was found that the two plots agree in that the function has a negative peak at a noise lag time of approximately 30 minutes.

8.4 CONCLUSIONS

The cross-correlation functions for the two sets of independent data on hoist position, current and amplitude of 300 Hz component did not have sufficient resolution to accurately determine lag times.

The points in the 44 point plots have a large variance which limits the accuracy of the peaks. In both the 44 and 125 point plots the resolution is limited by the sampling time.

The cross-correlation functions showed that all three of the parameters varied periodically with the same frequencies. To

CROSS CORRELATION FUNCTIONS OF ELECTRODE HOIST POSITION AGAINST AMPLITUDE OF THE 300 Hz COMPONENT IN THE ACOUSTIC NOISE.

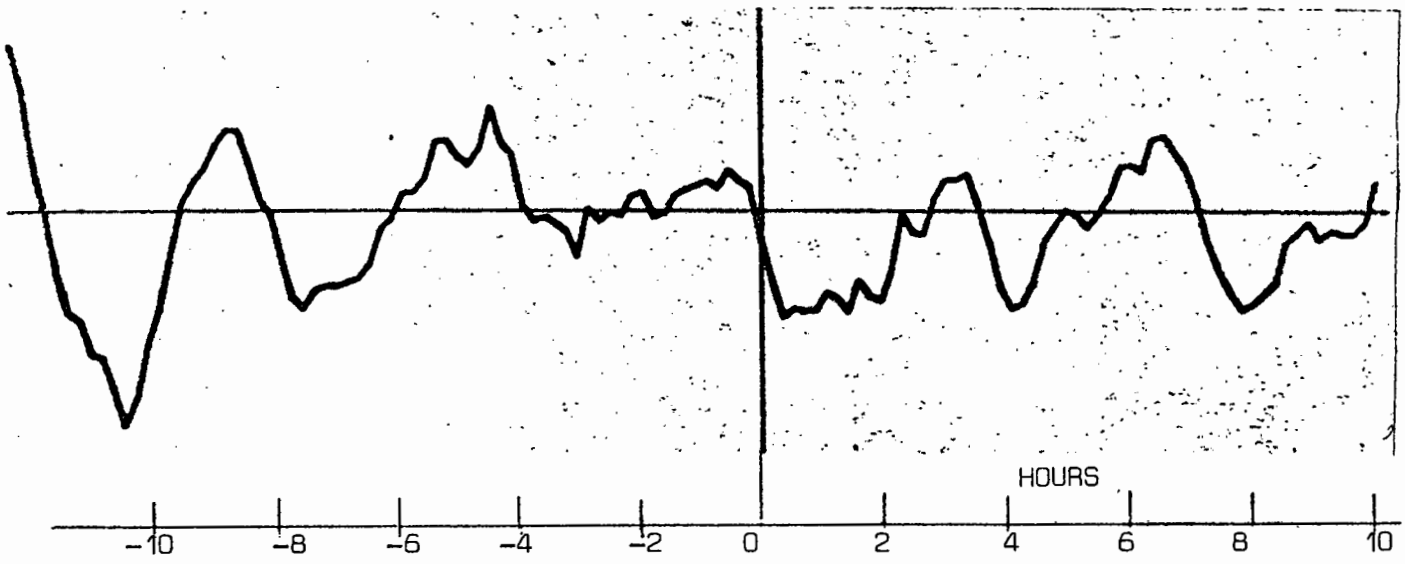

DIAGRAM 8.3

HOIST POSITION LAGS 300 Hz COMPONENT

HOIST POSITION LEADS 300 Hz COMPONENT

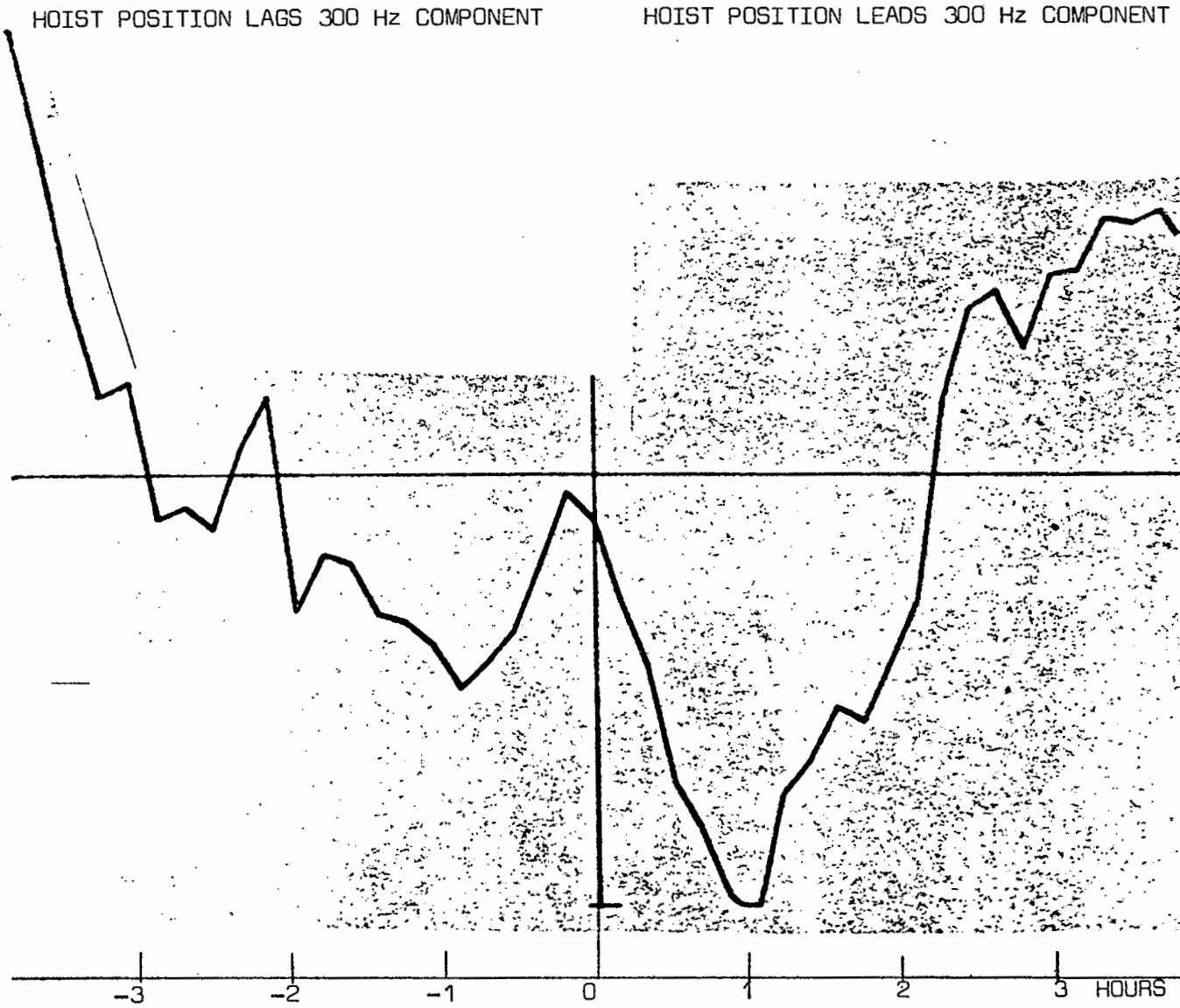

DIAGRAM 8.4

identify these frequencies the DFT of the 125 point cross-correlations were calculated. The 44 point cross-correlation had record lengths too short for accurate DFT analysis.

The DFT of the cross-correlation function is the cross spectral density function which indicates common frequencies in two data records.

A program was written which removed the mean value from the data and applied the cosine taper to the ends of the functions. The cross-correlation function does not require the formation of its mirror image as is required for the DFT of the autocorrelation function. The FFT was then applied which calculated the plots shown in Diagrams 8.5 and 8.6.

The following was noted from the plots:

(a) The error frequency component at 1/128h where h is the sample interval was absent in the plot relating to hoist position and was not dominant in the plot relating to current. This is due to the cross-correlation function performing more like a continuous function than the double-sided autocorrelation function.

(b) The plots were very similar in that both had distinct peaks at frequencies corresponding to periods of 11 hours 26 minutes and 3 hours 48 minutes. They can be described as a fundamental and a third harmonic.

FFT OF THE CROSS CORRELATION FUNCTION OF ELECTRODE CURRENT WITH THE AMPLITUDE OF THE 300 Hz COMPONENT IN THE ACOUSTIC NOISE. (CROSS SPECTRAL DENSITY PLOT)

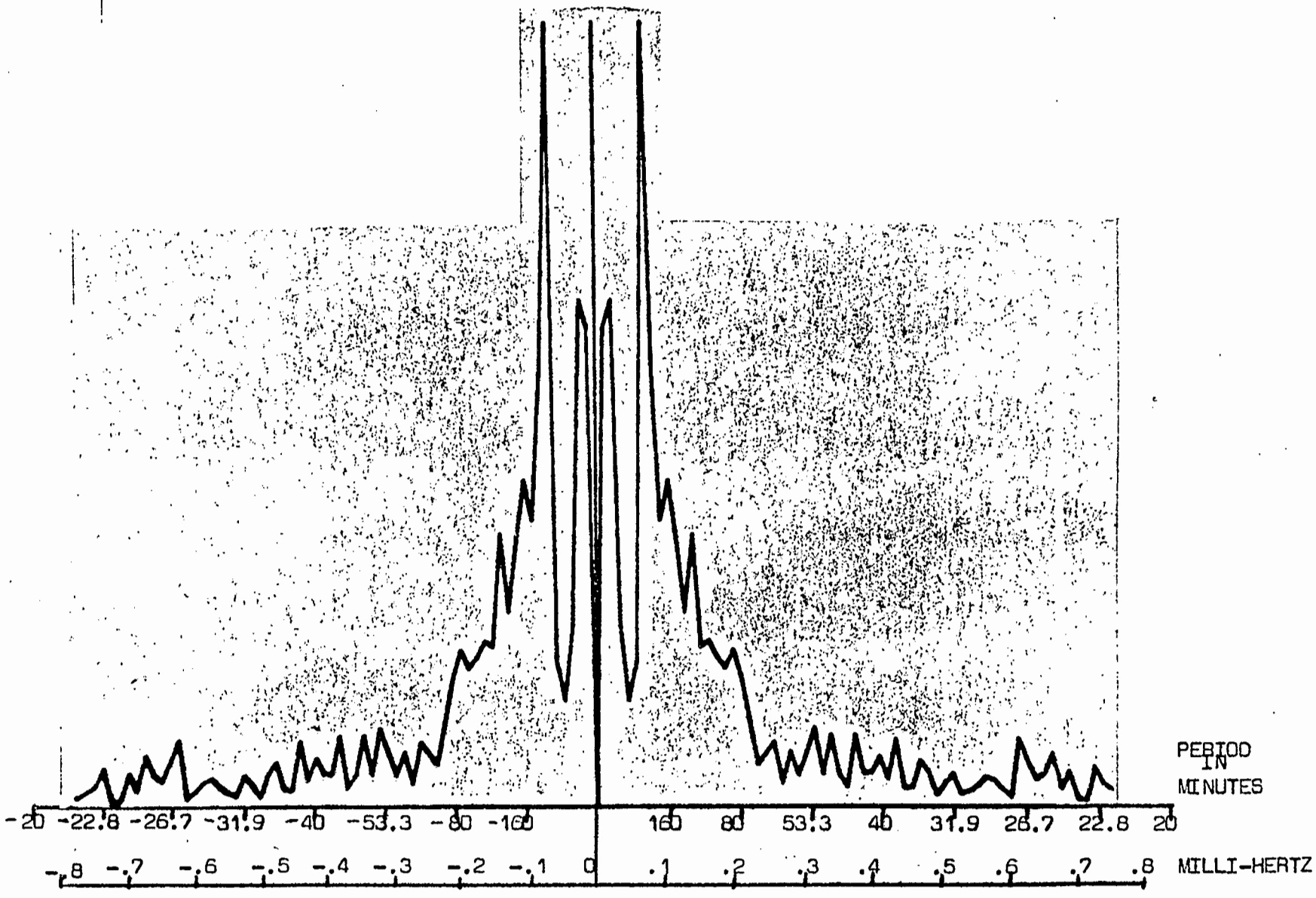

DIAGRAM 8.5

DIAGRAM 8.6

EET OF THE CROSS CORRELATION FUNCTION OF ELECTRODE HOIST POSITION WITH THE AMPLITUDE OF THE 300 Hz COMPONENT IN THE ACOUSTIC NOISE. (CROSS SPECTRAL DENSITY PLOT)

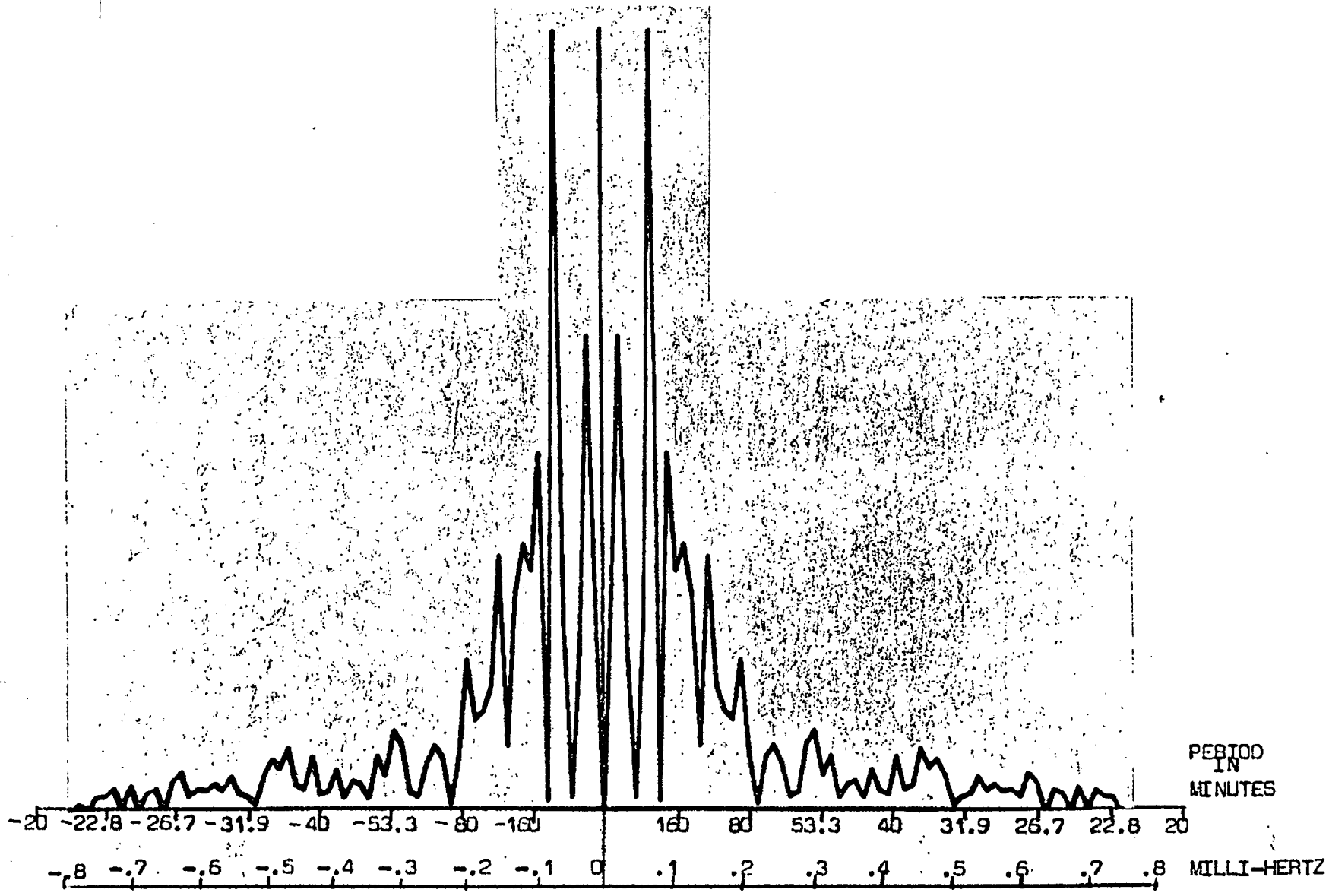

CONCLUSION

9.1 FURNACE OPERATING INFORMATION DETECTED IN THE ACOUSTIC NOISE

This project originated from a belief that furnace operators can hear 'how well' the furnace is operating, from the acoustic noise produced by the furnace.

The research was aimed at investigating this belief.

The instrumentation designed collected acoustic noise generated by the furnace. Appendix 10 is an instrumentation check done from an on-plant recording. It proves that the noise recorded is actual acoustic noise, not electrical noise pick-up.

A measure of 'how well' the furnace was operating was very difficult to achieve, as neither the furnace staff nor the researchers involved in investigating furnace operation could define what operating conditions indicated 'good' or 'bad' operation.

The furnace uses electrical power to melt ore. The power is applied via current flow through the furnace electrodes. This power 'injection' is dependent on the amount of current flowing and its conversion to heat via the undefined action at the electrode. The conversion is affected by the position of the electrode in a vertical plane as inferred from the electrode

hoist position.

From energy considerations, if the losses in the furnace are reasonable constant, than the heat produced to melt the ore is directly related to power injected into the furnace.

If the amount of ore melted reflects 'good' or 'bad' furnace operation, then from the above logic, the amount of current flowing in the electrode, and the position of the hoist holding the electrode give a measure of power injection and conversion and thus reflects 'good' or 'bad' operation.

The individual analysis described previously showed that, the two operating conditions chosen, the current and hoist positions varied with a definite period. The amplitude of the 300 Hz component in the acoustic noise varied with a similar period. Cross analysis proved that both operating conditions and the amplitude of the 300 Hz component in the acoustic noise have common frequencies.

The variations in the amplitude of the 300 Hz component in the acoustic noise are heard by the operators and gives them information about the electrode current and hoist position. This could explain the belief that the operators can 'hear' how well the furnace is operating.

The cross analysis was performed with two sets of sampled data records. The analysis agreed, but due to the second record being

only a third the length of the first record, and the fixed sample interval, the analysis accuracy was limited. Unfortunately these were the only sampled data records made, all the other acoustic noise records being continuous short term recordings. The furnace at the time of this date analysis was shut down for relining so further recordings could not be made.

The fixed sample interval of 10.75 minutes limited the number of in the data records which reduced the accuracy of the digital analysis technique and prevented accurate neasurement of lead or lag time in cross-correlation of records.

9.2 COMMENTS ON FURTHER ANALYSIS

The analysis used acoustic data collected near electrode 3 and data describing its hoist position and current. The acoustic noise at other electrodes is similar but not identical. Future analysis could be aimed at comparing the differences in operating conditions between the 3 electrodes, with the differences in the acoustic noise signals detected near the individual electrodes. This analysis would be very interesting but it is doubtful whether the conclusions would aid furnace operation.

The analysis of the furnace operating conditions was limited by the one minute sample format of the data. Thsi sampling interval is adequate for data-logging but limits the signal to a maximum frequency of 8 milli-Hertz. As described in Appendix 8, the acoustic noise could be created by rectification action of the arcing electrode. The variations in the periodic noise components could be caused by the variations in the arcing action. Future analysis could be directed at recording actual

current fluctuations and performing signal processing analysis to investigate the actual mechanism of energy conversion. The electrodes could be analyzed separately without the problem of inter-electrode interference.

Analysis could also be done using noie data samples collected at long intervals, e.g. 1 week. This would allow the noise to be correlated with furnace production. Noise signatures associated with 'good' and 'bad' operation could be determined.

The low level random noise not heard by the operators could carry information abour physical conditions in the furnace, e.g. bubbling and metal level. Future analysis could investigate these low level signals by filtering the 100 Hz component and its harmonics from the acoustic noise signals. This would be similar to the work done by Higgs (Ref. 1).

REFERENCES

1. Noise Statistics in an Electric Arc Furnace, by Roland W. Higgs, Emmanuel P. Papadakis and Walter K. Sheets.

   IEEE Transactions on Sonics and Untrasonics, Vol. SU-23 No. 1, January, 1976.

2. Random Data: Analysis and Measurement Procedures, by Julius S. Bendat and Allan G. Piersol.

3. George C. Marshall Space Flight Centre Vibration Manual by the MSFC Vibration Committee.

4. Fundamentals of Acoustics, by Kinsler and Frey.

5. N.I.M. Technical Memos Instruments Division, IB/CC 10.2.76 and 11.2.76. Reference Ian Barker.

6. Siliconic Application Note A N 74-6. November, 1974, Keith Davies.

7. Digital Processing of Signals, by B. Gold and C.M. Rader.

8. The Measurements of Power Spectra From the Point of View of Communications Engineering, by Blackman and Tukey.

9. The Fast Fourier Transform, by E.O. Brigham.

10. FOUR*ABS Fourier Transform Routines Package (MACC) U.C.T. Computer Centre Library.

A P P E N D I X 1.

This Appendix contains the data sheets for the accelerometer used in detecting the acoustic noise analysed.

The data sheets describe the Models 213E and 233E.

Model 213E was the accelerometer used.

ENDEVCO PRODUCT DATA

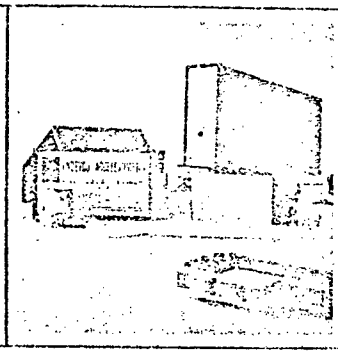

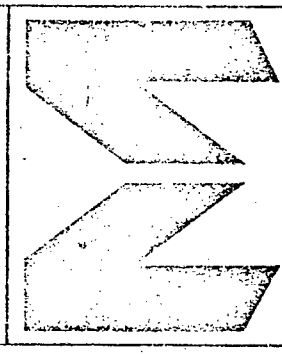

MODELS 213E 233E

Flat Charge Characteristics

HIGH SENSITIVITY ACCELEROMETERS

These accelerometers are versions of well-proven designs that have received wide acceptance in the field of shock and vibration measurement.

Piezite® Element Type P-8 crystal material combines high sensitivity, flat charge characteristics, high resonant frequency, broad temperature range, and high capacitance to give these accelerometers a high degree of versatility in the expanding field of shock and vibration measurement.

Model 233E is a premium version of the Model 213E. It features low transverse sensitivity and all-welded hermetic seal. In addition, the Model 233E operates to 260°C instead of 177°C. Models 213E and 233E utilize self generating piezoelectric crystals and do not require external power for operation.

ACTUAL SIZE

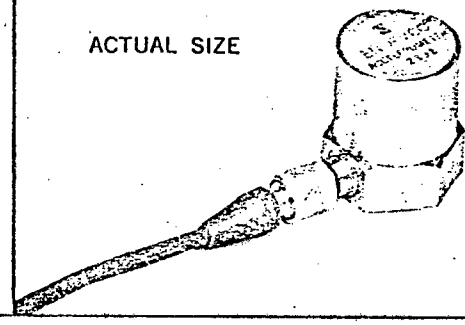

SPECIFICATIONS FOR MODELS 213E AND 233E ACCELEROMETERS

(According to ANSI and ISA Standards)

DYNAMIC

CHARGE SENSITIVITY	60 pC/g, nominal; 45 pC/g, min.
VOLTAGE SENSITIVITY[1]	45 mV/g, nominal
MOUNTED RESONANCE FREQUENCY	32,000 Hz, nominal
FREQUENCY RESPONSE (±5%)[2]	Charge: 4 to 6000 Hz, nominal[3] Voltage: 2 to 6000 Hz, nominal
TRANSVERSE SENSITIVITY	
213E	5%, max.
233E	3%, max., 1% on special selection
AMPLITUDE LINEARITY	Sensitivity increases approximately 1% per 150 g, 0 to 1000 g.
TRANSDUCER CAPACITANCE	1000 pF, ±20%
RESISTANCE	20,000 MΩ, min. at 22°C (72°F) 1000 MΩ, min. at 177°C (350°F) 500 MΩ, min. at 260°C (500°F) (233E only)

NOTES

[1]With 300 pF external capacitance.

[2]In shock measurements, minimum pulse duration for half-sine or triangular pulses should exceed 0.15 msec to avoid excessive high frequency ringing. (See Endevco Piezoelectric Accelerometer Manual.)

[3]Use ENDEVCO® 2640 Series or 2700 Series Charge Amplifiers.

TYPICAL TEMPERATURE RESPONSE

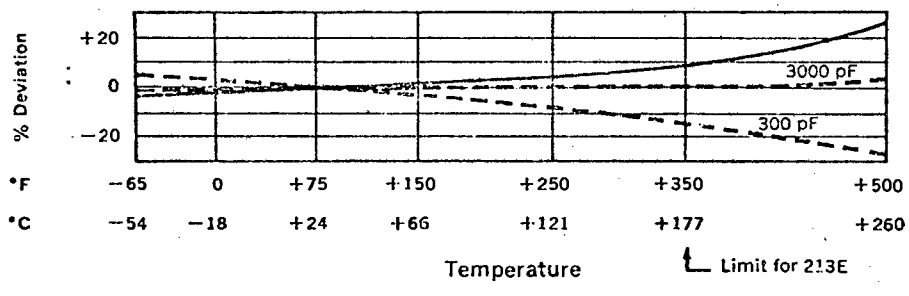

The solid curve shows the nominal charge-temperature response. The nominal voltage-temperature response is illustrated by the dashed curves with external capacitances as indicated.

TYPICAL FREQUENCY RESPONSE

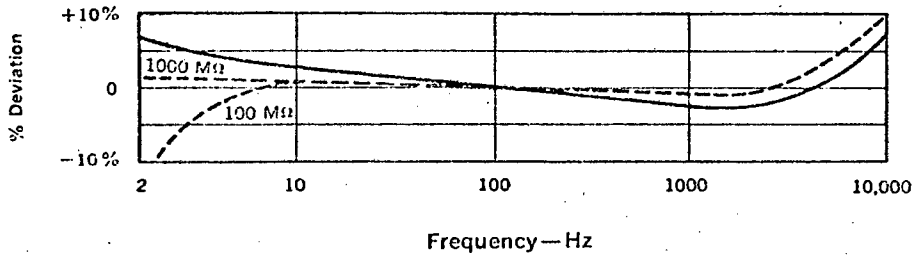

The solid line shows the charge-frequency response. The broken lines show the voltage-frequency response with the loads shown. Estimated calibration errors:
5 to 1000 Hz: ±1.5%
1000 to 10,000 Hz: ±2.5%

SPECIFICATIONS FOR MODELS 213E AND 233E

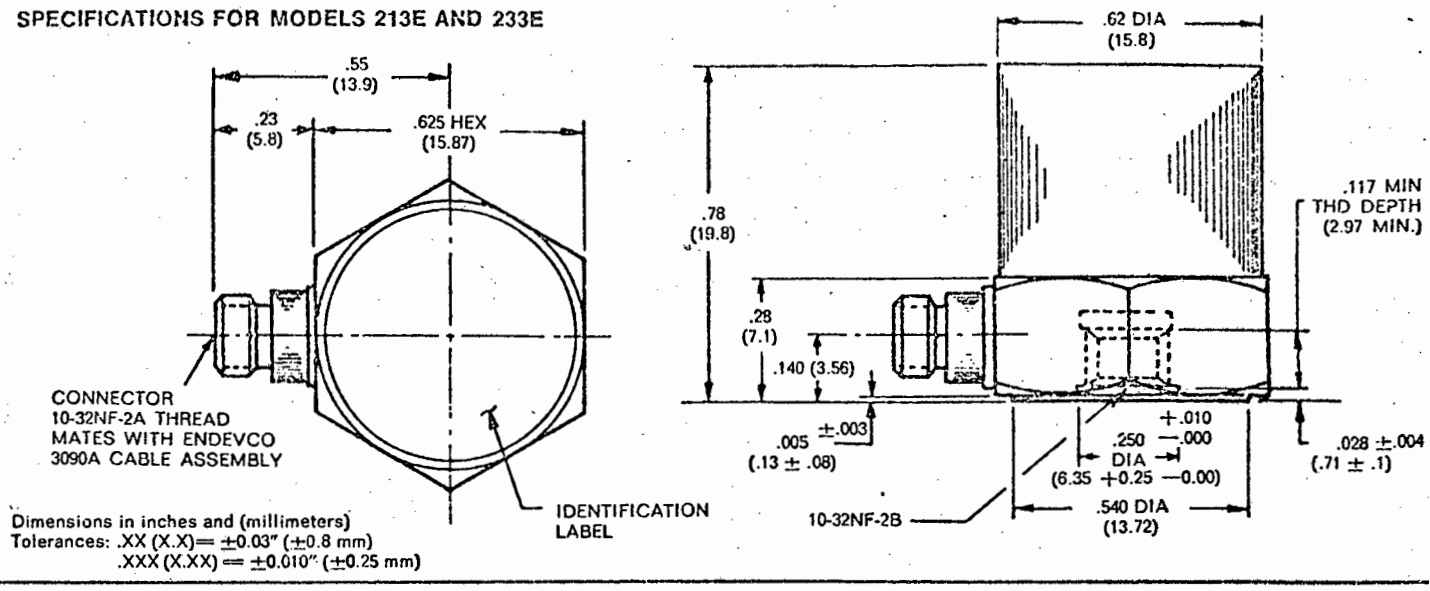

Dimensions in inches and (millimeters)
Tolerances: .XX (X.X)= ±0.03" (±0.8 mm)
.XXX (X.XX) = ±0.010" (±0.25 mm)

PHYSICAL

DESIGN	Single-Ended Compression
WEIGHT	32 grams (1.2 ounces) nominal
CRYSTAL MATERIAL	Piezite® Element Type P-8
CASE MATERIAL	Stainless Steel
CONNECTOR	Coaxial, 10-32 thread, mates with accessory cable.
MOUNTING	Tapped hole for 10-32 ENDEVCO® Mounting Stud. Recommended Mounting Torque: 2 Nm (18 in.-lb.)
GROUNDING	Signal return connected to case.
ACCESSORIES INCLUDED	Model 2981-4 Mounting Stud with 10-32 accelerometer mating thread and M5 metric thread, or Model 2981-3 with 10-32 to 10-32 threads.
	Model 3090A-120 Low Noise Cable Assy., 3 m (10 ft.), 300 pF nominal.
ACCESSORIES AVAILABLE	Model 2986M3 Insulated Mounting Stud with 10-32 accelerometer mating thread and M5 metric thread.
	Model 2986B Insulated Stud with 10-32 to 10-32 threads.

ENVIRONMENTAL

ACCELERATION LIMITS	Vibration: 1000 pk g, sinusoidal, in any direction Shock: 2000 g, in any direction.
TEMPERATURE	213E: —54°C to 177°C (—65°F to 350°F) 233E: —54°C to 260°C (—65°F to 500°F)
BASE STRAIN SENSITIVITY	25 equivalent g, nominal, at 250 μ strain.
MAGNETIC SENSITIVITY	0.00005 equivalent g per gauss, nominal, at 60 Hz.
ALTITUDE	Not affected
HUMIDITY	213E: Epoxy sealed 233E: All-welded hermetic seal

Continued product improvement necessitates that Endevco reserve the right to modify these specifications without notice.

RELIABILITY: Endevco maintains a program of constant surveillance over all products to ensure a high level of reliability. This program includes attention to reliability factors during product design, the support of stringent quality control requirements, and compulsory corrective action procedures. These measures, together with conservative specifications, have made the name Endevco synonymous with reliability.

CALIBRATION: Each unit is calibrated at room temperature for sensitivity, capacitance, transverse sensitivity, and charge-frequency response from 20 to 4000 Hz. Temperature calibration at —54°C (—65°F), 22°C (72°F), 177°C (350°F), (260°C for 233E), and other calibrations are furnished upon special order. See Calibration Service Bulletin No. 301.

Consult the Endevco Export Price Schedule or the nearest Endevco Representative for current prices.

A P P E N D I X 2.

The information in this Appendix is from the Endevco Instruction Manual on Piezoelectric Accelerometers.

ACCELEROMETER OPERATION

Equivalent Circuits of Piezoelectric Accelerometers.

The equivelent circuit for a piezoelectric transducer is shown in Figure A2.1. In practice, the internal resistance, R_s shown in circuit A2.1A normally exceeds 20,000 megohms and, thus, can be ignored when considering the over-all transducer performance. Similarly, effects due to the internal inductance are not significant until far beyond the upper frequency limit of the transducer and can also be ignored. The simplified circuit (Fig. A2.1b) is adequate for applications analysis.

The piezoelectric transducer is effectively a capacitor which produces a charge, q, accross its plates proportional to a force applied to the crystal. The open circuit voltage, e, out of the transducer is equal to the generated charge divided by the transducer capacitance,

or $e\ (\text{volts}) = \frac{q\ (\text{picocoulombs})}{Cp\ (\text{picofarads})}$. Thus, the transducer can also be represented as a voltage generator and a series capacitance (Fig. A2.1c).

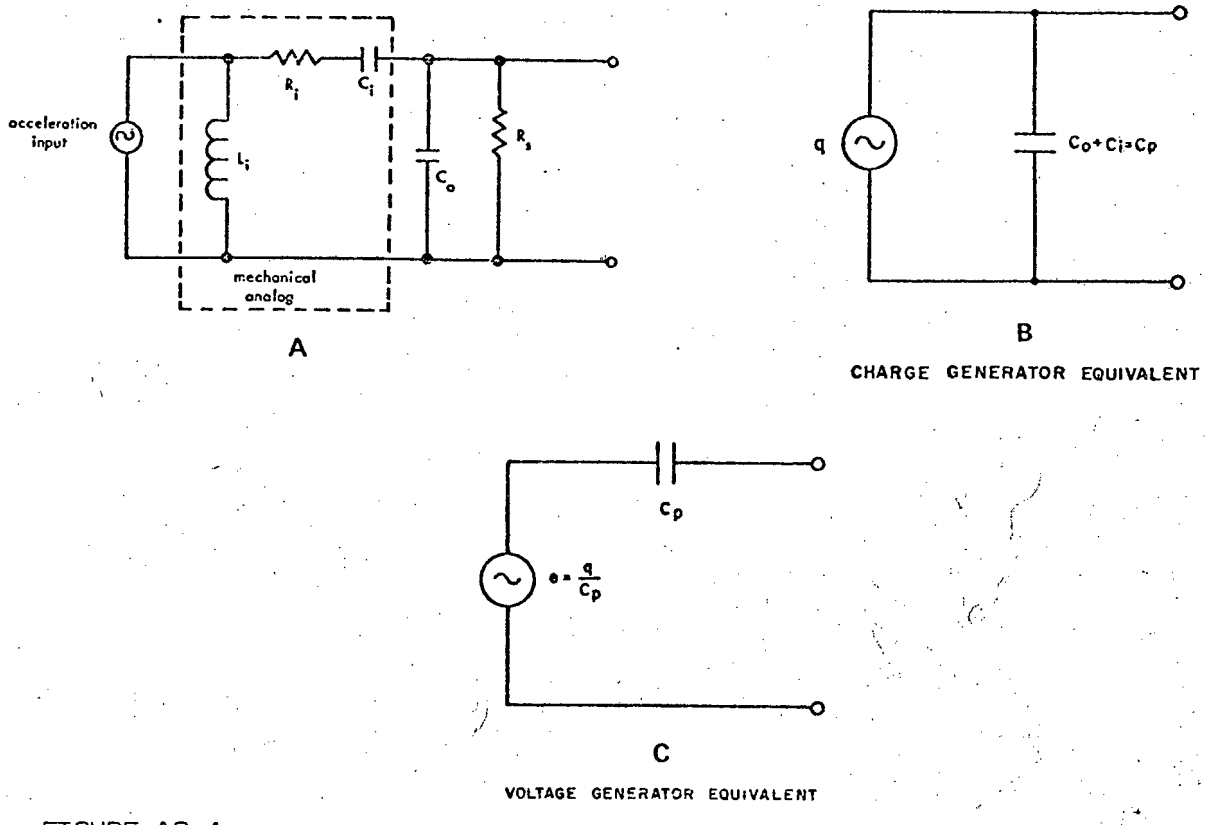

FIGURE A2.1

Equivalent circuits for a piezoelectric transducer (A) actual circuit, (B) charge generator equivalent, and (C) voltage generator equivalent.

Accelerometer Sensitivity

The sensitivity of an accelerometer is defined as the ratio of its electrical output to its mechanical input. It may be expressed in units of charge per unit of acceleration or voltage per unit of acceleration. It is most important the terms in which the respective parameters are expressed: e.g. average, rms, or peak.

Charge Sensitivity

Each accelerometer is provided with a charge sensitivity calibration, Q, expressed in picocoulombs per g(pC/g). This is measured directly or derived from Q EC, where Q is expressed in picocoulombs, E in Volts, and C in picofarads. This calibration is used when the accelerometer is operating into charge measuring electronics. Note that magnitude of sensitivity can be expressed in other terms:

$$\frac{\text{pC}}{\text{g}} = \frac{\text{rms pC}}{\text{rms g}} = \frac{\text{pk pC}}{\text{pk g}} = 1.41 \frac{\text{rms pC}}{\text{pk g}}$$

Voltage Sensitivity

Calibration cards also carry the accelerometer voltage sensitivity, E, in millivolts per g (mV/g) as calculated with a stated amount of external capacitance connected to the accelerometer.

Effect of Cables on Sensitivity

When performing measurements, the transducer circuit involves an external capacitance and a shunt resistance. The external capacitance C_t is commonly cable capacitance plus input capacitance of the associated amplifier. The shunt resistance R_i is commonly the input resistance of the associated amplifier. (Figure A2.2).

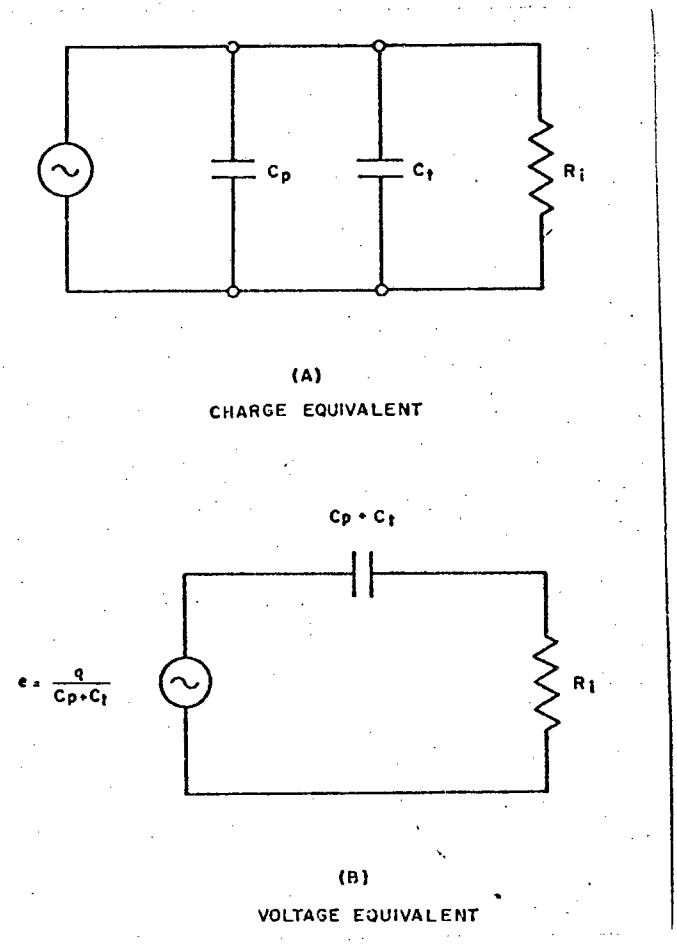

Figure A2.2. Equivalent circuits for a normal piezoelectric transducer system; (A) charge equivalent, and (B) voltage equivalent.

Since the charge generated does not change, regardless of the amount of external capacitance added, the charge sensitivity of the accelerometer remains unaffected by the length of interconnecting cable. This characteristic explains the practical advantage of a system incorporating charge measuring electronics rather than voltage amplifiers.

When using voltage amplifiers, the amount of external capacitance must be considered in establishing the signal at the input of the amplifier. With added capacitance, the output voltage (appearing accross R_i) becomes:

$$e = \frac{q}{C_p + C_t}$$

The total system capacitance during actual use may differ from the capacitance that was used in the original calibration. This changes the basic voltage sensitivity up or down by a calculable amount. The new sensitivity can be determined with either of two equations:

$$E = \frac{Q}{C_p + C_t} \times 1000 \qquad (1)$$

Where:

E = new sensitivity being determined, in millivolts per g (mV/g)

Q = factory supplied charge sensitivity, in picocoulombs per g (pC/g)

C_p = transducer internal capacitance, in picofarads (pF).

C_t = total capacitance external to the transducer for which E is being established, in picofarads (pF).

Another form of Equation 1 can be written as:

$$E = E_{cal} \frac{C_p + C_{cal}}{C_p + C_t} \qquad (2)$$

Where:

E = new sensitivity being determined, in mV/g.

E_{cal} = factory supplied voltage sensitivity, in mV/g.

FREQUENCY RESPONSE

Low Frequency Response

A piezoelectric accelerometer is a self-generating transducer that produces an electrical output signal that is proportional to acceleration, without the use of an external power source or carrier voltage. In practice, such a transducer cannot be used to measure constant or steady-state accelerations. At zero frequency no mechanical energy is being put into the system, thus electrical energy cannot be continuously removed.

When using charge amplifiers the system low frequency response is determined primarily by the low frequency response of the amplifier. The length of cable between transducer and amplifier will not affect the low frequency of the system, which is limited only by the characteristics of the amplifier.

When using voltage amplifiers, the low frequency response of a piezoelectric accelerometer is a function of the RC time constant of the accelerometer and the input resistance of the matching electronics.

Of course, the low frequency response of any accelerometer can be improved by swamping with additional shunt capacitance, such as long cables, to raise the RC time constant. However, this technique will also affect sensitivity as discussed on the preceding pages.

Actual response at any frequency can be measured from Figure A2.3.

Where:

f = frequency in Hz

R = input resistance of the matching amplifier in ohms

C = total capacitance in farads of the accelerometer, plus additional applied shunt capacitance, if any.

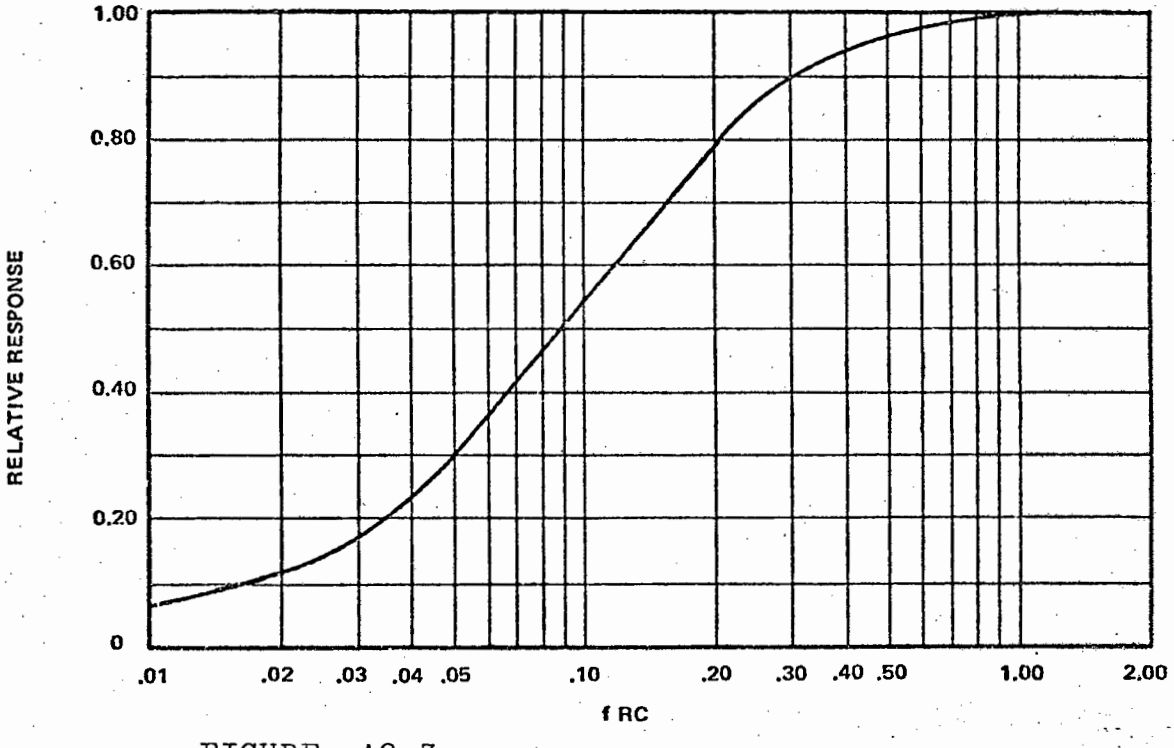

FIGURE A2.3
Low Frequency response vs. loading (voltage amplifiers).

APPENDIX 3.

LOW POWER VOLTAGE BUFFER.

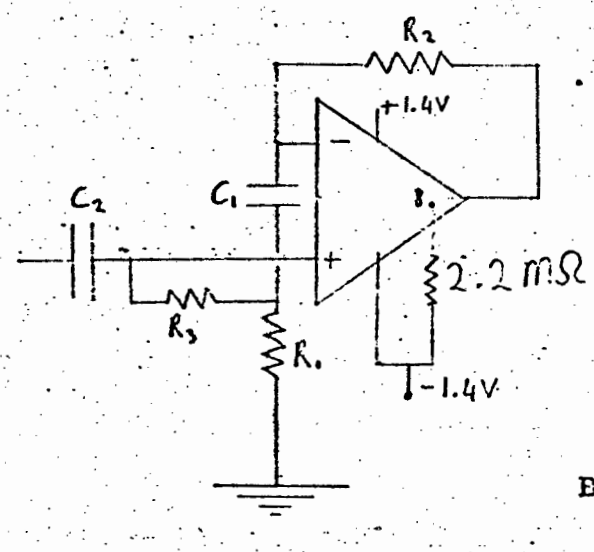

$R_2 = 0$

$R_3 = 10M\Omega$

$R_1 = 10K\Omega$

$C_1 = 1\mu F$

$C_2 = 1\eta F$

$$\text{Gain} = \left(1 + \frac{R_2}{R_1}\right) = 1 + \frac{0}{10^4} = 1$$

$$\text{Breakpoint at } \frac{1}{2\pi C_1 R_1} = \frac{1}{2\pi 10^{-6} 10^4} = \frac{100}{2\pi}$$

$$= \underline{15.92 \text{ Hz.}}$$

Device used LM4250 C

Set Current $\approx$ 1μA

Set resistor (pin 8 to -Ve) = 2.2 MΩ

Supply voltage ± 1.4V

Gain B.W product = 50 KHz

Slew rate 0.02 V/μS Open loop gain 10^5

Phase margin 30^0

Batteries MP 675 H 1.4 V 210 mAH.

A P P E N D I X 4.

This Appendix contains the specifications of the tape recorder used in recording the acoustic noise signals.

The recorder used was an EL 1020/07 portable instrumentation recorder completely wired for 7 channels equipped with 1 basic unit EL 1020/10 and 7 processing amplifiers EL 1020/20.

INTRODUCTION

The EL 1020 equipment can instantaneously and simultaneously record up to seven variable electrical signals at a high rate and in accurate mutual phase relationship, and reproduce them at the same or a different rate; each signal being the electrical equivalent of the magnitude of a phemomenon under investigation (e.g. temperature, position, pressure, flow rate) in analogue form i.e., the amplitude of the signal is proportional to the quantity to be recorded) or digital form (the quantity to be recorded being expressed numerically and then encoded into a train of pulses). The seven 'channels' are supplemented by an eighth one, the audio channel, for the recording of speech and other less critical information.

The signals can be recorded immediately after suitable amplification (direct recording, 'DR'), or they first modulate the frequency of a carrier generator incorporated in the recording channel ('FM' recording).

The latter method can be of advantage when particularly accurate recording of transient and drift phenomena is required. With frequency modulation, one track may be employed for the recording of an unmodulated carrier. Playback of this carrier will reveal any small but inevitable tape speed deviations, and this can be used for electronic flutter compensation in signals derived from other channels. This permits low tape speed recordings to be used at their full efficiency.

Each of the seven main channels has an all- in processing amplifier of the plug-in type.

This modular unit contains recording, playback and output amplifiers, a frequency modulator and a demodulator. The time constants of the networks and other circuits are automatically changed when the tape speed is changed. Each amplifier has a DR/FM switch, gain controls, a modulation meter and controls for calibration and signal level indication.

In the course of a recording operation, separate playback heads permit 'off tape' monitoring.

The magnetic erase, recording and playback heads are made of ferroxcube, a NiZn ferrite of high density, high wear-resistance, low losses and excellent magnetic properties.

The material permits the manufacture of fine and accurately positioned gaps handling very short wavelengths. Head currents and consequent temperature rises are low.

The tape is driven by two capstans, one before and one after the recording and playback head assemblies. The capstans are driven by a belt from the capstan motor. There are four tape speeds, 30, 15, 33/4 and 15/16 inch per second, accurately servo-controlled by a crystal oscillator with frequency dividers. A photo-diode is exposed through a slotted disc on the motor shaft. The resulting signal is compared with the signal from the crystal oscillator, by means of which the speed of the capstan motor is controlled. Slow playback (a maximum of 32-fold expansion can be obtained) facilitates re-writing the information in a pen recorder (strip chart); fast playback (up to 32-fold compression) permits visual analysis with the aid of oscilloscopes.

Recording is done after the IRIG standards on $\frac{1}{2}$" magnetic tape, kept and handled in a special cartridge, which is inserted and removed through a 'pillar-box' slot in the recorder front panel. The cartridge protects the tape against dust and damage. The tape is fully automatically threaded and unthreaded, and the machine can be operated by untrained personnel.

The recorded tape can be repeatedly played back on the equipment itself or, after it has been removed from the cartridge, on any other IRIG standardised recorder taking NARTB reels Likewise, it will play back IRIG recorded tapes from other machines.

The tape movement and the channel circuitry are controlled, via 'logic' circuits controlled by five pushbuttons and two rotary selectors. Operation it also possible by pushbuttons on a remote control box.

The audio channel serving the eighth track written on the tape edge has a microphone with switch, recording amplifier with automatic level control and a built-in loudspeaker.

All these recording and playback functions are combined in a relatively small piece of equipment, which can be lifted an moved by one man.

Apart from its power source, which may be the AC mains or a storage battery, the instrument is completely self-contained. As the mechanism is suspended in shock absorbers and the electronic circuitry is solid-state, it can be operated while travelling by air, road or rail. It will function in the vertical as well as in the normal horizontal position. It can also be mounted in a standard 19" rack by means of a mounting kit.

MECHANICAL LAY-OUT

The recorder basically consists of the following units:

* a frame with carrying handle, panels, brackets, etc:, protecting the interior and supporting the sub-assemblies, connectors, switches etc; this frame can be modified easily for mounting in standard 19" instrument racks.
* a tape deck

  Containing the tape transport and automatic threading mechanisms, the tape cartridge holder, the magnetic head assemblies for 7 channel operation and ancillary devices; this tape deck is mounted in shock absorbers.
* an amplifier compartment

  With rails and plug-in connectors for up to seven processing amplifiers, each amplifier carrying on its front panel the pre-set controls which are normally located behind a cover panel. The compartment is completely wired for 7 amplifiers.
* a power supply unit

  Comprising mains adapter, mains transformer, rectifiers and voltage stabilizing circuitry, a chopper circuit for battery supply and an oscillator section with dividers. The unit is cooled with a fan.

RECORDING METHODS

Depending on the signal to be recorded, a selection can be made from 2 recording methods.

1. Direct recording (DR)

   With this conventional recording system, the signal itself, after suitable amplification and superposition of H.F. bias (pre-magnetisation), a rather wide frequency range can be covered (see chapter E-4 Technical Data).
   The use of ferroxcube heads eliminates the necessity of electronic corrections in the recording amplifier.
   In the play-back section of the amplifier, the frequency response of the playback head only is corrected by L.C. and feedback circuits.

2. Frequency Modulated (F.M.) Recording

   The frequency (F_o) of a carrier signal generated in the recording amplifier is modulated by the amplitude of the incoming signal, with the result that the carrier frequency varies proportionally to the amplitude of the input signal. If, for example, the input voltage varies between + and -1 V, the frequency of the recorded signal will vary between fo + 0.4 fo and fo - 0.4 fo.
   The overall frequency sweep applied with this system is therefore 80 %.
   However, only the frequency of the recorded signal is of importance, i.e. the number of times that the signal becomes 0 V. The shape of the signal on the tape is of less importance.
   Irregularities of tape movement (flutter) cause undesired frequency variations which show up, after demodulation, as a spurious signal.
   This interference can be practically eliminated by recording an unmodulated carrier on an otherwise unused track. After demodulation, spurious signals, caused by "flutter" can thus be isolated and subtracted from the signal played back from the other tracks (see chapter G-11 Miscellaneous operations, point a).

TECHNICAL DATA

1. General data

Power supply voltage	110 V; 125 V, 220 V or 245 V ± 10 % 50 or 60 Hz or 24 V d.c. (± 1.5 V)
Power consumption	max. 200 VA
Position during operation	horizontal or vertical
Ambient temperature	In operation : 0°...+45°C Storage : -40°...+75°C.
Relative humidity	5..95 %, if not condensing
Dimensions	height 11.8 inch (300 mm) width 17.6 inch (450 mm) depth 24.6 inch (620 mm) Mounted in a 19 inch rack, the maximum depth is 20 inch (510 mm)
Weight	Depending on the number of channels from 100..121 lbs (46..55 kg).

2. Tape transport

Start time	< 8 sec. at 30 in/s ≤ 6 sec. at 15 in/s ≤ 4 sec. at 33/4 in/s ≤ 4 sec. at 15/16 in/s
Stop time	< 1 sec. at all speeds
Rewind time	< 5 min. for an 8-inch reel containing 1800 ft of tape.
Tape speeds	30 in/s. - 76 cm/s 15 in/s. - 38 cm/s 33/4 in/s. - 9.5 cm/s 15/16 in/s. - 2.375 cm/s
Speed ratio	32:1.
Playing time with long-play tape	at 30 in/s. : 11 minutes at 15 in/s. : 22½ minutes at 33/4 in/s. : 1½ hours at 15/16 in/s. : 6 hours
Playing time with extended play tape	at 30 in/s. : 22½ minutes at 15 in/s. : 45 minutes at 33/4 in/s. : 3 hours at 15/16 in/s. : 12 hours
Tape width	½ inch
Speed deviation	Within 0.2 % of the nominal value
Wow and flutter measured in a band width up to 300 Hz	at 30 in/s. max. 0.18 % peak at 15 in/s. max. 0.20 % peak at 33/4 in/s. max. 0.40 % peak at 15/16 in/s. max. 0.70 % peak

3. Heads

Number of channels	seven + one audio channel
Recording head	combined in two stacks
Playback head	combined in two stacks
Track width	0.05 ± 0.005 inch
Track spacing	0.07 inch
Spacing between stacks (gap-to-gap)	1.500 ± 0.001 inch
Gap scatter	< 0.02 mil (0.5 μm)
Gap azimuth	90° ± 1 minute of arc to the base plate
Gap length	recording head 3.5 μm ± 20 %
	playback head 1.9 μm ± 20 %
Head standards	IRIG specification 106-66
Inductances	recording head 0.1 mH ± 15 %
	playback head 2.0 mH ± 15 %
Cross-talk between adjacent tracks	better than-36 dB
Static skew measured between 2 adjacent tracks of the same head stack at 30 in/sec.	
	< 3 μsec.
Dynamic skew	3 μsec peak-to-peak at 30 in/sec
	(between the 2 outer tracks the total skew is about 8 μsec at 30 in/sec)

4. Direct Recording/Playback system

Frequency response	at 30 in/s. 250..100,000 Hz ± 3 dB
	at 15 in/s. 250.. 50,000 Hz ± 3 dB
	at 33/4 in/s. 250.. 12,500 Hz ± 3 dB
	at 15/16 in/s. 500.. 3,000 Hz ± 3 dB
2nd and 3rd distortion	≤ 1 %
Signal-to-noise ratio measured in	
a pass band from: 250 Hz to 100 kHz	at 30 in/s. -36 dB
250 Hz to 50 kHz	at 15 in/s. -36 dB
250 Hz to 12.5 kHz	at 33/4 in/s. -36 dB
250 Hz to 3 kHz	at 15/16 in/s. -36 dB
Input level adjustable	from 0.1 V r.m.s. to 5 V r.m.s. in 5 steps
Input impedance	> 18,000 Ω
Output level	1 V r.m.s. nominal across 1000 Ω
Output impedance	30 Ω
H.F. bias frequency	432 kHz

5. F.M. Recording/Playback system

Central frequency	at 30 in/s - 54 kHz
	at 15 in/s - 27 kHz
	at 33/4 in/s - 6750 Hz
	at 15/16 in/s - 1688 Hz
Max. frequency sweep	± 40 %
Overall frequency response	

Tape speed	Frequency range	Tolerance
30 ips	0 Hz...10 kHz	30 Hz 0 dB ± 0.5 dB
		5 kHz -1 dB ± 0.5 dB
		10 kHz -3 dB ± 0.5 dB
15 ips	0 Hz... 5 kHz	30 Hz -0 dB ± 0.5 dB
		2.5 kHz -1 dB ± 0.5 dB
		5 kHz -3 dB ± 0.5 dB
$3\frac{3}{4}$ ips	0 Hz...1250 Hz	30 Hz 0 dB ± 0.5 dB
		625 Hz -0.5 dB ± 0.5 dB
		1250 Hz -2.5 dB ± 0.5 dB
15/16 ips	0 Hz...312 Hz	30 Hz 0 dB ± 0.5 dB
		150 Hz -0.5 dB ± 0.5 dB
		312 Hz -2 dB ± 0.5 dB

On special request:

Overall frequency response:	the same frequency response, but with a tolerance of 0.5 dB instead of 3 dB at the upper frequency limits
Overshoot	: < 10 %
Rise time	: at 30 in/s - 30 µsec
	at 15 in/s - 60 µsec
	at 33/4 in/s - 240 µsec
	at 15/16 in/s - 1080 µsec
Input level	0.1 V-0.2 V-0.5 V-1 V-2 V or 5 V
(for max. frequency sweep)	(selection by calibrated attenuator switch)
Input impedance	18,000 Ω
Output level	1 V peak across 10,000 Ω
Output impedance	30 Ω

APPENDIX 5.

The notch filters were designed using Siliconix Application Note AN 74-6 (Reference 6). The filters used 3 LM308 operational Amplifiers to achieve a dual Integrator Resonator circuit which was arranged to give a band elimination second order transfer function of:

$$\frac{Ho\ (S^2 + \Omega^2)}{S^2 + Q_p + \omega_o^2} \qquad \text{where } Q_p = \frac{1}{2\zeta}$$

as shown in diagram A5.1

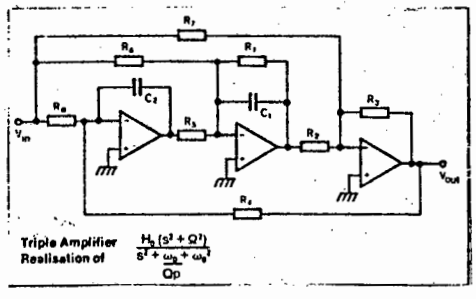

DIAGRAM A5.1

This can be written as

$$\frac{Vout}{Vin}(s) = -\frac{R_3}{R_7}\left\{\frac{s^2 - \left[\frac{R_1R_7 - R_7R_6}{R_1R_2R_6C_1}\right]s + \frac{R_7}{R_2R_5R_8C_1C_2}}{s^2 + \frac{1}{R_1C_1}s + \frac{R_3}{R_2R_4R_5C_1C_2}}\right\}$$

for band elimination the S term in the numerator must be zero;

therefore $R_1 R_7 = R_2 R_6$

then:

$$\Omega^2 = \frac{R_7}{R_2R_5R_8C_1C_2}$$

$$\omega_o^2 = \frac{R_3}{R_2R_4R_5C_1C_2}$$

$$Ho = -\frac{R_3}{R_7}$$

$$Qp = R_1C_1\sqrt{\frac{R_3}{R_2R_4R_5C_1C_2}}$$

$$R_1R_7 = R_2R_6$$

$$\frac{\omega_o}{Qp} = \frac{1}{R_1C_1}$$

To calculate the component values:

$$R_2 = R_3 = R_7$$

$$R_1 = R_6$$

Select $C_1 = C_2$

Select $R_5 = R_4$

Notch frequency $f_o = 2\pi SR$

and let $Q_p = 1.2$

The gain for $f < f_o = \frac{-R4}{R8}$

$f > f_o = \frac{-R3}{R7} = 1$

The notch frequency, and notch depth, can be adjusted independently by adjusting R_8 and R_6. The low frequency gain can then be set to 1 by adjusting R_4 which does not affect the notch frequency or depth.

Notch filters with notch frequencies of 50, 100, 150, 200, 300, 400 and 500 Hz were built and connected in series such that any combinations or all the notches could be switched into the line.

A P P E N D I X 6.

This appendix shows a list of the operating conditions recorded on digital magnetic tape. The Hoist Position and Secondary Current were found to have reliable data throughout the recording, but not all the channels were in reliable working order.

LIST OF VARIABLES RECORDED

Channel	Variable	Nominal range	Position in array RAF.
1	1)		53
2	2) Secondary current calculated from primary current.	0-100 × 100	54
3	3)		55
4	=)		13
5	2) Secondary power	0-10 × 1000	15
6	3)		14
7	1)		65
8	2) Power factor	0-1 × 10 000	66
9	3)		67
10	1)		20
11	2) Hoist position	0-1 × 10 000	21
12	3)		22
13	1)		62
14	2) Electrode resistance	0-1 × 10 000	63
15	3)		64
16	Total gas flow	0-5000 × 1	95+96
17	Carbon reduction	0-1000 × 1	91
18	CO	0-100 × 10	27
19	CO_2	0-100 × 10	28
20	CO/CO_2OR H_2	? or 0-10 × 100	(27/28) or 29
21	N_2	0-100 × 10.0	73
22	Power, MW	0-50 × 100.0	5
23	Power factor	0-1 × 10 000.0	52
24	Tap changer position	0-22 × 1	19
25	Average furnace resistance	0-2 × 1000.0	97

APPENDIX 7.

Taken from Reference 2.

STATIONARY RANDOM PROCESSES.

When a physical phenomenon is considered in terms of a random process, the properties of the phenomenon can hypothetically be described at any instant of time by computing average values over the collection of sample functions which describe the random process. For example, consider the collection of sample functions (also called the ensemble) which forms the random process illustrated in Figure A 7.1 .The mean value (first moment) of the random process at some time t_1 can be computed by taking the instantaneous value of each sample function of the ensemble at time t_1, summing the values, and dividing by the number of sample functions. In a similar manner, a correlation (joint moment) between the values of the random process at two different times (called the autocorrelation function) can be computed by taking the ensemble average of the product of instantaneous values at two times, t_1 and $t_1 + \tau$.

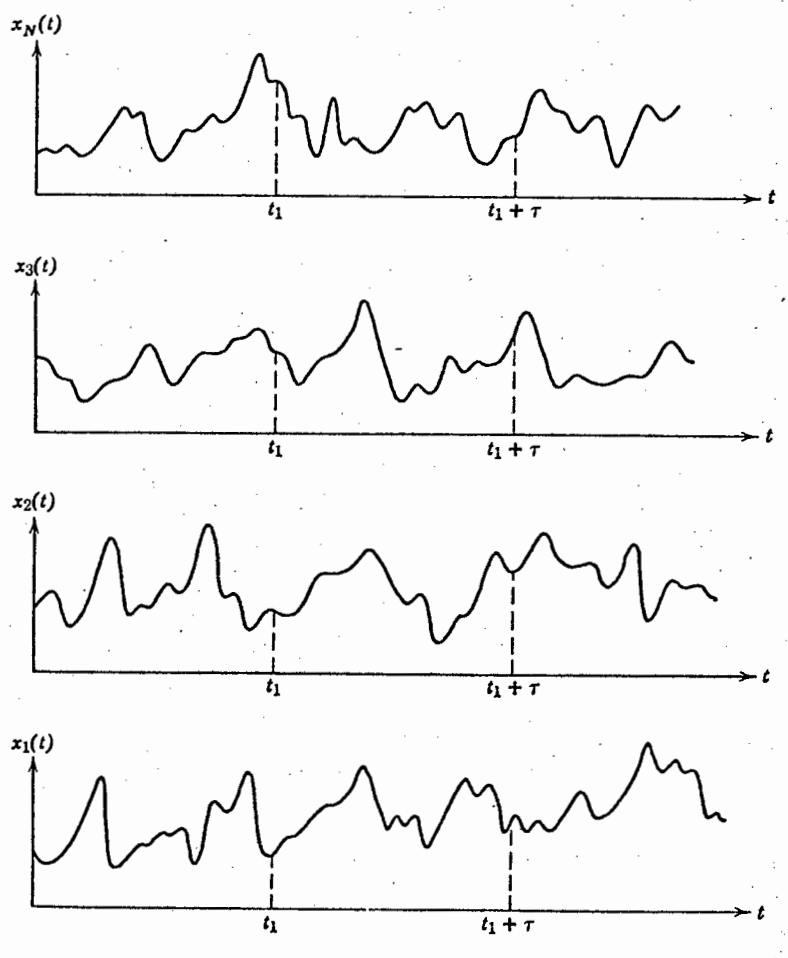

Ensemble of sample functions forming random process.

Figure A7.1

That is, for the random process {x(t)}, where the symbol { } is used to denote an ensemble of sample functions, the mean value $\mu_x(t_1)$ and the autocorrelation function $R_x(t_1, t_1 + \tau)$ are given by

$$\mu_x(t_1) = \lim_{N\to\infty} \frac{1}{N} \sum_{k=1}^{N} x_k(t_1)$$

$$R_x(t_1, t_1 + \tau) = \lim_{N\to\infty} \frac{1}{N} \sum_{k=1}^{N} x_k(t_1)\, x_k(t_1 + \tau) \qquad \text{A7.1}$$

where the final summation assumes each sample function is equally likely.

For the general case where $\mu_x(t_1)$ and $R_x(t_1, t_1 + \tau)$ defined in Equation A7.1 vary as time t_1 varies, the random process {x(t)} is said to be non-stationary. For the special case where $\mu_x(t_1)$ and $R_x(t_1, t_1 + \tau)$ do not vary as time t_1 varies, the random process {x(t)} is said to be weakly stationary or stationary in the wide sense. For weakly stationary random processes, the mean value is a constant and the autocorrelation function is dependent only upon the time displacement τ. That is, $\mu_x(t_1) = \mu_x$ and $R_x(t_1, t_1 + \tau) = R_x(\tau)$.

An infinite collection of higher-order moments and joint moments of the random process {x(t)} could also be computed to establish a complete family of probability distribution functions describing the process. For the special case where all possible moments and joint moments are time invariant, the random process {x(t)} is said to be strongly stationary or stationary in the strict sense. For many practical applications, verification of weak stationarity will justify an assumption of strong stationarity.

ERGODIC RANDOM PROCESSES.

The previous section discusses how the properties of a random process can be determined by computing ensemble averages at specific instants of time. In most cases, however, it is also possible to describe the properties of a stationary random process by computing time averages over specific sample functions in the ensemble. For example, consider the kth sample function of the random process illustrated in Figure A7.1. The mean value $\mu_x(k)$ and the autocorrelation function $R_x(\tau, k)$ of the kth sample function are given by

$$\mu_x(k) = \lim_{T\to\infty} \frac{1}{T} \int_0^T x_k(t)\, dt$$

$$R_x(\tau, k) = \lim_{T\to\infty} \frac{1}{T} \int_0^T x_k(t)\, x_k(t + \tau)\, dt \qquad \text{A7.2}$$

If the random process $\{x(t)\}$ is stationary, and $\mu_x(k)$ and $R_x(\tau,k)$ defined in Equation A7.2 do not differ when computed over different sample functions, the random process is said to be ergodic. For ergodic random processes, the time-averaged mean value and autocorrelation function (as well as all other time-averaged properties) are equal to the corresponding ensemble averaged values. That is, $\mu_x(k) = \mu_x$ and $R_x(\tau,k) = R_x(\tau)$. Note that only stationary random processes can be ergodic.

Ergodic random processes are clearly an important class of random processes since all properties of ergodic random processes can be determined by performing time averages over a single sample function. Fortunately, in practice, random data representing stationary physical phenomena are generally ergodic. It is for this reason that the properties of stationary random phenomena can be measured properly, in most cases, from a single observed time history record.

APPENDIX 8.

A HYPOTHESIS ON THE CAUSE OF THE PERIODIC COMPONENTS IN THE FURNACE ACOUSTIC NOISE

The voltage applied to the furnace electrodes is sinusoidal with a 50 Hz frequency. The manner by which the carbon electrode converts current to heat is not clearly defined but it is agreed that it is probably a resistance heating or arcing effect.

If arcing does occur the electrode could act as a full wave rectifier.

The Fourier series of a full wave rectified signal defined as

$$y = |\sin x| \quad \text{for} \quad -\pi < x < \pi$$

is

$$\frac{2}{\pi} - \frac{4}{\pi}\left[\frac{\cos 2x}{1.3} + \frac{\cos 4x}{3.5} + \frac{\cos 6x}{5.7} \ldots\ldots \frac{\cos nx}{(n-1)(n+1)}\right]$$

If sinx is a 50 Hz sinusoid then the full wave rectified signal contains a 100 Hz component and its harmonics. The amplitudes of the fundamental and its harmonics are

1, 0.198, 0.085, 0.047

This is similar to the acoustic noise signal which is dominated by 100 Hz fundamental and its harmonics. The amplitude variations of components in the acoustic noise could be due to changes in the rectified waveform caused by different arcing conditions.

APPENDIX 9.

The program listings in this appendix are:

1) CHAD*FURN.DATA 2 which reads (operating conditions) data from a data tape, and dumps it in a UNIVAC data file called 19.
2) CHAD*FURN.FIND locates the block position from inputted Date and Time information.

A P P E N D I X 10.

INSTRUMENTATION CHECK.

Plant Procedure.

The transducers being accelerometers, are only vibration sensitive and the procedure below was designed to isolate the transducers mechanically so that any signal recorded would indicate electrical noise pick-up in the cables or instrumentation. The problem of mechanically isolating the transducers without changing the routes of the cables was solved by hanging the transducers by rubber-bands as close to their mounting positions as possible. The mass of the transducer and the rubber bands formed a low pass system with a breakpoint below 100 Hz.

Analysis Results.

Plots A10.1, A10.2 and A10.3 show the auto-correlation function for the signals recorded with the transducers mounted in the above manner.

Plot A10.1 is the auto-correlation function for the signal from the top position electrode 3. $R_{xx}(0) = 0.021$.
Time scale is $\pm$ 400 msec.

Plot A10.2 is the auto-correlation signal from the top position electrode 2. $R_{xx}(0) = 0.0065$.
Time scale is $\pm$ 400 msec.

Plot A10.3 is the auto-correlation function signal from the mid-position electrode 3. $R_{xx}(0) = 0.01$.

Conclusion.

Plots A10.1 and A10.2 show random noise with very low value periodicities (less than 50 Hz). These periodicities are resonances of the catwalk structure transmitted to the transducers through the rubber bands.

Plot A10.3 shows a periodicity of 50 Hz, which could be a resonance of the structure from which the transducer was suspended. This is unlikely and the 50 Hz is more likely attributed to electrical hum pick-up.

For this reason, analyses of the noise was concentrated on the other transducers which had no evidence of electrical noise pick-up.

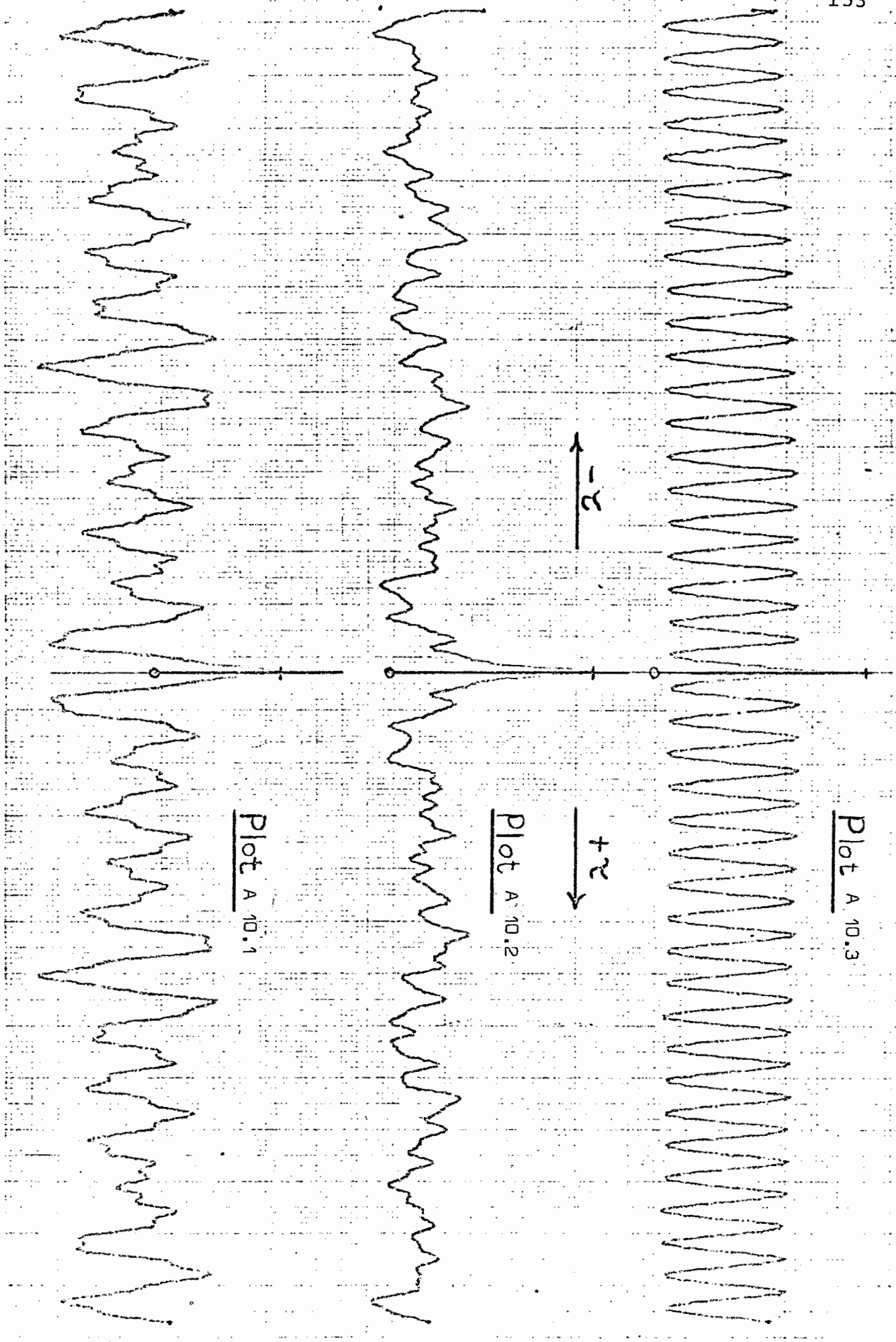
Plot A 10.1
Plot A 10.2
Plot A 10.3
-τ
+τ

A P P E N D I X 11

Taken from Reference 2.

MASKING BY PURE TONES.

It is difficult to hear and understand speech in the presence of a background of some other loud sound. Under such circumstances we say that the desired sound or signal is masked by the background and define the degree of masking as the extent to which the masking sound raises the threshold of audibility of the desired sound, the increase being customarily expressed in decibels. In general both the masked sound and the masking sound have highly complex wave forms and frequency structures. However, an understanding of the basic principles underlying this phenomenon is most readily obtained through a study of the special case in which both sounds are pure sinusoidal tones. In performing experiments of this type the masking tone is operated steadily at some particular intensity level, and the intensity of the signal tone is raised from a level below audibility to one that is just distinguishable. Typical results of experiments of this type are shown in Figure or two masking frequencies, (A) 400 cycles/sec and (B) 2000 cycles/sec. In each the frequency of the masked tone is indicated along the axis of abscissas, and the threshold shift in decibels for various intensities of the masking tone along the axis of ordinates.

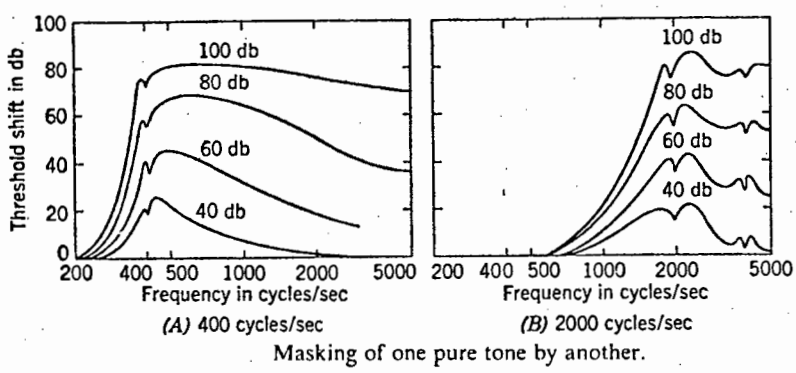

Masking of one pure tone by another.

It will be observed that the masking of one pure tone by another is most apparent when the two tones are of approximately the same frequency and also that in general a tone masks signals of higher frequency more effectively than it does those of lower frequency. For example, a signal having a frequency of 1000 cycles/sec and an intensity level of 40 dB is completely masked by a 400-cycle tone whose intensity level is 80 dB, but it is well above the threshold of audibility in the presence of a 2000-cycle tone of the same intensity. A consideration of the aural harmonics generated by the masking tone supplies an explanation of this effect.

For the 400-cycle, 80 dB tone these harmonics have frequencies of 800, 1200, 1600, etc., cycles/sec and have loudnesses approaching that of the fundamental, so that, since one or another of these harmonics will be of approximately the same frequency as any signal in the upper audible range, it will provide effective masking. On the other hand, the aural harmonics of the 2000-cycle tone have frequencies of 4000 cycles/sec or more and hence do not mask the 1000-cycle signal. The notch observed in each of the curves when the signal frequency is approximately the same as the masking frequency is due to the generation of beats, which aid in recognition of the presence of a signal.

From the results of experiments such as that described above it is possible to make qualitative predictions as to the manner in which pure tones should be expected to mask complex signals.

APPENDIX 12

Taken from:

"Digital Processing of Signals" by Gold B. and Rader C.M. (reference 7).

The Discrete Fourier Transform.

Introduction to the Discrete Fourier Transform.

The Discrete Fourier Transform is a modified version of the continuous Fourier Transform which is amenable to digital computer computation. The formation of the dicrete transform from the continuous transform is shown by considering the following example.

Let a function h(t) have a Fourier Transform H(f). (Fig. 1(a))
To determine the Fourier Transform of h(t) by means of digital analysis techniques, it is necessary to sample h(t) at regular intervals. By the sampling theorem, to represent h(t) completely the sampling frequency must be greater or equal to twice the highest frequency occuring in h(t).

Sampling is accomplished by multiplying h(t) by the sampling function. Fig.1b
The sampled function $\hat{h}(t)$ and its Fourier Transform are shown in Fig. 1c
This diagram shows the first modification of the original Fourier Transform pair. If as in this case, the sampling frequency is less than twice the highest frequency then aliasing or folding occurs. This problem is easily solved by choosing a smaller T.

The transform pair shown in Fig. 1c are unsuitable for machine computation due to the large number of points representing the curve. By applying a square window Fig. 1d the number of points are limited to N. The effect of this window is seen in Fig. 1e.

The transform of the window is a sinc(f) function which goes to a delta function as the size of the window goes to infinity. To reduce the ripple in Fig. 1 e. T_o must be as large as possible.

Fig. 1 e is still not acceptable because the frequency transform is a continuous function. The machine can only compute sample values of the frequency function, thus it is necessary to modify the frequency transform by the frequency sampling function Fig. 1 f.

A P P E N D I X 9.

The program listings in this appendix are:

1) CHAD*FURN.DATA 2 which reads 'operating conditions' data from a data tape, and dumps it in a UNIVAC data file called 19.
2) CHAD*FURN.FIND locates the block position from inputted Date and Time information.

```
C,AD,F,R,N(1),,DATA2
      1          DIMENSION IZAP(129),IZ(516),NTB(380)
      2     20   FORMAT(1A,80R1)
      3          INTEGER PKT(8)/0231622050505,0505050505050505/
      4          DATA (PKT(I),I=3,8) /6*0/
      5          INCLUDE SYS$.FTNL13.FIOP
      6          NARDS(PKT)=12^9
      7          BUFAD(PKT)=LOC(IZAP)
      8     C ***************SET MODE TO REWIND**********************
      9          FUNCT(PKT)=FREW
     10          CALL FIOJ(PKT)
     11     C ***************READ NO OF MINUTES DATA &BLOCKS SKIPPED*********
     12          READ 12,NRD,IC,NB,NE
     13          PRINT 5000
     14     5000 FORMAT(' MINUTES  BLOCKS  BEGIN  END  ')
     15          WRITE(5,12) NRD,IC,NB,NE
     16     C ***************SET MODE TO BLOCK SKIP &SKIP IC BLOCKS**********
     17          FUNCT(PKT)=FMF
     18          DO 42 N=1,IC
     19          CALL FIOJ(PKT)
     20     42   CONTINUE
     21     C ***************SET MODE TO READ BLOCK**********************
     22          FUNCT(PKT)=FR
     23          IB=0
     24          NP=0
     25     12   FORMAT()
     26       21 CALL FIOJ(PKT)
     27          IF(IB.GT.NRD) GO TO 92
     28          IM=0
     29          DECODE(516,100,IZAP,ICH)IZ
     30     100  FORMAT(6(80R1,/),36R1)
     31          DATA ICR,IDTE,IAT/0015,0104,0101/
     32     C ***************REMOVE CARIAGE RETURN CHARACTERS*___@@@@@@**********
     33          DO 72 I=1,516
     34          IF(IZ(I).NE.ICR) GO TO 72
     35          IM=IM+1
     36          DO 14 J=I,515
     37          IZ(J)=IZ(J+1)
     38     14   CONTINUE
     39     72   CONTINUE
     40          IF(IB.GT.NRD) GO TO 92
     41       103 IF(NP.NE.0) GO TO 24
     42     C ***************FIND DATE AND WRITE MINUTE BLOCKS OF DATA
     43     C ***************TO FILE 19
     44          DO 19 N=1,516
     45          IF(IZ(N).NE.IDTE) GO TO 19
     46          IF(IZ(N+1).NE.IAT) GO TO 19
     47          IF(N+379+IM-510)6,6,7
     48     7    NP=1
     49          JA=1
     50          DO 10 I=N,510-IM
     51          NTB(JA)=IZ(I)
     52          JA=JA+1
     53     10   CONTINUE
     54          GO TO 19
     55     24   IA=1
     56          DO 25 K=JA,380
     57          NTB(K)=IZ(IA)
     58          IA=IA+1
     59     25   CONTINUE
```

```
     60          GO TO 9
     61     6    WRITE(5,20)(IZ(K1),K1=N+NB,N+NE),(IZ(K1),K1=N,N+30)
     62          IB=IB+1
     63     19   CONTINUE
     64          GO TO 21
     65     9    WRITE(5,20)(NTB(K2),K2=NB,NE),(NTB(K2),K2=1,30)
     66          IB=IB+1
     67          NP=0
     68          GO TO 103
     69     101  CONTINUE
     70     92   PRINT 111
     71     111  FORMAT(' END JC RUN ')
     72          STOP
     73          END
```

```
CHAD*FORTRAN(1),FIND
      1             DIMENSION IZAP(129),IZ(516),NTB(23)
      2       20    FORMAT(1X,80R1)
      3             INTEGER PKT(16)/9231622050505,0J5050505J505/
      4             DATA (PKT(I),I=3,5) /6*0/
      5             DATA ICR,IDTE,NUL/3015,0104,0000/
      6             INCLUDE SYS$:FTNL18,FIOP
      7             HANDS(PKT)=129
      8             FUNCT(PKT)=FREW
      9             BUFAD(PKT)=LOC(IZAP)
     10             CALL FIOW(PKT)
     11             FUNCT(PKT)=FWF
     12             DO 103 J=1,70
     13             CALL FIOW(PKT)
     14       103   CONTINUE
     15             FUNCT(PKT)=FR
     16             READ 49,JMNTH
     17             READ 49,JDY1
     18             READ 49,JDY2
     19             READ 49,JTH1
     20             READ 49,JTH2
     21             READ 49,JTM1
     22             READ 49,JTM2
     23       49    FORMAT(R1)
     24             DO 12 K=1,1000
     25             CALL FIOW(PKT)
     26       25    NP=0
     27             DECODE(516,100,IZAP,ICH)IZ
     28       100   FORMAT(6(80R1*/),36R1)
     29             DO 72 I=1,516
     30             IF(IZ(I).NE.ICR) GO TO 72
     31             DO 14 J=I,515
     32             IZ(J)=IZ(J+1)
     33       14    CONTINUE
     34       72    CONTINUE
     35             IF(NP.EQ.1) GO TO 85
     36             DO 19 N=1,516
     37             IF(IZ(N).EQ.IDTE) GO TO 5
     38       18    IF(NP)19,19,25
     39       19    CONTINUE
     40       12    CONTINUE
     41       5     IF(N+26-515)86,86,2
     42       86    NMNTH=IZ(N+6)
     43             NDY1=IZ(N+8)
     44             NDY2=IZ(N+9)
     45             NTH1=IZ(N+17)
     46             NTH2=IZ(N+18)
     47             NTM1=IZ(N+20)
     48             NTM2=IZ(N+21)
     49             NSC1=IZ(N+23)
     50             IF(NMNTH.NE.JMNTH) GO TO18
     51             IF(NDY1.NE.JDY1) GO TO 18
     52             IF(NDY2.NE.JDY2) GO TO 18
     53             IF(NTH1.NE.JTH1) GO TO 18
     54             IF(NTH2.NE.JTH2) GO TO 18
     55             IF(NTM1.NE.JTM1) GO TO 18
     56             IF(NTM2.NE.JTM2) GO TO 18
     57       32    WRITE(5,50) K
     58       50    FORMAT()
     59             WRITE(5,20)(IZ(JP),JP=N,N+26)

     60             STOP
     61       2     CONTINUE
     62             DO 22 I=N,516
     63             IF(IZ(I).EQ.NUL) GO TO 28
     64       22    CONTINUE
     65       28    NTOT=I
     66             J4=1
     67             DO 23 J3=N,NTOT
     68             NTB(J4)=IZ(J3)
     69             J4=J4+1
     70       23    CONTINUE
     71             NP=1
     72             NL=NTOT+2-N
     73             GO TO 12
     74       85    K1=1
     75             DO 83 I=NL,27
     76             IZ(I)=IZ(K1)
     77             K1=K1+1
     78       83    CONTINUE
     79             DO 84 I2=1,NL-1
     80             IZ(I2)=NTB(I2)
     81       84    CONTINUE
     82             N=1
     83             GO TO 86
     84             END
```

A P P E N D I X 10.

INSTRUMENTATION CHECK.

Plant Procedure.

The transducers being accelerometers, are only vibration sensitive and the procedure below was designed to isolate the transducers mechanically so that any signal recorded would indicate electrical noise pick-up in the cables or instrumentation. The problem of mechanically isolating the transducers without changing the routes of the cables was solved by hanging the transducers by rubber-bands as close to their mounting positions as possible. The mass of the transducer and the rubber bands formed a low pass system with a breakpoint below 100 Hz.

Analysis Results.

Plots A10.1, A10.2 and A10.3 show the auto-correlation function for the signals recorded with the transducers mounted in the above manner.

Plot A10.1 is the auto-correlation function for the signal from the top position electrode 3. $R_{xx}(0) = 0.021$.

Time scale is $\pm$ 400 msec.

Plot A10.2 is the auto-correlation signal from the top position electrode 2. $R_{xx}(0) = 0.0065$.

Time scale is $\pm$ 400 msec.

Plot A10.3 is the auto-correlation function signal from the mid-position electrode 3. $R_{xx}(0) = 0.01$.

Conclusion.

Plots A10.1 and A10.2 show random noise with very low value periodicities (less than 50 Hz). These periodicities are resonances of the catwalk structure transmitted to the transducers through the rubber bands.

Plot A10.3 shows a periodicity of 50 Hz, which could be a resonance of the structure from which the transducer was suspended. This is unlikely and the 50 Hz is more likely attributed to electrical hum pick-up.

For this reason, analyses of the noise was concentrated on the other transducers which had no evidence of electrical noise pick-up.

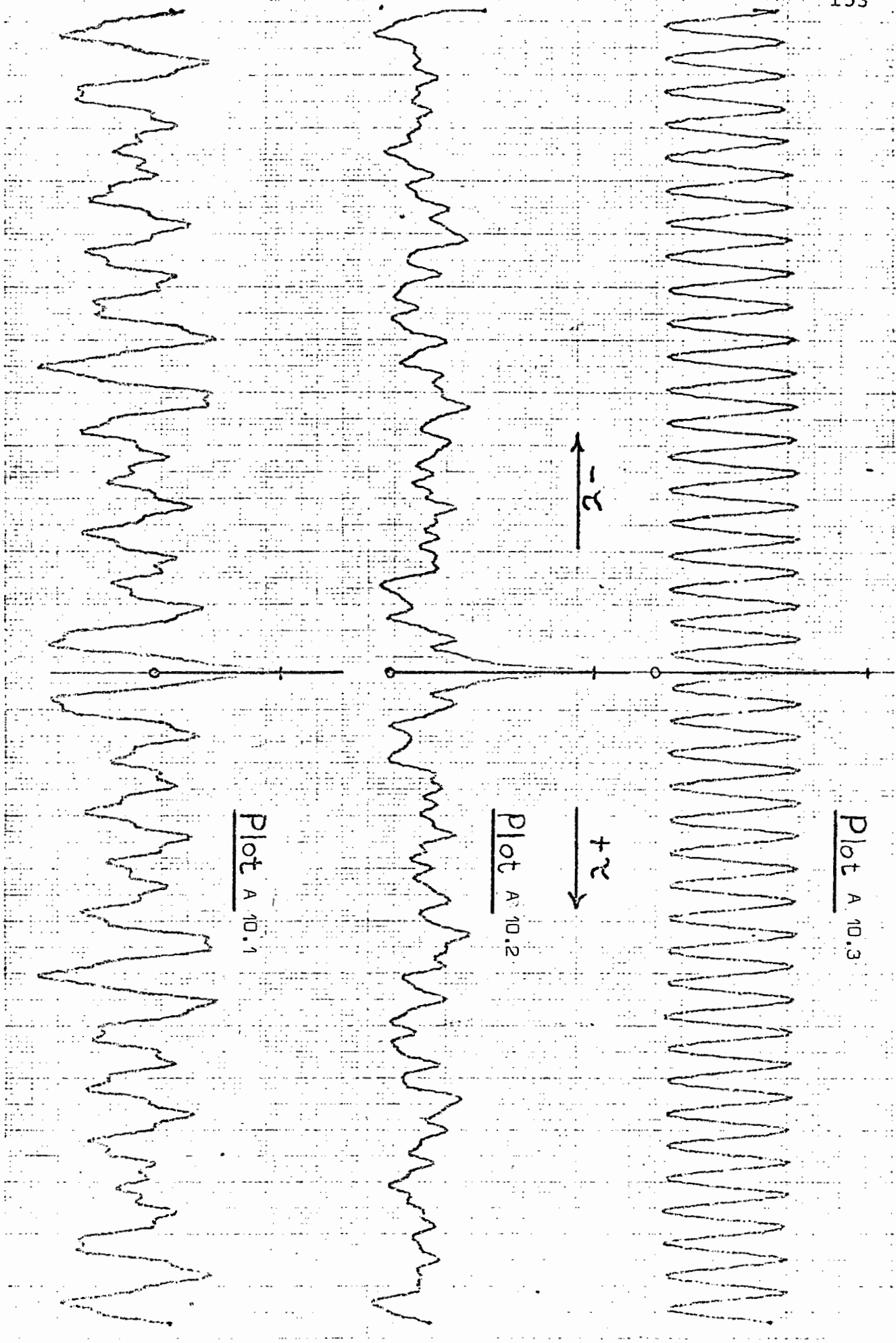
Plot A 10.1
Plot A 10.2
Plot A 10.3
2-
2+

A P P E N D I X 11 .

Taken from Reference 2.

MASKING BY PURE TONES.

It is difficult to hear and understand speech in the presence of a background of some other loud sound. Under such circumstances we say that the desired sound or signal is masked by the background and define the degree of masking as the extent to which the masking sound raises the threshold of audibility of the desired sound, the increase being customarily expressed in decibels. In general both the masked sound and the masking sound have highly complex wave forms and frequency structures. However, an understanding of the basic principles underlying this phenomenon is most readily obtained through a study of the special case in which both sounds are pure sinusoidal tones. In performing experiments of this type the masking tone is operated steadily at some particular intensity level, and the intensity of the signal tone is raised from a level below audibility to one that is just distinguishable. Typical results of experiments of this type are shown in Figure or two masking frequencies, (A) 400 cycles/sec and (B) 2000 cycles/sec. In each the frequency of the masked tone is indicated along the axis of abscissas, and the threshold shift in decibels for various intensities of the masking tone along the axis of ordinates.

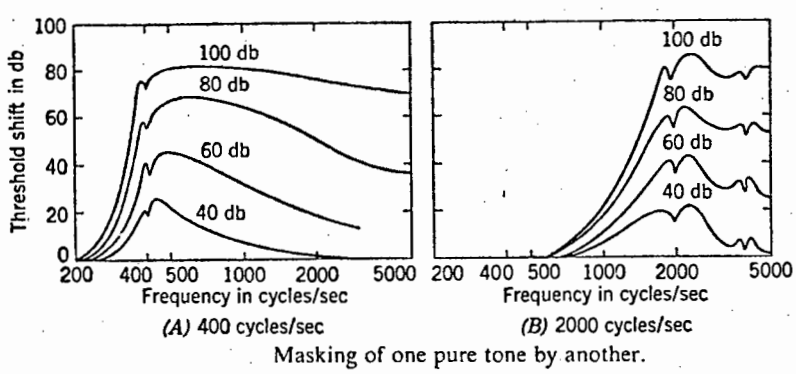

Masking of one pure tone by another.

It will be observed that the masking of one pure tone by another is most apparent when the two tones are of approximately the same frequency and also that in general a tone masks signals of higher frequency more effectively than it does those of lower frequency. For example, a signal having a frequency of 1000 cycles/sec and an intensity level of 40 dB is completely masked by a 400-cycle tone whose intensity level is 80 dB, but it is well above the threshold of audibility in the presence of a 2000-cycle tone of the same intensity. A consideration of the aural harmonics generated by the masking tone supplies an explanation of this effect.

For the 400-cycle, 80 dB tone these harmonics have frequencies of 800, 1200, 1600, etc., cycles/sec and have loudnesses approaching that of the fundamental, so that, since one or another of these harmonics will be of approximately the same frequency as any signal in the upper audible range, it will provide effective masking. On the other hand, the aural harmonics of the 2000-cycle tone have frequencies of 4000 cycles/sec or more and hence do not mask the 1000-cycle signal. The notch observed in each of the curves when the signal frequency is approximately the same as the masking frequency is due to the generation of beats, which aid in recognition of the presence of a signal.

From the results of experiments such as that described above it is possible to make qualitative predictions as to the manner in which pure tones should be expected to mask complex signals.

APPENDIX 12

Taken from:

"Digital Processing of Signals" by Gold B. and Rader C.M. (reference 7).

The Discrete Fourier Transform.

Introduction to the Discrete Fourier Transform.

The Discrete Fourier Transform is a modified version of the continuous Fourier Transform which is amenable to digital computer computation. The formation of the dicrete transform from the continuous transform is shown by considering the following example.

Let a function h(t) have a Fourier Transform H(f). (Fig. 1(a))
To determine the Fourier Transform of h(t) by means of digital analysis techniques, it is necessary to sample h(t) at regularintervals. By the sampling theorem, to represent h(t) completely the sampling frequency must be greater or equal to twice the highest frequency occuring in h(t).

Sampling is accomplished by multiplying h(t) by the sampling function. Fig.1b
The sampled function $\hat{h}(t)$ and its Fourier Transform are shown in Fig. 1c
This diagram shows the first modification of the original Fourier Transform pair. If as in this case, the sampling frequency is less than twice the highest frequency then aliasing or folding occurs. This problem is easily solved by choosing a smaller T.

The transform pair shown in Fig. 1c are unsuitable for machine computation due to the large number of points representing the curve. By applying a square window Fig. 1d the number of points are limited to N. The effect of this window is seen in Fig. 1e.

The transform of the window is a sinc(f) function which goes to a delta function as the size of the window goes to infinity. To reduce the ripple in Fig. 1 e. T_o must be as large as possible.

Fig. 1 e is still not acceptable because the frequency transform is a continuous function. The machine can only compute sample values of the frequency function, thus it is necessary to modify the frequency transform by the frequency sampling function Fig. 1 f.

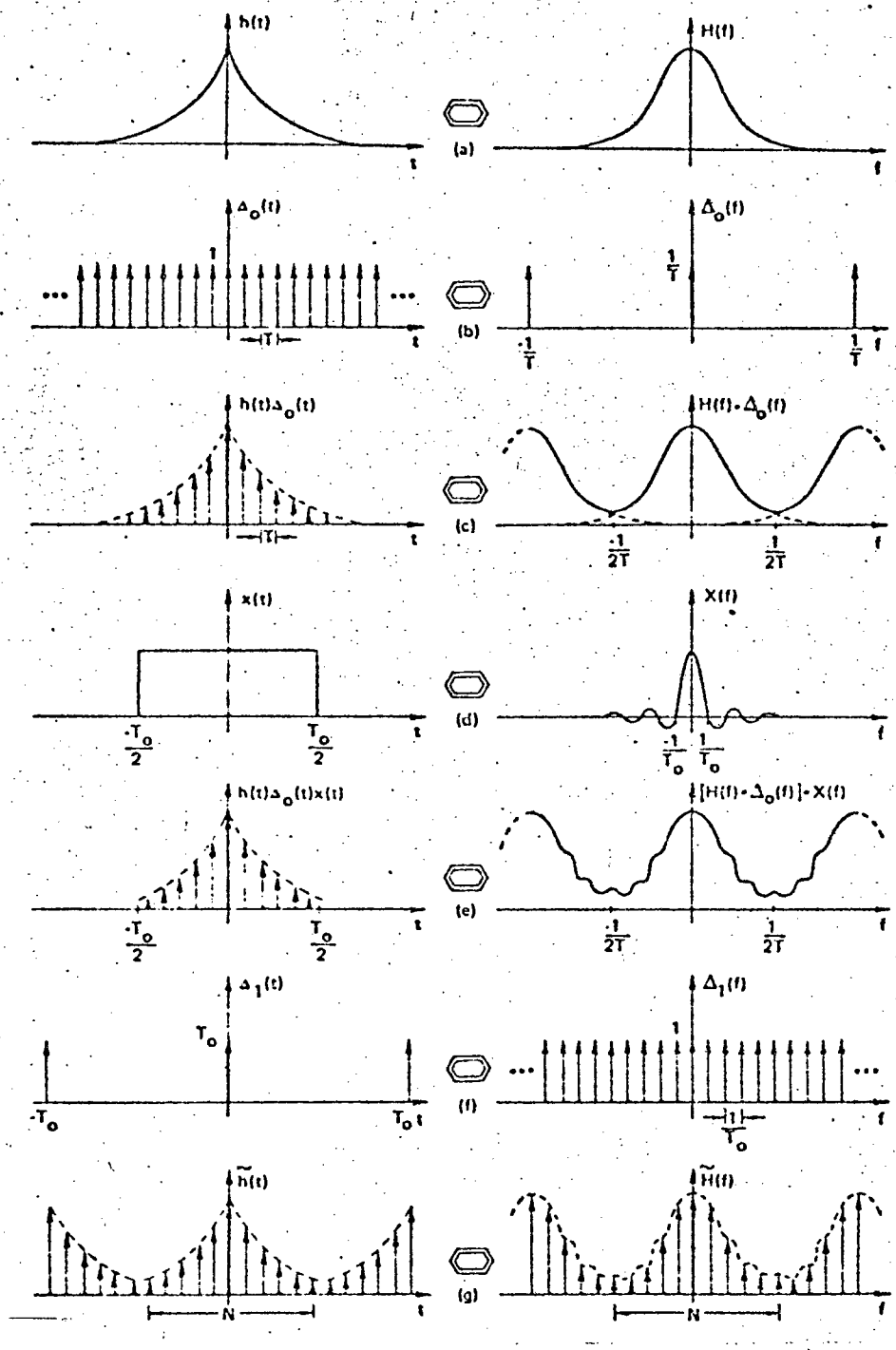
h(t)
H(f)
(a)
t
f
$\Delta_o(t)$
$\Delta_o(f)$
1
$\frac{1}{T}$
T
$\frac{-1}{T}$
$\frac{1}{T}$
(b)
$h(t)\Delta_o(t)$
$H(f)*\Delta_o(f)$
$\frac{-1}{2T}$
$\frac{1}{2T}$
(c)
x(t)
X(f)
$\frac{-T_o}{2}$
$\frac{T_o}{2}$
$\frac{-1}{T_o}$
$\frac{1}{T_o}$
(d)
$h(t)\Delta_o(t)x(t)$
$[H(f)*\Delta_o(f)]*X(f)$
(e)
$\Delta_1(t)$
$\Delta_1(f)$
T_o
$-T_o$
T_o
(f)
$\tilde{h}(t)$
$\tilde{H}(f)$
N
(g)

Figure 1.

The discrete Fourier transforms pair Fig.1(g) is acceptable as both the time and frequency domains are represented by discrete values. If the original time function is represented by N samples, the original Fourier transform H(f) is also represented by N samples.

The sampling in the time domain results in the periodic function of frequency, and the sampling in the frequency domain results in a periodic function of time. N time samples and N frequency samples represent one period of the time and frequency domain waveforms respectively. The Fourier transform algorithm assumes the 'window' of N points to be one period of a continuous wave and thus calculates the Fourier transform.

The extent to which the discrete Fourier transform approximates the continuous transform depends of the waveform being analysed. The following examples show the validity of the approximation. Differences in the two transforms arise because of the discrete transform requirement for sampling and truncation.

Consider the function h(t) and its transform H(f) in Fig. 2(a). The waveform is sampled by multiplication with the sampled function in Fig. 2 (b) giving the sampled wave in Fig. 2(c). There is no aliasing as T_o 2T and the Fourier transform in Fig.2(c) has an amplitude of A/2T due to sampling in the time domain. Fig.2(d) shows the rectangular function which truncates the input waveform. The length of the rectangle is chosen to be exactly the period of the input waveform. The transform of the rectangle is convolved with Fig.2(c) giving the result in Fig.2(e). A close up version is shown in Fig.3. A sinc(f) function is formed on each impulse of Fig2(c) and the sum is given by the dark line in Fig.3. The distortion of the resultant waveform is eliminated by the sampling of the frequency sampling function Fig.2(f) which samples at the zeroes of the sinc waveforms.

Multiplication of the frequency function Fig.2(e) and $\Delta_1(f)$ Fig.2(f) implies the convolution of the time functions in Fig.2(e) and 2(f). Because the sampled truncation waveform Fig.2(e) is exactly one period of the original waveform h(t) and since the time domain impulse functions of Fig.2(f) are separated by T_o, then their convolution yields a periodic as shown in Fig.2(g).

Comparing Fig.2(a) and Fig.2(g) we see that for the continuous case the time domain amplitude is A and goes to A/2 in the frequency domain, while for the continuous case the time domain amplitude is AT_o which goes to $T_oA/2T$ in the frequency domain.

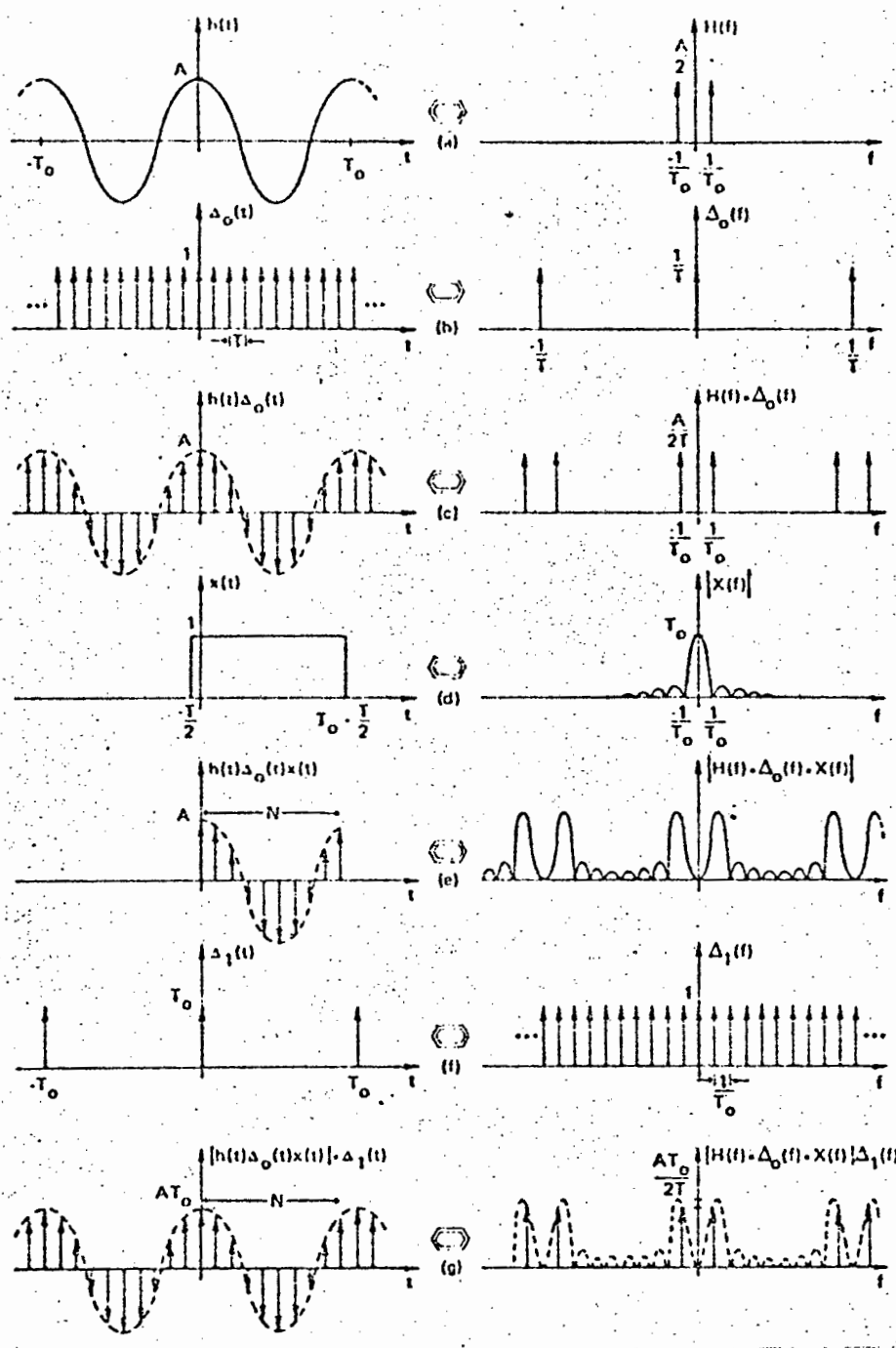

Figure 2.

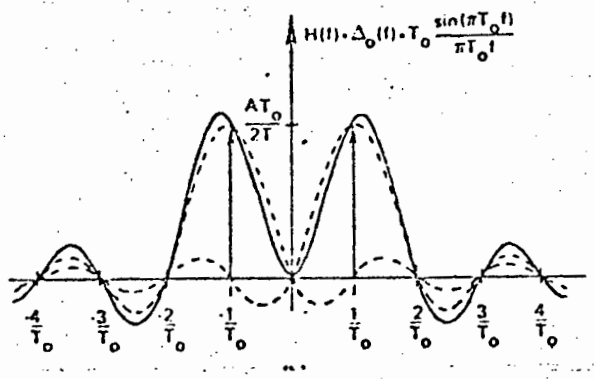

Figure 3.

Thus the discrete Fourier transform can be written as

$$H(n/NT) = T\sum_{k=0}^{N-1} h(kT)\exp(-j2\pi nk/N) \qquad n= 0,1,2,.....N-1$$

Equivalence of the continuous and discrete transforms require

1) the time domain function h(t) must be peroidic.
2) h(t) must be band limited.
3) the sampling rate must be at least twice the largest frequency component of h(t).
4) the truncation function x(t) must be an integer multiple peroid h(t) or x(t) must be non-zero over exactly one period.

The discrete Fourier transform implies periodicity in both the time and frequency domains, the N input samples must represent a period of a continuous waveform. If condition 4) is not satisfied leakage occurs resulting in errors.

Fig.4(a-g) show the same example as Fig.2(a-g) except that the truncation interval does not satisfy condition 4) above. (Figures 1-4 come from Ref. 2)

A P P E N D I X 13.

This program is the adopted form of the FFT program supplied by Dr. D. Swingler, Electrical Engineering Department. University of Cape Town.

The program produces a spectral density plot from a single sided autocorrelation function. The program first removes the mean value, then applies a cosine taper to the data before computing the FFT. The magnitude of the spectral density function is plotted with linear amplitude and frequency axis.

FFT PROGRAM.

```
1  CALL  ERASE
2  LET N= 128
3  DIM D(255)
4  LET Z1=-1
5  LET G1= 0
6  FOR J= 1 TO  255
7  LET D(J)= 0
8  NEXT J
9  FOR A= 1 TO  250 STEP  2
10  PRINT D(A+ 1)
11  NEXT A
12  LET J= 0
13  FOR I= 102 TO  124 STEP  2
14  LET I(I)=D(I)*COS( .2613*J)
15  LET J=J+ 1
16  NEXT I
17  FOR I= 1 TO  124
18  LET D( 124+I)=D(I)
19  NEXT I
20  FOR I= 124 TO  1 STEP -1
21  LET D(I)=D( 250-I)
22  NEXT I
23  LET Z= 0
24  LET D( 250)= 0
25  FOR I= 1 TO  250 STEP  2
26  LET Z=Z+D(I+ 1)
27  NEXT I
28  LET Z=Z/ 125
29  FOR I= 1 TO  250 STEP  2
30  LET I(I+ 1)=I(I+ 1)-Z
31  NEXT I
32  GOSUB 37
33  GOSUB 114
34  GOSUB 127
35  GOSUB 139
36  END
37  LET N= 128
38  LET I0= 8
```

```
39  LET I3=I0*N
40  LET I9= 1
41  FOR J3= 1 TO I3 STEP I0
42  IF (J3-I9)>= 0 THEN 64
43  LET T1=D(J3)
44  IF (J3+ 1)= 256 THEN 47
45  LET T2=D(J3+ 1)
46  GOTO 48
47  LET T2=G1
48  LET D(J3)=D(I9)
49  IF (J3+I9+ 2)= 512 THEN 58
50  IF (J3+ 1)= 256 THEN 54
51  IF I9= 255 THEN 56
52  LET D(J3+ 1)=D(I9+ 1)
53  GOTO 59
54  LET G1=D(I9+ 1)
55  GOTO 59
56  LET D(J3+ 1)=G1
57  GOTO 59
58  LET G1=G1
59  LET D(I9)=T1
60  IF I9= 255 THEN 63
61  LET D(I9+ 1)=T2
62  GOTO 64
63  LET G1=T2
64  LET I1=I3/ 2
65  IF (I9-I1)<= 0 THEN 69
66  LET I9=I9-I1
67  LET I1=I1/ 2
68  IF (I1-I0)>= 0 THEN 65
69  LET I9=I9+I1
70  NEXT J3
71  LET I1=I0
72  IF (A1-I3)>= 0 THEN 113
73  LET I2=I1* 2
74  LET U1= 6.28318/(I1*I2/I0)
75  LET U2=SIN(U1/ 2)
76  LET W1=-2*U2*U2
77  LET W2=SIN(U1)
78  LET W3= 1
79  LET W4= 0
80  FOR J1= 1 TO I1 STEP I0
81  FOR J3=J1 TO I3 STEP I2
82  LET K1=J3
83  LET K2=K1+I1
84  IF K2= 255 THEN 88
85  LET T1=W3*D(K2)-W4*D(K2+ 1)
86  LET T2=W3*D(K2+ 1)+W4*D(K2)
87  GOTO 90
88  LET T1=W3*D(K2)-W4*G1
89  LET T2=W3*G1+W4*D(K2)
90  LET D(K2)=D(K1)-T1
91  IF (K1+K2)= 510 THEN 100
92  IF K2= 255 THEN 96
```

```
 93  IF K1= 255 THEN 98
 94  LET D(K2+ 1)=D(K1+ 1)-T2
 95  GOTO 101
 96  LET G1=D(K1+ 1)-T2
 97  GOTO 101
 98  LET D(K2+ 1)=G1-T2
 99  GOTO 101
6100  LET G1=G1-T2
101  LET D(K1)=D(K1)+T1
102  IF K1= 255 THEN 105
103  LET D(K1+ 1)=D(K1+ 1)+T2
104  GOTO 106
105  LET G1=G1+T2
106  NEXT J3
107  LET T1=W3
108  LET W3=W3*W1-W4*W2+W3
109  LET W4=W4*W1+T1*W2+W4
110  NEXT J1
111  LET I1=I2
112  GOTO 72
113  RETURN
114  FOR J= 1 TO (N- 1) STEP  2
115  LET T1=D(J)
116  LET T2=D(J+ 1)
117  LET D(J)=D(J+N)
118  LET D(J+N)=T1
119  IF (J+N)= 255 THEN 123
120  LET D(J+ 1)=D(J+ 1+N)
121  LET D(J+ 1+N)=T2
122  GOTO 125
123  LET D(J+ 1)=G1
124  LET G1=T2
125  NEXT J
126  RETURN
127  LET P= 0
128  FOR K= 1 TO N
129  IF K= 128 THEN 132
130  LET D(K)=D( 2*K- 1)↑ 2+D( 2*K)↑ 2
131  GOTO 133
132  LET D( 128)=D( 255)↑ 2+G1↑ 2
133  LET D(K)=SQR(D(K))
134  IF D(K)>P THEN 136
135  GOTO 137
136  LET P=D(K)
137  NEXT K
138  RETURN
139  CALL  POINT,-1,-1
140  CALL   LINE, 1,-1
141  CALL  POINT,(-1+ 2/N),D( 1)* 2/P- 1
142  FOR K= 2 TO N
143  CALL   LINE,(-1+ 2*K/N),D(K)* 2/P- 1
144  NEXT K
145  LET Y9= 2/N
146  CALL  POINT,Y9,-1
147  CALL   LINE,Y9, 1
148  CALL  POINT,-1,-1
149  PRINT ""
150  RETURN
151  END
152  END
```